



Multi-electrode system design and optimization for cardiac implants

Islam Seoudi

► To cite this version:

Islam Seoudi. Multi-electrode system design and optimization for cardiac implants. Other. Télécom ParisTech, 2012. English. NNT : 2012ENST0027 . tel-01081680

HAL Id: tel-01081680

<https://pastel.hal.science/tel-01081680>

Submitted on 10 Nov 2014

HAL is a multi-disciplinary open access archive for the deposit and dissemination of scientific research documents, whether they are published or not. The documents may come from teaching and research institutions in France or abroad, or from public or private research centers.

L'archive ouverte pluridisciplinaire **HAL**, est destinée au dépôt et à la diffusion de documents scientifiques de niveau recherche, publiés ou non, émanant des établissements d'enseignement et de recherche français ou étrangers, des laboratoires publics ou privés.



Doctorat ParisTech

THÈSE

Pour obtenir le grade de docteur délivré par

Télécom ParisTech

Spécialité “Electronique et Communications”

Présenté et soutenue publiquement par

Islam SEOUDI

5 juin 2012

Multi-electrode System Design and Optimization for Cardiac Implants

Directeur de thèse : **Amara AMARA**

Jury

M. Marc Belleville, Chief Scientist, CEA-Leti

M. Jean-Michel PORTAL, Professeur, Ecole Polytechnique Universitaire de Marseille

M. Christian PIGUET, Professeur, CSEM

Mme Lirida NAVINER, Professeur, Telecom ParisTech

M. Alain RIPART, Vice-President, Sorin CRM

M. Daniel KROISS, Vice-President & Chief Scientific Officer, Sorin CRM

M. Amara AMARA, Directeur de Recherche, ISEP

Mme Karima AMARA, Ingénieur Project, Sorin CRM

RAPPORTEUR

RAPPORTEUR

EXAMINATEUR

EXAMINATEUR

EXAMINATEUR

INVITE

DIRECTEUR DE THESE

CO-DIRECTEUR DE THESE

T
H
È
S
E

Télécom ParisTech

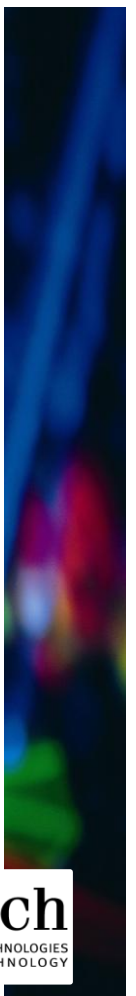
Grande école de l'Institut Télécom – membre fondateur de ParisTech

46, rue Barrault – 75634 Paris Cedex 13 – Tél. + 33 (0)1 45 81 77 77 – www.telecom-paristech.fr

Title: Multi-Electrode System Design and Optimization for Cardiac Implants

Abstract: Cardiac implants like ICD (Implantable Cardioverter Defibrillator) are life saving devices in cases of sudden cardiac arrhythmias. In other conditions like the one of heart failure, cardiac implants like CRT (Cardiac Rhythm Therapy) are prescribed to restore the coordinated contraction of the heart. Such treatment consists of the delivery of localized electrical stimuli to the cardiac tissue via electrodes in the stimulation lead. Conventionally the stimulation lead come either in unipolar or bipolar configuration (1 or 2 electrode) which have been found to be sufficient for pacing the right atrium and right ventricle, studies have shown the benefits of a multi-electrode system for pacing left ventricle essential for cardiac resynchronization. This thesis discusses the design and optimization of a multi-electrode system capable of alleviating the limitations and constraints related to left ventricular stimulation. We first present a chip implementation of such multi-electrode system. It was taped out in 0.18 μm technology and occupies 2.25x5.35 mm² area . The chip also features a specially designed communication protocol and is compliant with the existing standards. It enables low power operation and allows quick configuration. Thereafter we present the design and implementation of a default connection unit (DCU) to ensure the compatibility of our multi-electrode lead with pacemakers not designed specifically to control such a lead. Like the multi-electrode chip the DCU unit was taped out in 0.18 μm technology, occupies 2.2 x 1.75 mm² area and harvests the stimulation energy to power itself. Finally we present a proof of concept study for the adaptation and integration of non-volatile memory technologies within the multi-electrode system. New technologies were explored which drastically improve the performance of the multi-electrode system. The employment of such technologies enhanced our multi-electrode system by eliminating the need of repetitive configuration of electrodes, thereby saving power and reducing latency. The benefits also included smaller area and compatibility with any pacemaker in the market. Through simulations we proved the feasibility of these technologies for our implant applications.

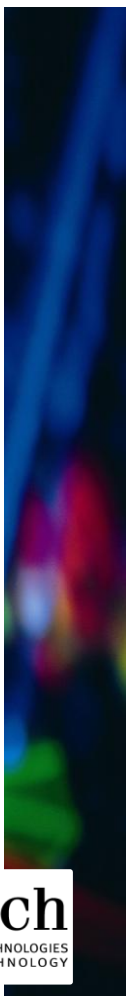
Keywords : Cardiac pacemakers, multi-electrode, stimulation, medical implants, switching, MOS, non-volatile, memories



Titre : Conception et Optimisation de Système Multi-électrodes Pour Les Implants Cardiaques

Résumé: Les implants cardiaques tels que les défibrillateurs implantables sont des appareils permettant de sauver la vie dans le cas de troubles de l'arythmie cardiaque soudaine. Tandis que dans le cas des attaques cardiaques, les implants CRT sont utilisés pour rétablir la cadence de la contraction cardiaque. De tels traitements consistent en l'application de stimulations locales au tissu cardiaque via des électrodes se trouvant dans les sondes de stimulation. Ces dernières se présentent soit dans une configuration unipolaire ou bipolaire ; qui ont prouvé leur efficacité pour stimuler le ventricule droit et l'oreillette droite ; des études ont montré l'efficacité de la sonde multi-électrode dans la stimulation du ventricule gauche indispensable pour la resynchronisation cardiaque. Cette thèse traite de la conception et l'optimisation d'un système multi-électrodes capable d'éviter les limitations et les contraintes liées à la stimulation du ventricule gauche. Tout d'abord, une réalisation de ce système est présentée et fabriqué dans une technologie 0.18 μm . Le circuit a également un protocole de communication spécifique. Il permet une opération basse consommation et une configuration rapide. Ensuite, la conception et la réalisation d'une unité de configuration par default est présentée. Cette unité assure la compatibilité de notre sonde avec les stimulateurs cardiaques du marché. Finalement, une étude pour l'adaptation et l'intégration des technologies mémoire non-volatile dans la sonde est présentée. De telles technologies améliorent considérablement le système en évitant le besoin de reconfiguration des sondes et en conséquence réduire la latence et la consommation.

Mots clés: implants cardiaques, pacemaker, multi-électrodes, sondes, switching, MOS, mémoires non volatile



Acknowledgment

I would like to thank Mr. Renzo Dal Molin for this exceptional opportunity to work with him at the Advanced Research Department of Sorin Group from where this thesis work started. I would like to thank Professor Amara for accepting me as his student for which I'm grateful. I was lucky enough to have Professor Amara as my PhD director. He gave the example how an advisor can be as a father for his student, offers him unlimited support without counting, and lighting the dark paths full of doubts and unclear ideas.

I am grateful to Karima Amara for revealing all the secrets of digital electronics design for me. She also taught me how to insist and dig after the promising ideas and to be equipped with patience in order to convert them into meaningful inventions. I am also grateful to Jean-Francois Debroux and Marc Laflutte for revealing all the secrets of analog electronics design for me and for their unquestionable support and sincere advice.

I will strongly remember Alaa Makdissi with his rich scientific discussions and his enormous capacity to retrieve solutions for persistent problems. I want to thank him for his sincere advice and support.

All my thanks and gratitude I would present them to my friend Ashutosh who gave a perfect example for how a friend can support sincerely and generously his friend. When talking about generosity, I cannot forget Balwant Godara for being so kind, helpful and generous in giving me advice.

I would like to thank all my colleagues with whom I enjoyed to work:

Sir Julien Ardelean, Sebastien Jackard and all the "advanced research", Fabrice Gayral, Bruno Eon, Jean-Claude Bierg, Didier Gourgousse, Jean-Pierre Noel, Jean-Yves and all the R&D, Bruno, Adel, Etienne, Wen, Nabil and all V&V, Emmanuel Bigen and all System design at Sorin.

I am also grateful to Francis Chan Wai Po, Costin Anghel, Andrei Vladimirescu and wish all the best for Hraziia, Rutwick, Adam and Khaja in their Phd.

In such special moments, special persons are always remembered because without them I wouldn't have reached this achievement today. To my father Zakaria and my mother Elham I owe them this achievement and nothing can be presented to them in return other than an eternal thanks and gratitude.

To my wife Salma I present my gratitude for her support in many difficult periods of this thesis and for always pushing me forward to reach my goals.

To my brothers Yahia, Ahmed and Nour: thanks for your continuous support and for urging me constantly towards higher achievements and bigger success.

To all my Seoudi and Hammouda families I dedicate this work.

Contents

Acknowledgment	5
Contents	7
List of Figures	12
List of Tables	15
Résumé de la thèse en Français	17
Chapitre 1: Introduction	18
Chapitre 2: Les Implants de Stimulation Cardiaque	21
Système de stimulation cardiaque implantable	22
Thérapie de resynchronisation cardiaque (CRT)	23
Chapitre 3: Système Multi-Electrodes Pour La Stimulation Ventriculaire Gauche: Conception et Mise en Œuvre	25
Système Multi-Electrode : Principe & Contraintes	25
Conception et implémentation du système	26
Résultat de Mesure	31
Chapitre 4: Unité de Connexion Par Défaut	32
Les choix et défis de conception	33
Le Principe de l'opération du DCU	34
Résultats	35
Chapitre 5 : L'Amélioration de la Sonde Multi-Electrode en Utilisant La Technologie des Mémoires Non-Volatiles	35
1 Chapter 1	40
2 Chapter 2	44
2.1 Introduction	46
2.2 Human Heart and Cardiac Implant Evolution	46
2.2.1 Heart failure condition	48
2.2.2 Arrhythmias	48
2.2.3 First Implantable pacemaker	48
2.2.4 Demand Pacemaker	49

2.2.5	Rate-Responsive Pacemaker	49
2.3	Implantable Cardiac Stimulation System	49
2.3.1	Pulse Generator (Implant - CAN)	51
2.3.1.1	Power source	51
2.3.1.2	Output circuit	52
2.3.1.3	Sensing Unit	56
2.3.1.4	Control unit	58
2.3.2	Leads	59
2.3.2.1	Unipolar	60
2.3.2.2	Bipolar	60
2.4	Cardiac Resynchronization Therapy (CRT)	61
2.4.1	Phrenic nerve stimulation	62
2.4.2	Limited choice of stimulation site	62
2.4.3	Lead displacement	62
2.5	Conclusion	63
	References	64
3	Chapter 3	66
3.1	Introduction	68
3.2	Multi-electrode System: Principle & Constraints	69
3.1.1	Compliance with standards	70
3.1.2	Communication protocol: Power and Configuration	71
3.3	State of the Art	71
3.3.1	Implementation Strategies for LEC	72
3.3.1.1	Centralized Structure	72
3.3.1.2	Distributed Structure	73
3.3.1.3	Direct Structure	74
3.4	System Design & Implementation	74
3.4.1	Adopted Strategy	74
3.4.2	Implant and lead electrode controller (IEC & LEC)	75
3.4.2.1	Power Storage Unit	77

3.4.2.2	Control Unit	78
3.4.2.3	Oscillators	78
3.4.2.4	OTP Memory	79
3.4.2.5	Main Switching Unit	79
3.4.2.6	Auxiliary Switching Unit	79
3.4.2.7	Charge Pump	80
3.4.3	Communication Protocol	80
3.4.3.1	Power pulses	83
3.4.3.2	Event Synchronization bits	83
3.4.3.3	Configuration bits	83
3.4.3.4	Double Stimulation	87
3.4.4	Comparison	88
3.5	Distributed Structure	88
3.6	Measurement Results	89
3.7	Conclusion	92
	Publications	93
	References	93
4	Chapter 4	95
4.1	Introduction	97
4.2	Design Challenges and Choices	98
4.3	DCU Operation Principle	100
4.4	System Implementation	100
4.4.1	Architecture	100
4.4.2	MOS Sizing	105
4.4.3	Gate capacitance sizing	106
4.4.4	Noise	107
4.5	Results	107
4.6	Conclusion	110
	Publications	111
	References	111

5	Chapter 5	113
5.1	Introduction	115
5.2	Enhancements to the Multi-Electrode	115
5.3	Advanced Non-Volatile Memory Technologies	117
5.3.1	Nanotube RAM (NRAM)	117
5.3.1.1	NRAM Application for Multi-Electrode Switching Unit	120
5.3.2	Resistive RAM family	122
5.3.1.1	Magnetic Tunnel Junction (MTJ)	122
5.3.1.2	Memristance	128
5.3.1.3	Memristance Behavioral Model	130
5.3.1.4	Adapting Memristance Cell for Cardiac Stimulation applications	132
5.2	Conventional Non-Volatile Memory Technology: Flash Memory	137
5.2.1	Theoretical background	137
5.2.2	Flash cell model	139
5.2.2.1	Program Sequence using Channel Hot Electron Method	139
5.2.2.2	ERASE Sequence using Fowler Nordheim Injection method	141
5.2.2.3	Observed Characteristics of the Flash Cell	142
5.2.2.4	Operation Window expansion to adapt with our application	142
5.2.2.5	Evolution of VT with QFG0 (simulation)	143
5.2.3	Non-Volatile Switching Unit Using Flash Memory Cell	144
4.3.1	Case 1: MOS Switch connects Cathode to Electrode	146
	Case 2: MOS Switch connects Anode to Electrode	148
5.2.4	Summary	151
5.3	Conclusion	153
	Publications	153
	References	154
6	Chapter 6	157
	List of Publications	161

List of Figures

Figure 0-1: système de conduction du cœur.....	21
Figure 0-2: (a) défibrillateur Implantable (b) Pacemaker Implantable	22
Figure 0-3: CRT pacemaker avec trios sondes de stimulation connectés au cœur	23
Figure 0-4: Illustration de système multi-électrodes avec ses deux unités de contrôle à l'intérieur de l'implant et la sonde (conforme aux normes)	26
Figure 0-5: schéma bloc de LEC.....	28
Figure 0-6: les phases différentes du protocole de communication	29
Figure 0-7: (a) une sonde de stimulation bipolaire simple, (b) une sonde multi-électrodes avec LEC, (c)) une sonde multi-électrodes avec DCU activée qui le transforme en une sonde bipolaire.....	32
Figure 0-8: schéma bloc de l'unité de contrôle la sonde avec le DCU	33
Figure 0-9: circuit du DCU	34
Figure 0-10: Microphotographie de la puce DCU.....	35
Figure 0-11: Remplacement de l'unité de commutation principal et l'unité de connexion par défaut par la nouvelle unité de commutation non-volatile à l'intérieur de l'unité de contrôle de la sonde (LEC)	37
Figure 2-2: Conduction system of the heart [5]	47
Figure 2-3: (a) implantable defibrillator (b) Implantable pacemaker [9]	50
Figure 2-4: block diagram of Dual chamber pacemaker [8]	51
Figure 2-5: simple circuit diagram for a stimulation channel	53
Figure 2-6: membrane potential during ventricular action potential.....	54
Figure 2-7: strength-duration curve.....	55
Figure 2-8: a) electrode-tissue interface b) interface equivalent circuit c) ideal and real stimulation pulse	56
Figure 2-9: sensing channel block diagram.....	57
Figure 2-10: Main phases of pacing cycle in a cardiac pacemaker.....	59
Figure 2-11: (a) endocardial leads [22] (b) Epicardial leads [23]	59
Figure 2-12: Illustration of unipolar stimulation/sensing.....	60
Figure 2-13: Illustration of bipolar stimulation/sensing.....	60
Figure 2-14: CRT pacemaker with three stimulation leads connected	61
Figure 3-1 : (a) illustration for the positions of bipolar leads in the different heart chambers, (b) multi-electrode lead replaces the bipolar left ventricular lead of figure (a)	68
Figure 3-2: Multi-electrode system components. The number of control lines equals the number of electrodes in the lead	69
Figure 3-3: Illustration of multi-electrode system with its two control units in the implant and inside the lead (norm compliant).....	70
Figure 3-4: Centralized structure for the multi-electrode system	72
Figure 3-5: Distributed structure for the multi-electrode system	73
Figure 3-6: Abstraction of the main parts of the system implementation	75
Figure 3-7: (a) phases of conventional pacing cycle (b) pacing cycle after the insertion of the multi-electrode preparation phase	76
Figure 3-8: block diagram of the LEC (centralized structure)	77
Figure 3-9: example for bidirectional communication between IEC and LEC.....	81
Figure 3-10: the different phases of the communication protocol	82
Figure 3-11: different types of bits that compose the configuration train.....	83
Figure 3-12: Example of error in estimation during calibration phase. (LEC; Lead-Electrode Controller)	85
Figure 3-13: Example of error in data decoding due to frequency difference	85

Figure 3-14: Biphasic stimulation pulses as an example of double stimulation mode	87
Figure 3-15: Block diagram of multi-electrode system (distributed structure).....	89
Figure 3-16: LEC chip microphotograph	90
Figure 3-17: Errors in decoding before and after the application of our communication protocol.....	91
Figure 3-18: signal on P&C line as observed during chip validation	91
Figure 4-1: (a) Simple bipolar stimulation lead, (b) Multi-electrode stimulation lead with an electrode-controller LEC, (c) Multi-electrode stimulation lead with the DCU activated resulting in a bipolar lead	97
Figure 4-2: Lead Electrode Controller blockdiagram including the DCU	99
Figure 4-3: DCU circuit	101
Figure 4-4: MAX-MIN generator circuit	102
Figure 4-5: circuit and symbol of S1 switch	103
Figure 4-6: Circuit and symbol of S2 switch	103
Figure 4-7: Simulation results of DCU in its active state	108
Figure 4-8: Simulation results of DCU in its inactive state	108
Figure 4-9: DCU chip microphotograph	109
Figure 5-1: Replacement of main switching unit and default connection unit by the new non-volatile switching unit inside the lead electrode-controller unit	116
Figure 5-2: single walled carbon nanotube [18].....	117
Figure 5-3: NRAM cell in erased state (left) Programmed state (right) [24].....	118
Figure 5-4: measured values for ON/OFF resistances (left), measured voltages and currents (right) [16]	119
Figure 5-5: An example for the non-volatile switching unit in the multi-electrode system ..	120
Figure 5-6: MTJ states [2]	122
Figure 5-7: FIMS cell (a) read phase (b) write phase [13]	123
Figure 5-8: toggle cell anatomy - SAF layers [17, 18].....	124
Figure 5-9: toggle sequence	125
Figure 5-10: STT structure [2]	126
Figure 5-11: Memristance model	128
Figure 5-12: Memristance Voltage and current curves	129
Figure 5-13: (a) memristance symbol (b) behavioral model circuit in LT Spice.....	130
Figure 5-14: (upper pane) input voltage sine wave of amplitude 1V and 0.5 Hz frequency against the measured current across the cell. (lower pane) the variation of state variable w with the input voltage	131
Figure 5-15: plot of voltage against current presented in the upper pane of fig. 5-14. The result is the double hysteresis curve.....	131
Figure 5-16: effect of increasing the full length D of the model on the double hysteresis curve (behavior)	132
Figure 5-17: recheck of model correct behavior at all the voltage range after increasing D to 28nm.....	133
Figure 5-18: model's resistance evolution with an applied positive ramp voltage signal.	133
Figure 5-19: model's resistance evolution with an applied negative ramp voltage signal. ...	134
Figure 5-20: Memristance model switching delay for different positive voltage applied across the cell	135
Figure 5-21: (upper pane) applied positive voltage pulse sequence and the memristance cell resistance is plotted. (lower pane) the measured current across the cell in the two directions. The missing part of the current waveform signifies a stable current value.....	136
Figure 5-22: Flash memory cell showing the structure of its floating gate transistor [20]	137
Figure 5-23: Programming window of flash cell [20].....	137

Figure 5-24: symbol for the generated flash cell - Program sequence	139
Figure 5-25: Program sequence waveforms for reference VerilogA Flash cell.....	140
Figure 5-26: Program sequence waveforms for the generated symbol of Flash cell	140
Figure 5-27: Symbol for the generated flash cell - Erase sequence	141
Figure 5-28: Erase sequence waveforms of reference VerilogA Flash cell	141
Figure 5-29: Erase sequence waveforms for the generated symbol of Flash cell	142
Figure 5-30: (a) default operation window of the flash cell model, (b) application adapted operation window of the model.....	143
Figure 5-31: Threshold voltage change with varying QFG0 @ $V_{tuv} = 1V$	144
Figure 5-32: concept schematic.....	145
Figure 5-33: Flash cell erased (ON) to block the connection between Cathode and Electrode1	146
Figure 5-34:Flash cell programmed (off)to enable the connection between Cathode and Electrode1.....	147
Figure 5-35: Flash cell is erased (ON) to enable the connection between Anode and Electrode1.....	148
Figure 5-36: Flash cell is programmed to block the connection between Anode and Electrode1	150
Figure 5-37: A. Electrode = Cathode, B. Electrode = Anode, C. Electrode = not connected 151	
Figure 5-38: example of complete system	152

List of Tables

Table 0-1: Charecterictiques de la puce	31
Table 2-1: normalized values for stimulation energy [11]	52
Table 2-2: parameters of stimulation channel	53
Table 3-1: Bipolar lead vs. Multi-electrode lead.....	69
Table 3-2: comparison of our solution with other multi-electrode systems found in patents..	88
Table 3-3: Chip Summary	90
Table 4-1: Operation modes	99
Table 4-2: example for MOS sizing	105
Table 4-3: example of capacitance sizing	106
Table 4-4: Chip Summary	107
Table 5-1: switching unit specification for cardiac stimulation	117
Table 5-2: NRAM features summary [19, 22]	119
Table 5-3: STT features.....	127
Table 5-4: Memristance model parameters [19]	132
Table 5-5: typical bias voltages for flash cell [23]	138
Table 5-6: Characteristics summary	142
Table 5-7: $QFG0 = 0$ and $V_T = 1V$	147
Table 5-8: $QFG0 = -8.5e-16$ and $VT = 9.07V$	148
Table 5-9: $QFG0 = 0$ and $VT = 1V$	149
Table 5-10: $QFG0 = -8.5e-16$ and $VT = 9.07V$	150

Résumé de la thèse en Français

Chapitre 1: Introduction

Au cours des dernières années, la qualité des soins s'est beaucoup améliorée. Grâce à la recherche dans le domaine de la santé, aux nouvelles découvertes technologiques, les êtres humains vivent non seulement plus longtemps, mais les thérapies suivies sont également de meilleure qualité ; elles réduisent les chances de progression des maladies et permettent leur diagnostic de manière plus précoce. Toutefois, il est important de noter que, malgré ces progrès, il est nécessaire de continuer les efforts de recherche afin de faire face à des pathologies telles que celles liées à des complications cardio-vasculaires qui affectent une grande partie de la population.

Dans plusieurs études, on estime que les maladies cardiovasculaires sont la cause principale de décès, en particulier dans les sociétés industrielles avancées. Aux États-Unis les maladies cardio-vasculaires sont la première cause de décès. Dans le monde entier, on estime à environ 40% le taux de décès résultant de complications cardiaques.

Dans cette thèse, nous nous pencherons sur les implants cardiaques utilisés dans le traitement cardio-vasculaire, en particulier les stimulateurs cardiaques et les défibrillateurs. Nous nous pencherons sur la description de base de ces appareils d'un point de vue électronique et nous allons également présenter leurs évolutions. En outre, nous présenterons nos résultats de recherche qui contribuent tant à l'amélioration de la fonctionnalité qu'à l'augmentation de l'efficacité de ces dispositifs en terme de volume, de performances et de consommation en puissance. Le plan de cette thèse est le suivant:

Au chapitre 2, nous présentons le fonctionnement de base du cœur, les maladies cardio-vasculaires importantes et les dispositifs utilisés pour gérer ces maladies. Nous détaillons l'évolution des implants cardiaques et de leurs composants de base. Par la suite, nous analysons en détail l'insuffisance cardiaque, une des maladies cardio-vasculaires les plus répandues. Par ailleurs, nous discutons de la stimulation bi-ventriculaire qui est le mécanisme utilisé pour gérer l'insuffisance cardiaque.

Au chapitre 3, nous présentons un système multi-électrodes pour résoudre le problème de la stimulation bi-ventriculaire. Nous présentons les défis de conception, la méthodologie de conception et les contraintes d'un tel système. Nous détaillons également les solutions existantes et leurs limites. Enfin, nous présentons les performances et les résultats du système qui a été conçu.

Au chapitre 4, nous détaillons la conception d'un bloc supplémentaire du système multi-électrodes que nous avons présenté dans le chapitre 3. L'ajout de ce bloc à notre sonde multi-électrodes permet de résoudre le problème de la compatibilité de notre système avec les stimulateurs cardiaques existants. Nous présentons en détail la méthodologie de conception, les contraintes et les performances de ce système.

Au chapitre 5, nous examinons les nouvelles technologies au-delà du CMOS standard, visant à rendre notre sonde multi-électrodes plus intelligente, plus petite et plus performante. Nous présentons plusieurs technologies candidates qui peuvent être utilisées dans notre système. Nous discutons de leurs points forts, leurs points faiblesses. Finalement, au travers de simulations nous démontrons la faisabilité de l'utilisation de certaines de ces technologies dans le cadre de l'application visée.

Les principales contributions de cette thèse sont les suivantes:

Conception et mise en œuvre d'un système multi-électrodes: Nous avons conçu et mis en œuvre un système multi-électrodes qui est capable de stimuler plusieurs sites dans la chambre cardiaque. Notre solution est entièrement configurable et répond aux contraintes de taille et de consommation en puissance imposée par la nature de notre application. Notre puce a été fabriquée en technologie 0,18 μm et occupe 2.25x5.35 mm². La puce, conforme aux normes en vigueur dans le domaine médical, dispose également d'un protocole de communication dédié. Il permet un fonctionnement à faible puissance et permet une configuration rapide. A notre connaissance, notre étude est la première publiée dans son genre.

Conception et mise en œuvre de l'unité de connexion par défaut: Nous avons implémenté une unité de connexion par défaut pour la puce multi-électrodes qui a permis l'exploitation de notre sonde multi-électrodes par des stimulateurs cardiaques qui ne sont pas conçus spécifiquement pour le contrôle de cette dernière. La solution élargit donc la compatibilité de notre sonde à tous les stimulateurs cardiaques du marché. Dans ce chapitre, nous discutons et nous apportons des solutions aux principaux défis liés à un environnement très contraignant comme celui du cœur humain. Cette unité a été fabriquée en technologie 0,18 μm , elle occupe 2,2 x 1,75 mm² de surface. Cette unité est capable de récupérer l'énergie nécessaire de son fonctionnement depuis l'énergie de stimulation envoyée au cœur.

Preuve de faisabilité de l'intégration des technologies de mémoire non volatile dans le système multi-électrodes: De nouvelles technologies ont été explorées qui améliorent

considérablement les performances du système multi-électrodes. L'emploi de ces technologies a amélioré notre système en éliminant le besoin de configuration répétitive des électrodes, économisant ainsi la consommation en puissance et réduisant la latence. Des avantages supplémentaires ont été obtenus au niveau de la taille de la puce et sa compatibilité avec tout autre stimulateur sur le marché. Nous avons exploré plusieurs technologies non volatiles, comme les NRAM, MRAM, Memristance et Flash. Grâce aux simulations, nous avons prouvé la faisabilité de ces technologies pour nos applications. Nous croyons que ces technologies seront utilisées pour concevoir la prochaine génération des sondes à faible puissance et haute performance.

Chapitre 2: Les Implants de Stimulation Cardiaque

Dans ce chapitre, on parle d'abord du fonctionnement de base du cœur et les dysfonctionnements possibles du système cardiovasculaire. Puis on parlera de l'évolution des implants cardiaques utilisés dans le traitement de ces dysfonctionnement ou maladies.

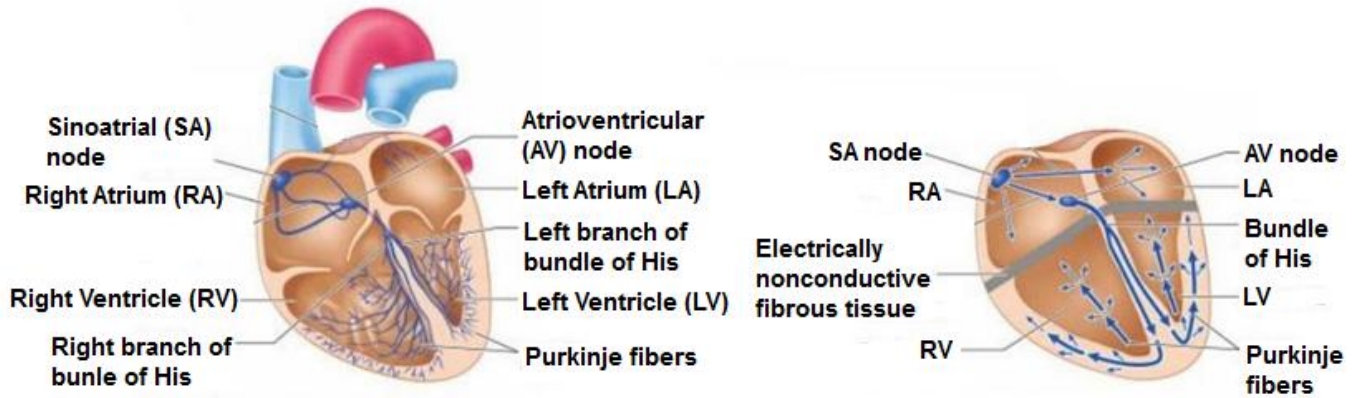


Figure 0-1: système de conduction du cœur

Le cœur humain et l'évolution de l'implant cardiaque

Le cœur est composé de quatre cavités, deux cavités reçoivent le sang désoxygéné de différentes parties du corps, et deux cavités pompent le sang oxygéné de nouveau pour les parties du corps. Si jamais la quantité de sang pompé par le cœur est diminuée pour une raison quelconque, cela pourrait provoquer une perte de connaissance ou même la mort (l'insuffisance cardiaque).

Le fonctionnement du cœur est maintenu par un système de conduction électrique très complexe. Toute activité électrique dans un cœur normal est initiée par le nœud sino-auriculaire connu comme le pacemaker naturel du cœur. L'impulsion électrique se propage dans le système de conduction du cœur comme illustré dans la figure 0-1. Toute perturbation dans ce système de conduction conduit à une condition pathologique critique connue sous le nom d'arythmie.

Les implants cardiaques de nos jours offrent le traitement requis pour beaucoup de maladies comme l'insuffisance cardiaque et la protection contre les situations potentiellement mortelles comme les arythmies.

Le premier pacemaker implantable stimulait le cœur avec des impulsions électriques d'une largeur et d'amplitude fixes à une fréquence fixée à 60 battements par minute. Ensuite, un nouveau concept a été introduit par l'arrivée de ce qu'on appelle « On Demand Pacemaker » où l'activité du cœur est

détectée grâce à un simple capteur dans le pacemaker et en fonction de cela, la stimulation adéquate est générée. Cette nouveauté a contourné les inconvénients de la stimulation à fréquence fixe.

Avec la recherche permanente dans l'optimisation de la stimulation cardiaque en fonction des besoins du patient, une étape supplémentaire a été franchie au-delà de la simple détection de l'activité électrique du cœur du patient. Dans les années 1980, des capteurs plus intelligents ont été incorporés dans le stimulateur cardiaque pour mesurer certains paramètres relatifs à l'activité physique du patient tels que le mouvement du corps, la respiration et la pression artérielle

Système de stimulation cardiaque implantable

Les implants cardiaques sous ses deux déclinaisons – pacemaker ou défibrillateur - se composent d'un générateur d'impulsion électrique implanté sous la peau de la poitrine. Ce générateur est branché au cœur au moyen d'une sonde électriquement isolée de l'extérieur et insérée puis fixée à l'intérieur de cœur (figure 0-2). Les sondes de stimulation sont équipées à leur extrémité par des électrodes pour faire l'interface électrique avec les tissus cardiaques.

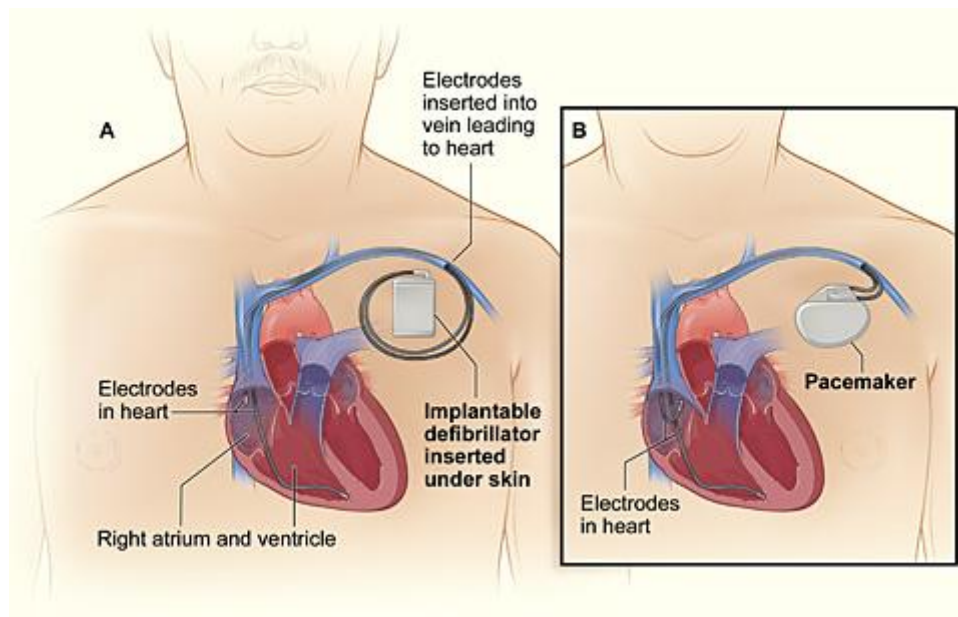


Figure 0-2: (a) défibrillateur Implantable (b) Pacemaker Implantable

Le nombre de sondes à insérer dans le cœur varie en fonction du nombre des cavités du cœur à stimuler selon l'état du patient et la décision de son médecin. Soit une cavité (l'oreillette droite RA), soit deux cavités (l'oreillette droite RA et le ventricule droit RV) ou au maximum trois cavités en ajoutant le ventricule gauche LV comme dans le cas de la thérapie de resynchronisation cardiaque (CRT).

Thérapie de resynchronisation cardiaque (CRT)

La contraction ventriculaire non synchronisée est l'un des principaux symptômes de l'insuffisance cardiaque. Les dispositifs de CRT traitent ce problème par la stimulation de deux ventricles RV et LV simultanément afin de resynchroniser leurs contractions.

Comme illustré dans la figure 0.3, les sondes de l'oreillette droite RA et le ventricule droit RV sont insérées et fixées à l'intérieur de ces cavités. Contrairement au cas du ventricule gauche, où la sonde doit être fixée à l'extérieur de la cavité. La sonde est insérée à travers une des veines ventriculaires au voisinage de la paroi externe du ventricule gauche (paroi libre). Une fois la paroi libre du ventricule gauche atteinte, une position stable de la sonde doit être obtenue avec la meilleure réponse cardiaque à la stimulation.

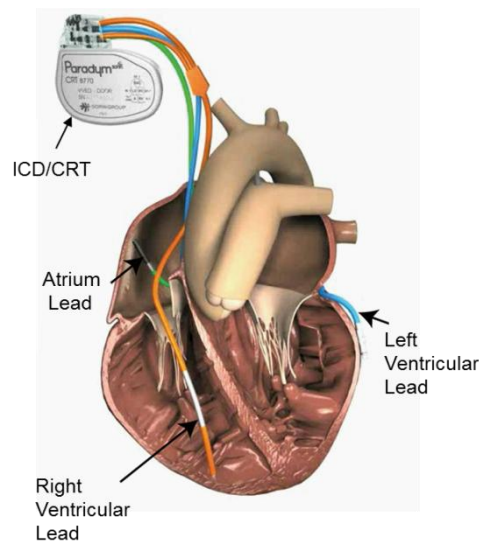


Figure 0-3: CRT pacemaker avec trios sondes de stimulation connectés au cœur

En plus de cette procédure compliquée, une stimulation ventriculaire gauche connaît un certain nombre de difficultés telles que:

- La stimulation du nerf phrénique souvent provoquée par la stimulation du ventricule gauche qui génère des effets indésirables chez le patient comme le hoquet et les crampes abdominales. Un moyen d'éviter cela est de placer la sonde dans une autre veine. Si cela n'est pas possible, certaines études ont montré que cela peut être évité en changeant la distance inter-électrode dans la sonde
- Le choix limité du site de stimulation pour le médecin face à la diminution de diamètre de la veine qui l'oblige à fixer le conducteur à un certain point et choisir le meilleur site de

stimulation disponible. L'emploi d'un nombre limité d'électrodes à l'intérieur de la sonde bipolaire limite encore davantage ce choix dans les veines du ventricule gauche

- le déplacement de la sonde qui peut causer une inhibition de la réponse cardiaque à la stimulation. Dans ce cas, une autre intervention chirurgicale semblable à la première est nécessaire afin de repositionner la sonde ventriculaire gauche.

Ce type de complications est inévitable à cause des sondes bipolaires ordinaires qui ne proposent pas une solution non-invasive. Pour cela nous présenterons dans le prochain chapitre le processus de conception d'un système multi-électrodes de stimulation qui pallie les limites de la stimulation ventriculaire gauche.

Chapitre 3: Système Multi-Electrodes Pour La Stimulation Ventriculaire Gauche: Conception et Mise en Œuvre

Ce chapitre présente un système multi-électrodes pour faire face aux limitations de la stimulation du ventricule gauche. Dans ce chapitre, nous allons montrer comment le système multi-électrodes offre aux médecins une plus grande souplesse dans le choix du meilleur site de stimulation pour leurs patients, ce qui permet une meilleure gestion de la stimulation du nerf phrénique. En outre, nous verrons aussi que le système de multi-électrodes réduit considérablement la probabilité des interventions chirurgicales qui est nécessaire pour repositionner la sonde en cas de déplacement de cette dernière. Ainsi, la sonde multi-électrodes permet un meilleur traitement et une meilleure gestion des maladies cardiaques.

Système Multi-Electrode : Principe & Contraintes

La figure 0-4 montre le système multi-électrodes et ses composants. Similaire aux systèmes classiques de stimulation cardiaque, le système multi-électrodes est composé d'un implant (pacemaker), une sonde multi-électrodes et des électrodes. En raison de la multiplicité des électrodes destinées à être activées sélectivement, un contrôleur d'électrode est nécessaire pour définir l'activité et la polarité de chaque électrode individuellement dans la sonde.

Comme tout système, notre système multi-électrodes avait ses contraintes qui nous ont poussé de trouver des solutions de contournement en phase de conception. La première contrainte était comment contrôler l'ensemble des électrodes (plus que 3 électrodes) dans la sonde tout en respectant les normes qui limitent le nombre de fils qui traversent le connecteur de l'implant à 2 ou 3 fils. Nous avons fait un choix de conception de distribuer le contrôleur des électrodes sur deux parties. La première réside dans l'implant même (Implant Electrode Controller - IEC), et la deuxième est transférée de l'implant à la sonde (Lead Electrode Controller - LEC) comme c'est illustré dans la figure 0-4. De cette façon le nombre de fils qui traversent le connecteur est de 2 ou 3 (conforme à la norme) et chaque électrode a son fil de contrôle. IEC et LEC communiquent mutuellement via 2 à 3 fils de contrôle.

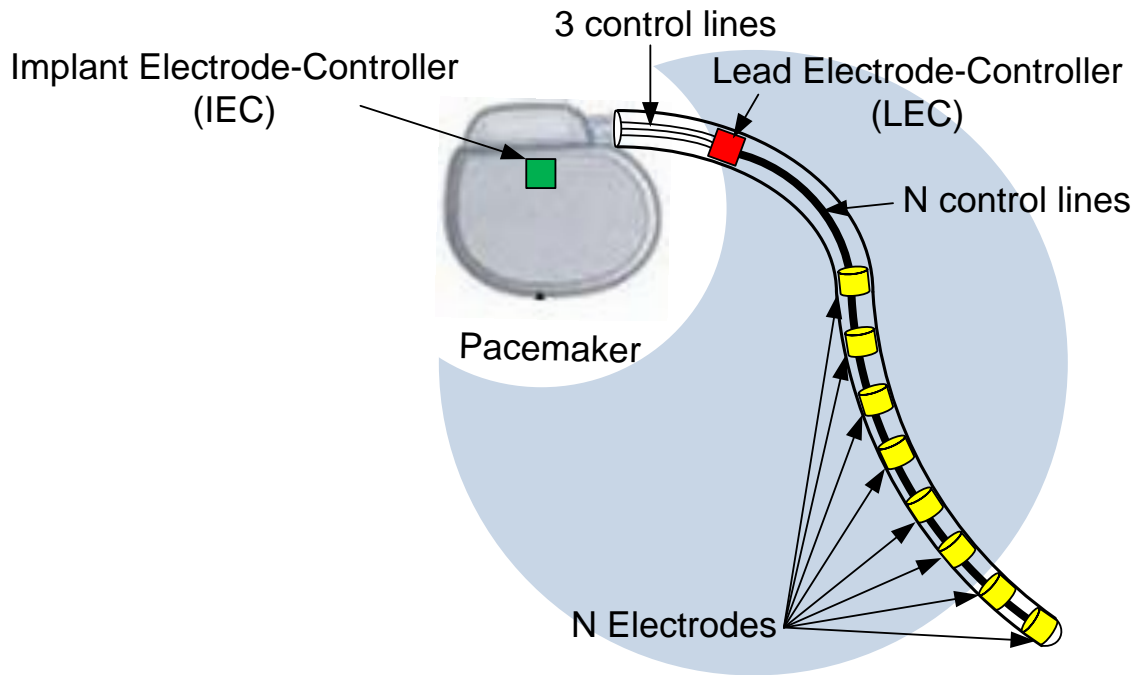


Figure 0-4: Illustration de système multi-électrodes avec ses deux unités de contrôle à l'intérieur de l'implant et la sonde (conforme aux normes)

Ayant choisi d'utiliser un contrôleur d'électrodes séparé à l'intérieur de la sonde, nous avons été confrontés au défi évident de son alimentation. La taille du LEC à l'intérieur de la sonde doit être très petite qui exclut l'utilisation d'une batterie comme source d'alimentation possible. Nous avons donc choisi d'alimenter ce LEC par le stimulateur via un fil dédié.

Puisque le IEC dans l'implant doit contrôler le LEC pour configurer/gérer les électrodes, un protocole de communication est nécessaire entre eux. Par ailleurs, afin de minimiser le nombre de fils, nous avons choisi de réutiliser le même fil que nous avons utilisé pour l'alimentation. Le protocole de communication adopté pour notre système sera discuté en détail dans ce chapitre.

Conception et implémentation du système

Nous avons fait le choix d'utiliser une interface à 3 fils entre le connecteur et le stimulateur LEC. 2 fils (anode et cathode) sont utilisés exclusivement pour la stimulation et l'acquisition de signaux cardiaques. La troisième ligne est dédiée au protocole de communication entre le stimulateur cardiaque (maître) et le LEC (esclave). Ce protocole de communication porte l'alimentation et les bits de configuration nécessaires pour la fonctionnalité du LEC. L'avantage de cette méthode est que ni les impulsions d'alimentation ni les données ne sont mélangées avec les lignes de stimulation.

Par ailleurs, nous nous sommes engagés à assurer la compatibilité de notre sonde multi-électrodes avec tous les stimulateurs du marché. Nous l'avons pris en compte en mettant en place une unité de commutation auxiliaire dans le LEC dont le rôle est de garder un lien actif entre le stimulateur cardiaque et le cœur du patient par au moins deux électrodes sans aucune consommation d'énergie. Cette unité auxiliaire permet également d'obtenir une faible consommation d'énergie pour l'ensemble du système.

Nous avons également inclus une fonction supplémentaire appelée stimulation double. Elle permet d'appliquer deux impulsions de stimulation consécutives. La première et la deuxième stimulation peuvent être soit appliquées sur la même configuration d'électrodes ou sur deux configurations différentes. Cette fonction ouvre une voie de recherche clinique qui peut démontrer son utilité dans l'amélioration de la stimulation cardiaque.

Une unité de contrôle à l'intérieur d'un implant classique (pacemaker) gère la séquence d'actions et d'événements au sein du cycle de stimulation. Ce cycle de stimulation se compose de trois phases: la détection, la stimulation et la décharge

- Lors de la phase de détection, la chaîne de détection d'un pacemaker filtre et analyse les signaux cardiaques acquis pour détecter des troubles de l'activité cardiaque du patient.
- En cas de trouble cardiaque détecté, une demande de stimulation est générée qui déclenche le circuit de sortie pour démarrer la phase de stimulation et de fournir une impulsion électrique au cœur sur les électrodes configurées.
- Ensuite la phase de décharge élimine les charges résiduelles provenant de l'interface électrode-tissu et le chemin de la stimulation/détection.

Dans notre système multi-électrodes, une phase supplémentaire a été insérée entre la demande de stimulation et sa livraison. Cette phase de préparation a pour mission de fournir à la LEC dans la sonde l'alimentation nécessaire et les bits de configuration des électrodes.

Nous avons conçu la LEC, sous la forme d'un ASIC (Application-Specific Integrated Circuit) pour être inséré à l'intérieur de la sonde, comme illustré dans la figure 0-5 où nous présentons les blocs principaux de la puce LEC.

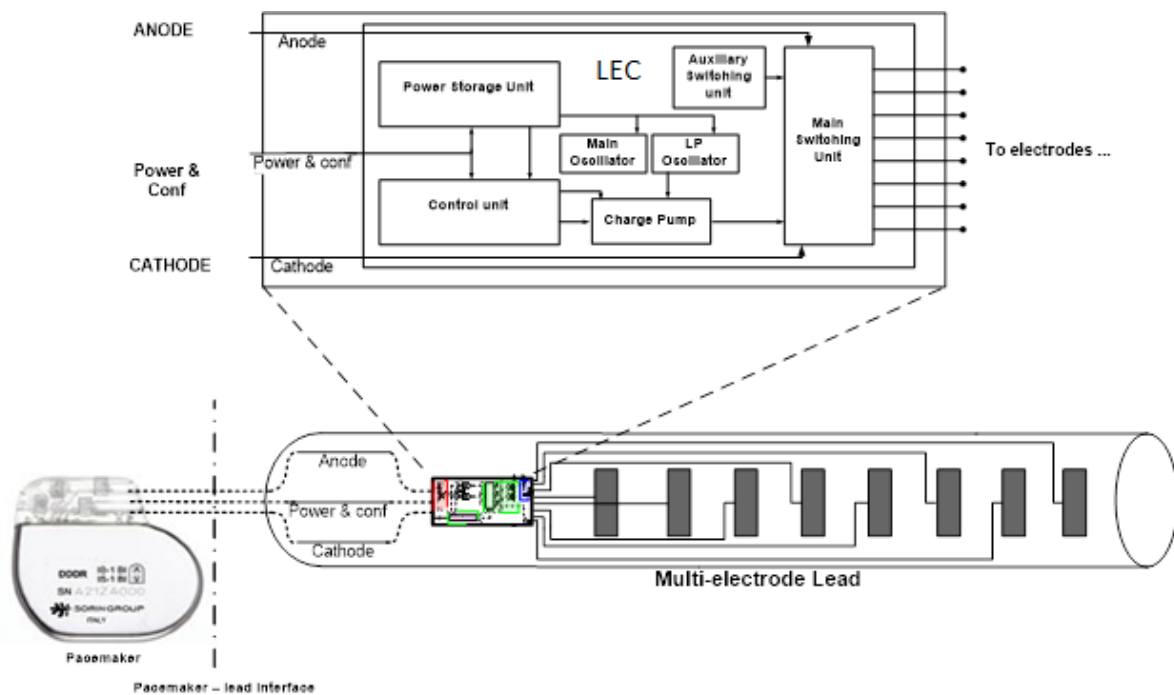


Figure 0-5: schéma bloc de LEC

L'unité de stockage d'énergie est la seule source d'énergie pour le LEC qui assure sa fonctionnalité pendant un cycle cardiaque complet. Les impulsions d'alimentation envoyées par l'implant sont stockées dans un condensateur dans le LEC. Un condensateur avec une taille considérable serait nécessaire pour maintenir l'énergie suffisante pour le circuit de la puce. Grâce au protocole mis en place, plusieurs impulsions de puissance sont prévues pour permettre la réduction de la taille de la capacité de stockage et de la recharger régulièrement.

L'unité de contrôle est la logique dans laquelle le protocole de communication est mis en œuvre. Le rôle premier de cette unité est de faire la différence entre les impulsions électriques et les bits de configuration. Elle achemine les impulsions électriques à l'unité de stockage d'énergie, et s'appuie sur des oscillateurs locaux pour décoder les bits de configuration. En outre, l'unité de contrôle active les deux unités de commutation ; principale et auxiliaire à des moments précis selon les données de configuration décodées qui indiquent l'état souhaité et la polarité de chaque électrode dans la sonde

L'unité de commutation principale définit le chemin de la stimulation du stimulateur cardiaque au cœur, elle est composée principalement des commutateurs MOS haute tension afin de supporter des tensions élevées (dizaines de volts) et des courants élevés (des dizaines de mA) de stimulation fournies au cœur.

Le chemin entre le stimulateur et les électrodes configurées doit être maintenu en gardant les commutateurs MOS configurés actif. L'unité de contrôle maintient cette stimulation pendant les phases de décharge. Pendant la phase de détection, l'unité de commutation auxiliaire prend en charge ce rôle pour transmettre les signaux cardiaques au stimulateur.

L'unité de commutation auxiliaire est activée dans le LEC lorsque le niveau d'alimentation diminue. Cette unité est capable de maintenir la connexion entre les électrodes et le stimulateur cardiaque, sans aucune alimentation électrique. Dans une première mise en œuvre, nous avons utilisé des interrupteurs JFET. Ils sont normalement actifs, tandis que pour les déconnecter une alimentation est nécessaire pour forcer l'état inactif. C'est le cas pendant la phase de détection. Il est difficile d'estimer une durée fixe pour cette phase, afin de dimensionner le condensateur de stockage.

Un autre avantage de l'utilisation d'une telle unité de commutation auxiliaire est d'assurer une compatibilité avec n'importe quel stimulateur du marché. Le fait que cette unité est connectée sans source d'énergie, elle assure une connexion minimale dans la sonde multi-électrodes afin d'agir comme une sonde bipolaire simple. Cette connexion est indépendante de tout protocole de communication spécifique qui peut exister dans n'importe quel système multi-électrodes. C'est un atout supplémentaire pour notre système par rapport aux autres solutions multi-électrodes.

Protocole de Communication

Dans notre mise en œuvre de ce test-chip, nous avons implémenté un protocole de communication unidirectionnel (IEC-> LEC) et nous avons choisi la fréquence d'horloge de l'implant à 1MHz. Cela a ajouté un autre défi pour l'LEC de décoder correctement la configuration envoyée en un seul coup, car il ne sera pas renvoyé d'IEC.

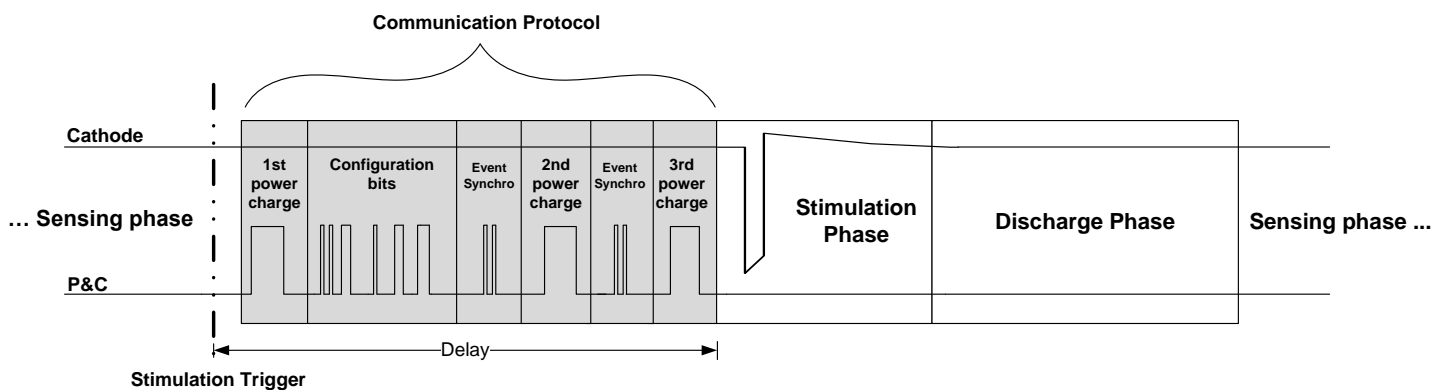


Figure 0-6: les phases différentes du protocole de communication

- Impulsions d'Alimentation:

Les phases de recharge ont été placées avant chaque activité consommant de l'énergie prévue pour les circuits de LEC. En plus du réveil (Wake-Up) du LEC, cette première phase assure qu'il y a suffisamment d'énergie pour la phase de configuration. La dernière phase d'alimentation est placée juste avant la phase de stimulation pour faire en sorte que l'unité de commutation a une énergie suffisante pour maintenir l'état des électrodes configurées lors de la phase de stimulation et la phase de décharge qui intervient juste après.

- Bits de synchronisation d'événements

Ils sont insérés avant les actions à effectuées par le LEC à un moment précis. En outre, ces bits de synchronisation d'événement aident l'unité de contrôle du LEC à différencier entre les bits de communication et les impulsions d'alimentation

- Bits de configuration

Ils transportent les informations de l'activité et de la polarité de chaque électrode dans la sonde multi-électrodes. Cette information est nommée ici "bits de données". D'autres types de bits tels que "calibration" et "sync" complètent la structure des bits de configuration.

Le décodage de données est basé sur le comptage des cycles d'horloge par bit pour l'acquisition de sa valeur à son milieu. En raison du déphasage entre l'oscillateur du LEC et celui du stimulateur cardiaque qui pourrait à tort estimer le nombre de bits côté LEC, nous mettons en place trois mécanismes:

- Calibration: ce mécanisme évalue le nombre de cycles d'horloge qui composent un bit en fonction de l'oscillateur du LEC.
- Synchronisation des données: dans une trame, un bit de synchronisation est ajouté après chaque 4 bits de données. Cela nous aide à éviter la propagation des erreurs dans la trame. Cette approche est similaire à la communication de données asynchrones « start-stop » utilisées dans la synchronisation de caractère en ASCII.
- Synchronisation de trame : chaque trame est décalée dans le temps de façon à être synchronisé avec l'horloge LEC. Cela garantit que le décodeur compte correctement la longueur de chaque bit uniquement sur la base de cycles d'horloge complets. (En nombre de cycles d'horloge).

Résultat de Mesure

La puce LEC a été fabriquée en technologie 0.18 μ m. Cette technologie est adaptée pour la haute tension présente dans l'impulsion de stimulation. Le Tableau 0-1 résume les caractéristiques de la puce.

Table 0-1: Charecterictiques de la puce

Technologie	0.18 μ m
Surface	2.25x5.35 mm ²
Courant moyenne consommee par cycle cardiaque	206.3 nA
Temps pour la configuration	2 ms
Frequence d'horloge	1 MHz
La tension d'operation	1.8V
La tolerance sur la frequence d'horloge	-20% to 40%

Notre protocole de communication mis en œuvre tolère une différence de fréquence de l'oscillateur, que ce soit dans le sens croissant ou décroissant, grâce à la phase d'étalonnage et les calculs ci-joints qui ont permis d'affiner l'estimation de la longueur de bit. L'échelle de fréquence tolérée a été observée entre de - 20% à +40% tel que ça apparaît dans le tableau.

Chapitre 4: Unité de Connexion Par Défaut

Le système multi-électrodes nécessite la présence de contrôleurs compatibles entre eux dans la sonde et le stimulateur cardiaque (le LEC et IEC). Dans le chapitre précédent, nous avons décrit notre propre implémentation de ces deux contrôleurs, mais dans le monde réel, des situations peuvent surgir qui limitent le fonctionnement d'une telle solution. Une situation, qui se produit fréquemment, est le remplacement du stimulateur cardiaque en raison de l'épuisement de la batterie, ou un dysfonctionnement général du stimulateur cardiaque. Les médecins souvent remplacent les stimulateurs cardiaques implantés par modèle récent.

Toutefois, étant donné que la mise en œuvre de système multi-électrodes est propre à nous, la sonde multi-électrodes ne peut pas être utilisée avec un nouveau stimulateur cardiaque qui n'est pas explicitement conçu pour contrôler le LEC dans la sonde. C'est pourquoi la compatibilité de la sonde est cruciale.

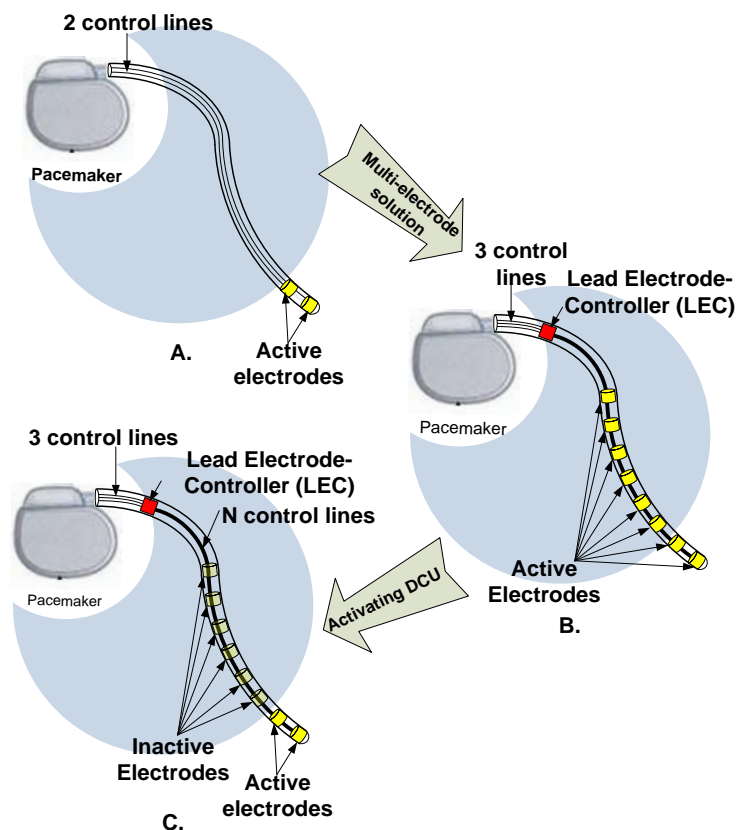


Figure 0-7: (a) une sonde de stimulation bipolaire simple, (b) une sonde multi-électrodes avec LEC, (c)) une sonde multi-électrodes avec DCU activée qui le transforme en une sonde bipolaire

Dans ce chapitre, nous présentons une solution pour résoudre le problème de compatibilité de la sonde en ajoutant une structure de commutation au LEC existant. Cette structure de commutation,

appelée DCU (Unité de connexion par défaut), permet à la sonde multi-électrodes de fonctionner comme une sonde bipolaire standard (fig. 0-7c) sans avoir besoin de configuration supplémentaire ou d'alimentation. Le DCU est conçu pour être autonome et indépendant de tout protocole de communication entre un stimulateur cardiaque et son contrôleur dans la sonde.

Notre structure DCU peut être adaptée à n'importe quel procédé technologique, car elle est basée sur des transistors MOS ordinaires et présente donc une solution versatile. Les solutions existantes étaient basées sur des composants discrets et donc n'étaient pas viables en raison de contraintes de taille de la puce LEC.

Les choix et défis de conception

Malgré le fait que le DCU est intégré à l'intérieur du LEC, ils fonctionnent alternativement. Puisque la ligne P&C est également utilisée pour la communication en dehors de l'alimentation, un protocole spécifique a dû être mis au point à cet effet. En outre, comme le DCU est actif lorsque le LEC est inactif, il rend le DCU transparent vis à vis du protocole de communication entre le LEC et le stimulateur. Par conséquent, la ligne P&C ne peut pas être utilisée pour fournir l'énergie nécessaire au DCU comme c'est le cas avec le LEC. Par conséquent, *le DCU a été conçu pour utiliser directement l'énergie disponible sur l'Anode et la Cathode.*

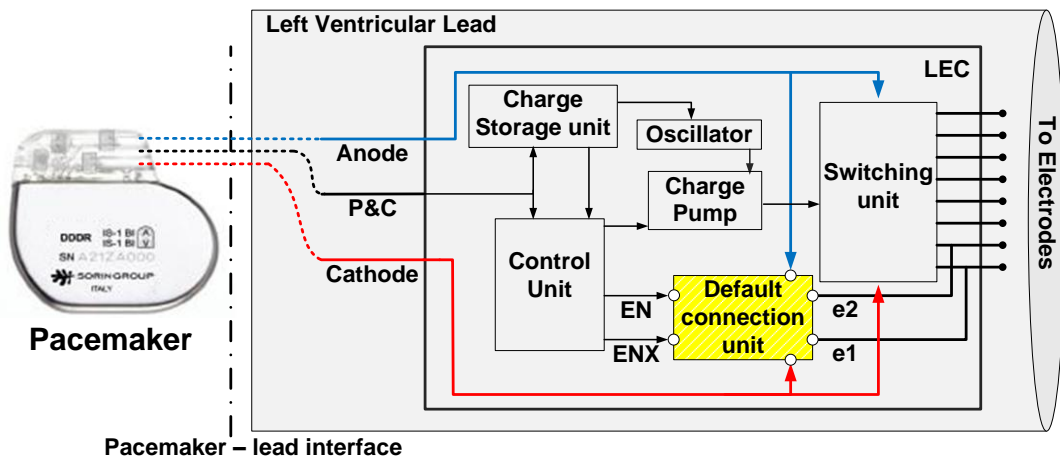


Figure 0-8: schéma bloc de l'unité de contrôle la sonde avec le DCU

Entre l'Anode et Cathode, la source d'énergie est disponible uniquement pendant la phase de stimulation, qui dure au maximum 1 ms, tandis que le DCU doit fonctionner pendant quelques secondes, voire quelques minutes en fonction de la durée des phases de décharge et de détection. Le DCU a été conçu pour utiliser cette source d'énergie limitée et fonctionner de manière fiable pour l'ensemble du cycle de stimulation.

Le Principe de l'opération du DCU

Le DCU fonctionne dans le mode par défaut lorsque le LEC est inactif. Il a quatre entrées (anode, cathode, FR et ENX) et deux sorties (E1 et E2) comme illustré dans la figure 0-9. EN & ENX sont des signaux de commande générés par l'unité de contrôle du LEC afin d'activer/désactiver le DCU. Les sorties E1 et E2 sont connectées à deux des électrodes de la sonde multi-électrode. Ces deux électrodes sont nommées ci-après électrodes par défaut. Celles sont partagées entre l'unité de commutation du LEC et le DCU. Notez que lorsque le DCU est actif, il prend le contrôle total des électrodes par défaut (LEC est inactif).

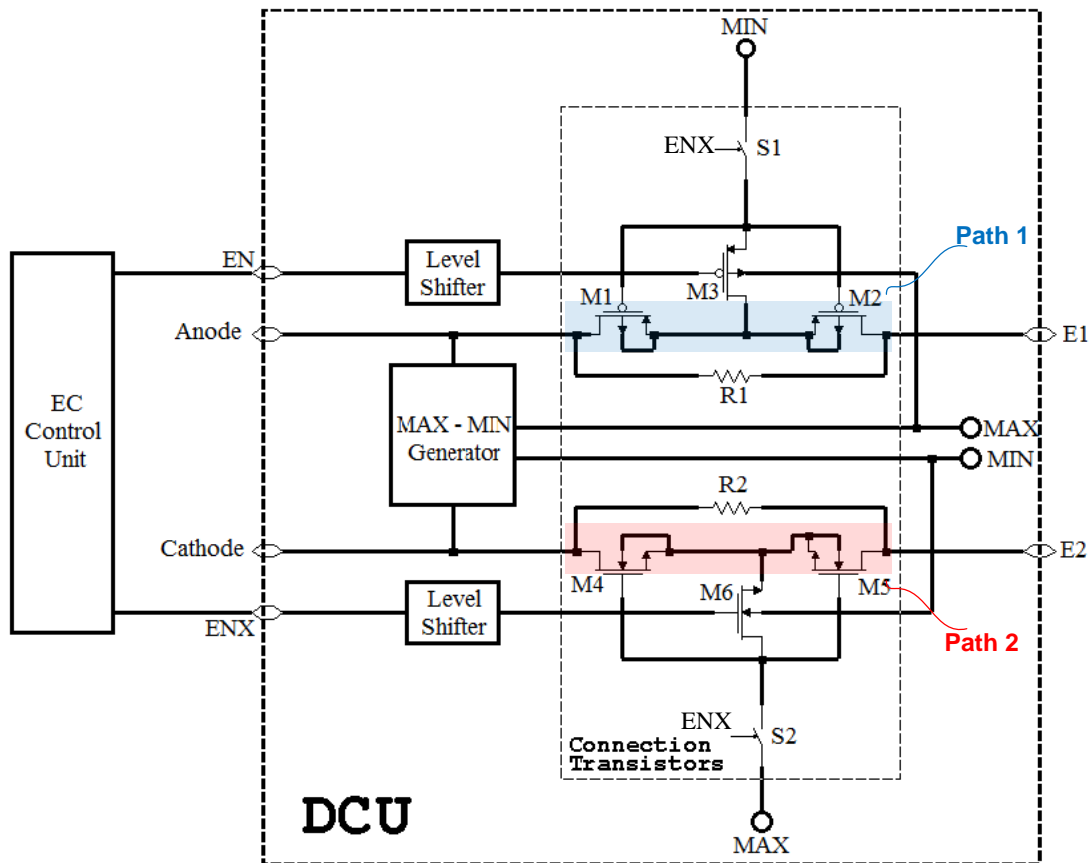


Figure 0-9: circuit du DCU

Le DCU lorsqu'il est activé crée deux connexions entre ses entrées et ses sorties. Une connexion entre l'anode et E1 et l'autre entre la cathode et E2. Ces connexions sont marquées (fig. 0-9) comme «Path1" et "Path2". Les deux chemins doivent être maintenus pendant les trois phases du cycle de stimulation décrit précédemment. Lorsque le DCU est désactivé, il doit couper les connexions des deux chemins «Path1" et "Path2".

Résultats

La puce DCU a été fabriquée en technologie 0,18 μm . la microphotographie de la puce est montré dans la Fig. 0-10. Afin de faciliter la validation de la puce en dehors de l'unité d'électrode-contrôleur, nous avons dupliqué les cellules Anode et Cathode (cellules Path1 et Path2 de la fig.0-9) dans leurs états actif et inactif. Ainsi il suffit d'appliquer une impulsion de stimulation entre anode et cathode, puis observer l'état des deux électrodes de chaque cellule.

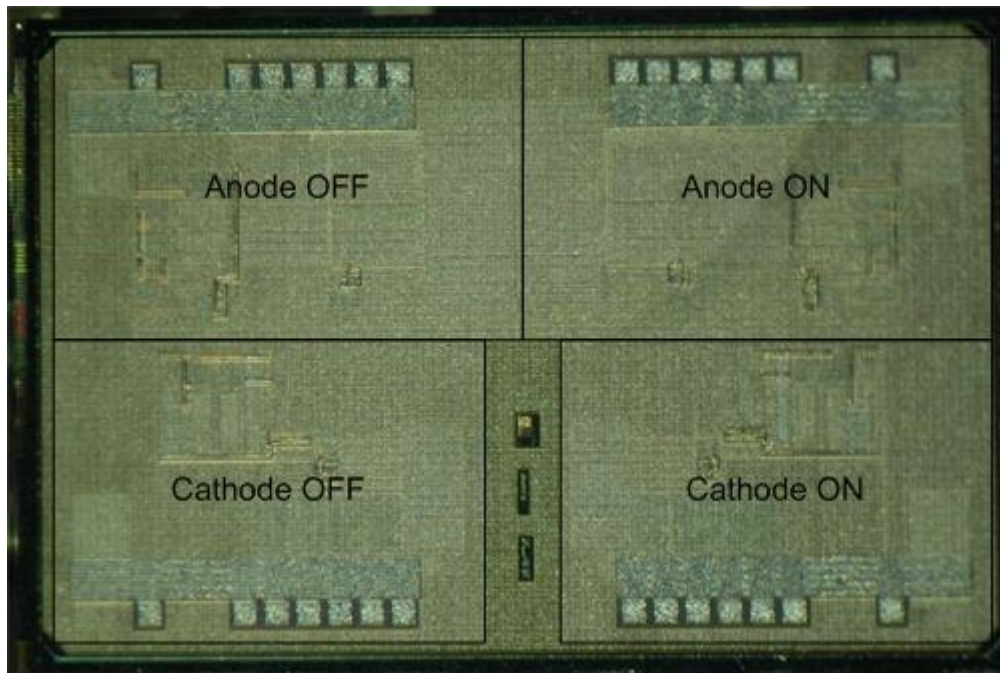


Figure 0-10: Microphotographie de la puce DCU

Le DCU distingue notre système multi-électrodes et constitue une avancée par rapport à l'unité de commutation auxiliaire présentée au chapitre 3 car il est intégré dans le processus de la technologie utilisée dans la puce de LEC.

Chapitre 5 : L'Amélioration de la Sonde Multi-Electrode en Utilisant La Technologie des Mémoires Non-Volatiles

Dans le chapitre 3, nous avons présenté un système multi-électrodes capable de la stimuler sur plusieurs sites. Nous avons également présenté les défis et les contraintes de conception d'un tel système. Dans le chapitre 4, nous avons fait progresser notre contribution en ajoutant à la sonde multi-électrodes une unité de connexion par défaut (DCU), qui permet la compatibilité de notre sonde multi-électrodes avec tout autre stimulateur cardiaque qui n'est pas spécifiquement conçu pour le contrôler. Cependant, alors que la solution DCU résout le problème de compatibilité, il le fait en restreignant la sonde multi-électrodes en la transformant en sonde bipolaire standard. Cette approche non seulement réduit l'avantage fonctionnel d'une sonde multi-électrodes, mais limite également l'avantage thérapeutique d'une telle solution.

Dans ce chapitre, nous nous appuyons sur l'expérience acquise pour pallier à ces limitations. Nous allons explorer les technologies qui peuvent améliorer la sonde multi-électrodes tout en gardant toutes ses caractéristiques fonctionnelles, et améliorer davantage et de façon radicale la consommation énergétique et la taille. En outre, la solution présentée permettra également à la sonde d'intégrer la fonctionnalité DCU, garantissant ainsi l'absence de tout problème de compatibilité. Pour ce faire nous allons tirer parti de nouvelles technologies qui vont au-delà des frontières du CMOS standard.

Nous explorons les technologies qui nous offrent la possibilité de la mémorisation d'une configuration donnée en l'absence d'alimentation: les mémoires non volatiles peuvent être intégrées dans l'unité de contrôle de la sonde (LEC) pour remplacer complètement l'unité de commutation principal et l'unité de connexion par défaut par une nouvelle unité de commutation non volatile comme c'est illustre la figure 0-11.

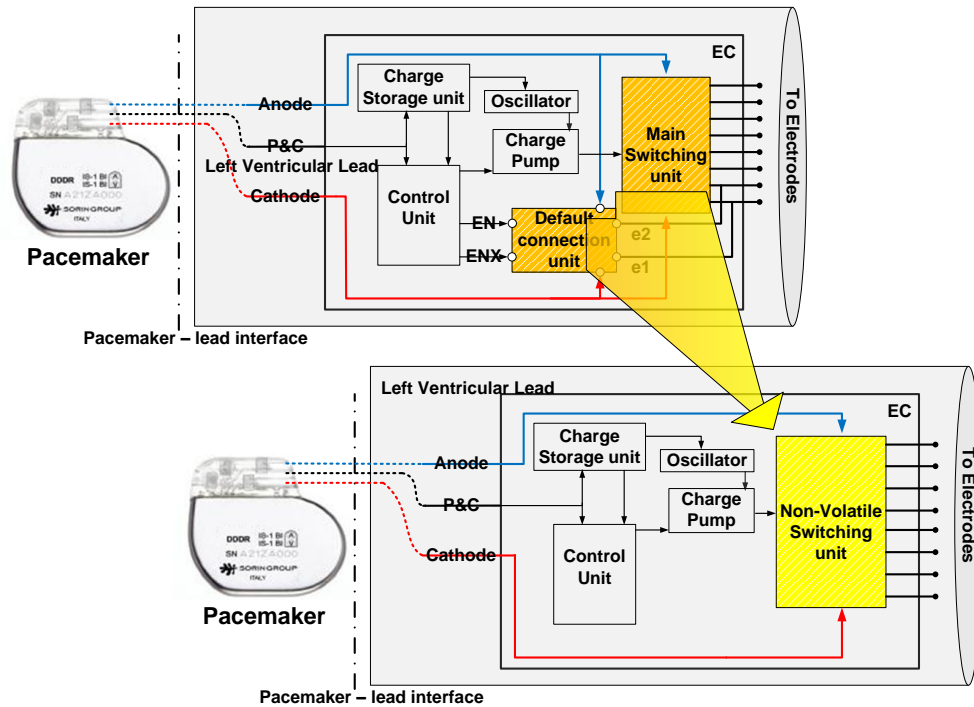


Figure 0-11: Remplacement de l'unité de commutation principal et l'unité de connexion par défaut par la nouvelle unité de commutation non-volatile à l'intérieur de l'unité de contrôle de la sonde (LEC)

Notez que conserver le dernier état configuré du système multi-électrodes nous permettra d'éviter la répétition de la reprogrammation du système. Cela permettrait non seulement une réduction de la consommation en énergie (un objectif clé de la conception), mais aussi d'éliminer la latence (due à la programmation) et en plus le remplacement du stimulateur ne conduirait pas à des problèmes d'incompatibilité. Ainsi, la mémorisation d'état nous conduirait à une solution gagnant-gagnant, où nous adressons tous nos défis de conception et de compatibilité.

Dans les sections 5.3 et 5.4 nous avons détaillé l'état de l'art des technologies non volatiles et nous avons présenté des résultats de simulation ainsi que l'étude de faisabilité en vue de son intégration au sein de notre système. Voici le résumé de toutes ces directions:

- Nous avons vu à quel point une technologie électromécanique à base de nanotubes de carbone comme les NRAM peut être prometteuse pour notre application. Ses états stables de commutation, la très grande variation des résistances à l'état passant et bloqué; sa vitesse et sa petite taille en font d'elle la candidate idéale pour notre application.
- STT MTJ et Memristance ont été regroupées sous la famille RAM résistive pour leurs caractéristiques communes du point de vue applicatif. Après nos investigations, nous sommes parvenus à la conclusion que leur intégration dans notre système n'est pas faisable en raison de leur instabilité face à des tensions et des courants importants de stimulation.

- Finalement, nous avons étudié les cellules de mémoire flash et nous avons proposé une nouvelle structure où les cellules flash sont associées à des transistors MOS pour faire des commutateurs non volatils. Dans cette structure la tension et le courant de stimulation passent à travers les transistors MOS, tandis que les cellules flash sont utilisées pour définir et conserver l'état du transistor MOS.

Nous avons breveté le concept de l'intégration des technologies de mémoire non volatile dans les implants cardiaques.

Fin du Résumé

Chapter 1

General Introduction

In the recent years the standards of health care delivery have improved by leaps and bounds. Thanks to path-breaking research, new discoveries, new materials and advancements in technology, human beings not only live longer lives, but are administered better therapy which reduces the chances of disease progression and enables early detection of maladies. However it is important to note, that despite these advancements there is scope and need for much improvement especially in dreaded medical conditions such as cardiovascular complication which affect a large section of our population.

In various studies it is estimated that cardiovascular diseases are the principal cause of death especially in advanced industrial societies [1] [2]. In United States alone cardiovascular diseases are reported to be the number one cause of death [3]. Worldwide it is estimated that around 40% of all human deaths are due to cardiac complications [4].

In this thesis we will look at cardiac implants used to manage cardiovascular therapy, particularly pacemakers and defibrillators. We will look at the basic construction of these devices from an electronics perspective and we will also discuss their evolution. Furthermore, we will present our research results which we believe will enhance these devices by improving their functionality and making them more efficient. The chapter wise plan of this thesis is as follows:

In chapter2 we present basic functioning of heart, the prominent cardiovascular diseases and the devices used to manage these diseases i.e. cardiac implants. We discuss in detail, evolution of cardiac implants and their basic components. Thereafter we discuss in detail one of the most prevalent cardiac malady i.e. heart failure. Furthermore, we discuss bi-ventricular stimulation which is the mechanism used to manage heart failure.

In chapter3 we present the multi-electrode system to address the problem of biventricular stimulation. We present the design challenges the design philosophy and the constraints of such a multi-electrode system. We also discuss in detail the existing solutions and their limitations. Finally, we present the performance and results of the system which was designed by us.

[1] Kadish A, Mehra M. Heart failure devices: implantable cardioverter-defibrillators and biventricular pacing therapy. *Circulation* 2005; 111:24/3327.full <http://circ.ahajournals.org/content/111/24/3327.full>

[2] Zipes DP, Wellens HJ. Sudden cardiac death. *Circulation*. 1998; 98: 2334–2351.

[3] Myerburg RJ, Interian AJ, Mitrani RM, Kessler KM, Castellanos A. Frequency of sudden cardiac death and profiles of risk. *Am J Cardiol*. 1997; 80: 10F–19F.

[4] S. A.P. Haddad, R.P.M. Houben and W. A. Serdijn “The Evolution of Pacemakers” *IEEE EMB Magazine*, Vol. 25, No. 3, May/June 2006, pp38 – 48.

In chapter 4 we present the design of an additional block of the multi-electrode system we presented in chapter 3. The addition of this block to our multi-electrode lead solves the problem of compatibility of our multi-electrode system with existing pacemakers. As in chapter 3 we present in detail the design philosophy, constraints and the performance/results of our system

In chapter 5 we look at new technologies beyond the standard CMOS, which can make our multi-electrode lead smarter, smaller and more performant. We present several candidate technologies which can be applied in our multi-electrode. We discuss their strengths, weakness and their merits and demerits. Finally through simulations we prove the feasibility of some of these technologies for our application.

The main contributions of the thesis are as follows:

Design and implementation of a multi electrode system: We designed and implemented a multi-electrode system which is capable of multi-site and multiple stimulation. Our solution is completely configurable and meets the drastic constraints of area and power imposed by nature of our application. Our chip was taped out in $0.18\ \mu\text{m}$ technology and occupies $2.25 \times 5.35\ \text{mm}^2$ area. The chip also features a specially designed communication protocol and is compliant with the existing standards. It enables low power operation and allows quick configuration. To the best of our knowledge our study is the first published study of its kind.

Design and implementation of default connection unit: We implemented a default connection unit block for the multi-electrode chip which enabled the operation of a multi electrode lead with pacemakers not designed specifically to control such a lead. The solution therefore enlarges our lead compatibility to cover all pacemakers in the market. In the chapter we also discuss and provide solutions to the key challenges of such design in a constrained cardiac environment. Like the multi-electrode block the DCU block was taped out in $0.18\ \mu\text{m}$ technology, occupies $2.2 \times 1.75\ \text{mm}^2$ area and harvests the stimulation energy to power itself.

Proof of concept of the non-volatile memory technologies in the multi-electrode system: New technologies were explored which drastically improve the performance of the multi-electrode system. The employment of such technologies enhanced our multi-electrode system by eliminating the need of repetitive configuration of electrodes, thereby saving power and reducing latency. The benefits also included smaller area and compatibility with any pacemaker in the market. We explored several nonvolatile technologies, like NRAM, MRAM, Memristance and Flash. Through simulations we proved the feasibility of these technologies for our implant applications. We believe such technologies will be leveraged to design the next generation ultra-low power and ultra-high performance leads.

Chapter 2

Cardiac Stimulation Implants

2.1 Introduction

Cardiac stimulation implants are life saving devices of about the size of a child's palm, implanted in the patient's chest to manage different disorders that may affect the heart. We will start this chapter by presenting the basic functioning of heart, the main cardiovascular disorders and how cardiac implants address those disorders. We will then discuss the evolution of cardiac implants and their basic components. Thereafter we discuss in detail one of the most prevalent cardiac malady i.e. heart failure. Furthermore, we discuss bi-ventricular stimulation which is the mechanism used to manage heart failure.

2.2 Human Heart and Cardiac Implant Evolution

The heart is one of the most important organs in our body. It is a muscular organ which pumps blood through the network of arteries and veins known as the cardiovascular system. As shown in figure 2-1, the heart is composed of four chambers: two receiving chambers; Right Atrium (RA) & Left Atrium (LA) and two pumping chambers; Right Ventricle (RV) & Left Ventricle (LV) as shown in figure 2-1.

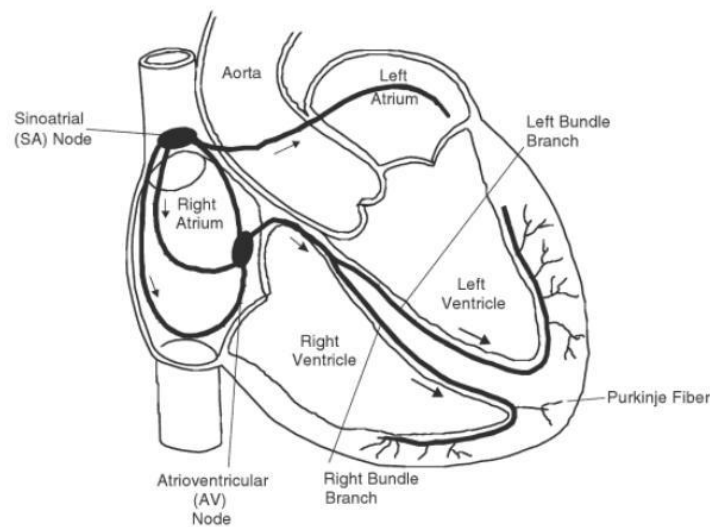


Figure 2-1: Heart Chambers [6]

Each minute the heart beats approximately 72 times. During this short period, RA pumps about 5 liters [5] of deoxygenated blood to the lungs while LV pumps about 5 liters of oxygenated blood to the rest of the organs. The amount of blood pumped each minute by the left ventricle is termed “cardiac output”. A significant decrease in this amount decreases the oxygen level in the organs which may lead to loss of conscious or even death if the affected organ was the brain.

The heart is composed of two types of muscle cells; *contractile* and *autorhythmic* cells. Contractile cells represent the majority (99%) and are responsible for the heart contraction which leads to the mechanical pumping. Autorhythmic cells are less in number but play the vital role in initiation and conduction of action potentials. Action potential is defined as the rapid change of membrane electrical potential during excitation and then leads to transmission of electrical impulses travelling across the membrane. This action potential initiation and conduction done by autorhythmic cells is responsible for the rhythmic and coordinated contraction of the heart chambers.

Figure 2-2 shows the electrical conduction system of the heart which governs its rhythm of contraction. Each heart beat is initiated by an electrical signal generated at the Sinoatrial node (SA node) located at the top of the right atrium. This electrical signal creates a depolarization wave that spreads rapidly in the right and left atria (RA & LA) causing them to contract. Due to electrical insulation between atria and ventricles, the depolarization wave does not reach the ventricles. Instead, the electrical activity reaches the ventricles via a second node called Atrioventricular node (AV node). This node is connected to a bundle of specialized cells called “Bundle of His” which divides into right and left bundle branches inside right and left ventricles respectively. These branches divide further into tiny fibers called “Purkinje fibers” to disperse rapidly the electrical signal inside the ventricles [6].

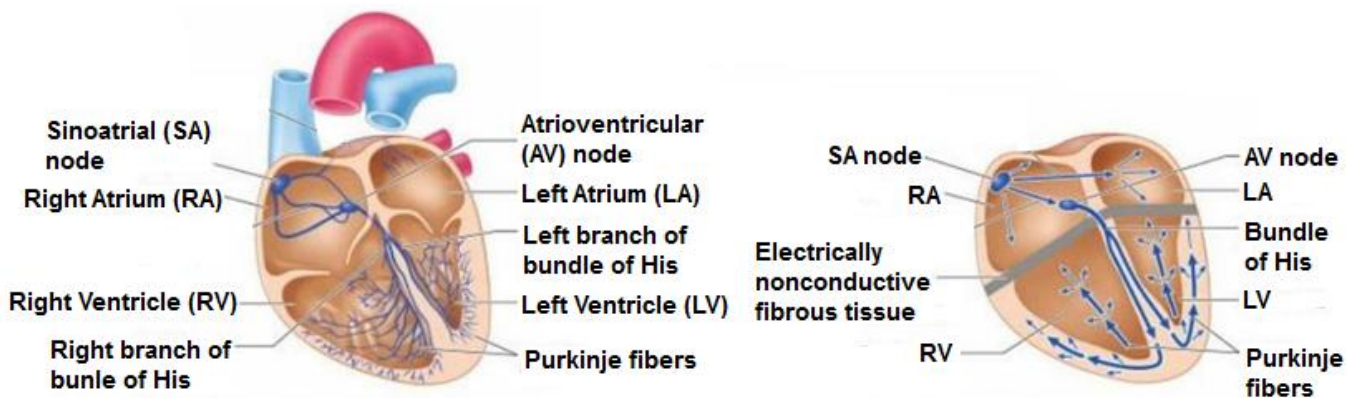


Figure 2-2: Conduction system of the heart [5]

In this electrical conduction system, the SA node acts as the natural pacemaker which sets the rate at which the heart beats. Any disturbance in this conduction system causes cardiac disorders such as arrhythmias or heart failure.

2.2.1 *Heart failure condition*

Heart failure is a progressive condition affecting patients whose heart cannot pump enough blood to meet the needs of their body. This condition is associated with uncoordinated ventricular contractions and causes symptoms like breathing difficulty and lack of energy. The first method of treatment is medication. Thereafter Cardiac Resynchronization Therapy (CRT) pacemakers are prescribed for patients with moderate to severe heart failure. Cardiac Resynchronization Therapy pacemakers do not have the ability to treat abnormal fast rhythm (VT and VF) with rapid pacing or a defibrillation shock.

2.2.2 *Arrhythmias*

Arrhythmia is defined as an abnormal heart rhythm which can be too fast or too slow, or irregular. Arrhythmias can be a life-threatening condition which may lead to a cardiac arrest. Cardiac arrest rarely gives any warnings, and once it occurs it requires an immediate intervention from a doctor or emergency medical personnel to provide a shock (defibrillation) in order to restore normal heart rhythm. Well, these kinds of resources are not always available in proximity of the patient. For patients whom medication was not sufficient to address the cause of such arrhythmias, Implantable cardioverter defibrillator (ICD) can offer a protection against such life-threatening condition.

Nowadays an implantable cardioverter defibrillator ICD with a cardiac rhythm therapy CRT is available and offers the required treatment for heart failure condition and protection against life-threatening situations.

The cardiac implant is generally implanted just under the chest skin and it delivers the electrical stimulation via specialized wires (called leads) to the chambers of heart. To deliver the electrical stimulation to the tissue the lead is equipped at its end with electrodes. Generally in the simplest embodiment, the number of electrodes is either two (bipolar) or one (unipolar).

2.2.3 *First Implantable pacemaker*

In 1959, the engineer Wilson Greatbatch developed the first fully implantable pacemaker [7]. It delivered electrical pulses of fixed width and amplitude at **fixed rate** of 60 beats per minute (bpm). It was powered by ten mercury-zinc cells battery that gave it an estimated lifetime of five years.

The limitation of this asynchronous (fixed rate) pacemaker was the delivery of stimulation pulses at fixed rate regardless of the cardiac activity. This activity competes with the natural activity of the heart leading sometimes to cardiac disorders.

2.2.4 Demand Pacemaker

In June 1964, Berkovits introduced a new concept of cardiac pacemakers named “Demand pacemakers” which became the basis for all modern pacemakers [7].

Unlike the asynchronous pacemakers first implanted, demand pacemakers keep track of natural cardiac activity through the usage of sensing amplifier. As long as the natural cardiac activity is detectable, the pacemaker does not deliver any stimulation pulses. However, once the natural cardiac activity is missing, the pacemaker restores the cardiac rhythm.

Another advantage of demand pacemaker over asynchronous one is the longer lifetime of the battery due to controlled activity.

2.2.5 Rate-Responsive Pacemaker

With the continuous search for optimization of cardiac pacing according to the patient’s needs, a further step was taken beyond the simple detection of electrical activity of the patient’s heart. In the 1980s sensors were incorporated in the pacemaker to measure some parameters relevant to the patient’s physical activity such as body motion, respiration and blood pressure. In the Rate-Responsive pacemakers, the pacing rate is determined as a function of the quantities measured by the sensors.

Since then the implantable cardiac pacemakers or defibrillators did not cease to evolve in the direction of better optimization of pacing according to the patient’s need. Modern cardiac implants have become very complex systems.

2.3 Implantable Cardiac Stimulation System

Cardiac pacing/defibrillation systems are composed of a **pulse generator** and **stimulation leads** that connect this pulse generator to the patient’s heart. Stimulation leads are equipped at their extremity by **electrodes** to electrically interface with heart tissues.

The implanting operation is performed either under heavy sedation or complete anesthesia. The doctor first makes a “pocket” under the chest skin in which the pulse generator will be inserted. Leads are then passed through veins and fixed in heart chambers. The number of leads to be inserted depends on the number of heart chambers assigned for pacing (one lead/chamber). This decision is

made by the doctor depending on the patient's needs, either one chamber pacing (RA) or double chamber pacing (RA and RV) or maximally triple chamber pacing (RA, RV and LV).

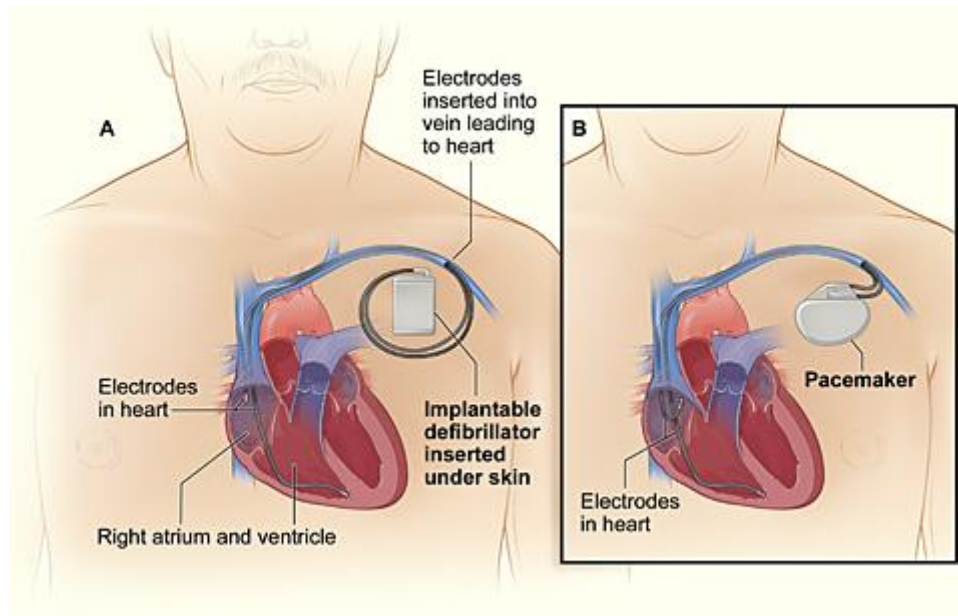


Figure 2-3: (a) implantable defibrillator (b) Implantable pacemaker [9]

Figure 2-3 shows as example for the position of the cardiac implant whether a defibrillator (fig. 2-3a) or pacemaker (fig. 2-3b) and the leads fixed in two heart chambers RA and RV (dual chamber pacing mode).

After leads insertion and before their final fixation, the doctor has to test the cardiac response to stimulation in order to determine the best site for stimulation.

Pulse generator is powered by batteries of limited lifetime estimated to last 7 or 10 years depending on the pacing activity. Several months before the battery is expected to run out, the pulse generator is replaced in an operation similar to the original implant. The pocket in the chest is re-opened and the new pulse generator is connected to existing leads only if they are tested to be in good state. Leads are occasionally replaced and their replacement can be more complex than the replacement of pulse generator.

In the following subsections we will discuss the basic components of a pulse generator and the leads features.

2.3.1 Pulse Generator (Implant - CAN)

Pulse generator is a hermetically sealed titanium case which prevents body fluids from entering in contact with its circuitry. It encloses circuitry of mainly four functional types as shown in figure 2-4:

- Power source
- Control unit
- Sensing circuit for each chamber
- Output circuit for each chamber

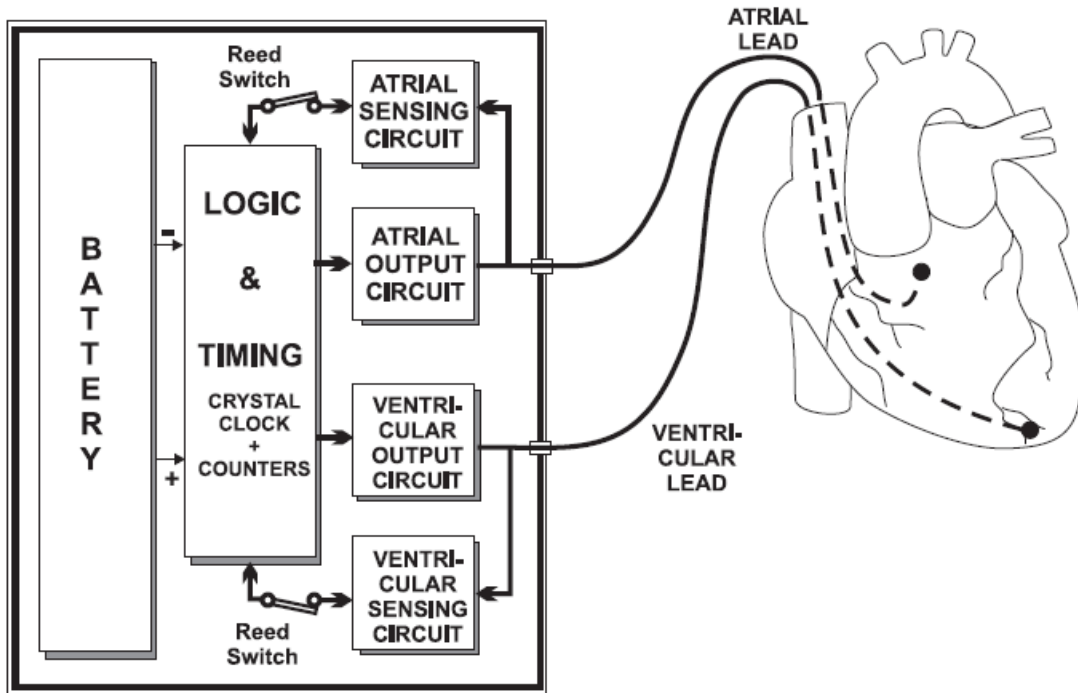


Figure 2-4: block diagram of Dual chamber pacemaker [8]

2.3.1.1 Power source

The most critical aspect of the power source of an implantable medical device is its lifetime. The longer its lifetime, the less the number of surgeries needed for a cardiac stimulator replacement. In cardiac pacemakers, lithium-iodine batteries are used as a power source as they do not produce gas and can be hermetically sealed [1]. The energy required for stimulation is determined by two parameters: pulse amplitude and stimulation frequency. As these parameters vary from patient to another, a normalized model is followed to reach an average estimation of needed energy for stimulation. Using these normalized values given in table 1, an average power consumption of 2.8uA is deduced for single chamber stimulation. This value doubles if two chambers are paced (dual chamber pacing). In order for the battery to last for 10 years, an average consumption of 11.4uA is required.

Table 2-1: normalized values for stimulation energy [11]

PARAMETER	NORMALIZED VALUE
PULSE AMPLITUDE	2.5V
PULSE DURATION	0.5 MS
STIMULATION FREQUENCY	72 PPM
LEAD/TISSUE IMPEDANCE	500 Ω

Lithium-iodine batteries capacitance is measured in ampere-hours (Ah) [2]. 1 Ah is equivalent to 114uA year [11]. Compromise has to be reached between battery's lifetime and its size in implantable devices with the continuous demand to decrease the size while keeping long lifetime.

Of course battery drainage is more significant in the case of implantable defibrillators due to the higher pulse amplitude used in cardiac shock. This makes the lifetime of defibrillators less than that of pacemakers. Other types of lithium iodine batteries are used in defibrillators which permit higher currents drain and lower internal impedance.

2.3.1.2 Output circuit

The output circuit is also known as "Stimulation channel" has the role of generating a voltage pulse of certain amplitude and duration sufficient to trigger an action potential wave in cardiac cells and stimulate the heart. This stimulation pulse is routed to electrodes interfacing with cardiac tissues through controlled switches.

Figure 2-5 illustrates a simplified stimulation channel for bipolar stimulation. V_B is the output of the voltage multiplier used to generate chosen stimulation amplitude in a programmable manner starting from the battery voltage. In a first phase of the stimulation channel operation, "Charge" switch is closed to charge the tank capacitor (C_{tank}) to the programmed amplitude. For the stimulation channel to deliver the stimulation impulse between Anode and Cathode electrodes interfacing with the heart, the "Discharge" switch opens and "STIM" switch closes for the programmed pulse duration. C_{tank} discharges its energy through the discharged series capacitor C_{series} to the Cathode. C_{series} has two roles [11]:

- Prevent the passage of DC current to the heart, which is an important safety condition
- Helps in discharging the electrode-tissue interface which helps in alleviating electrode polarization effect as will be discussed later in this chapter.

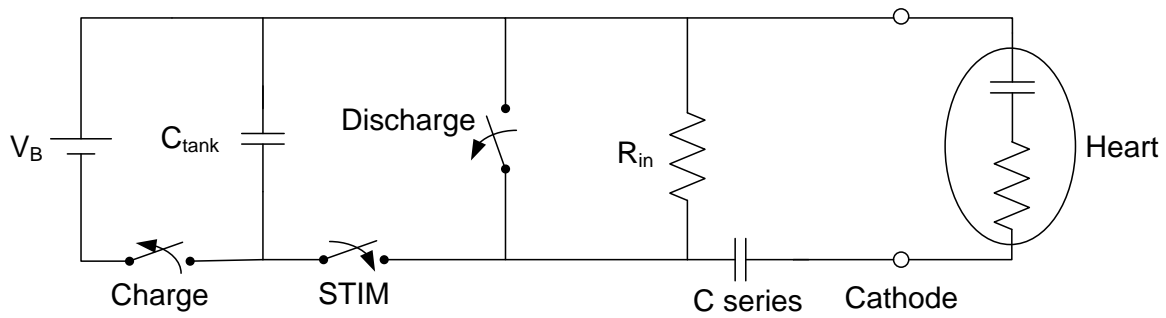


Figure 2-5: simple circuit diagram for a stimulation channel

Just after the simulation ends, STIM switch is opened and Discharge switch is closed during a period long enough to discharge the electrode-tissue interface as well as C series. This phase is called “Discharge phase” necessary for clearing residual charges that may mask sensed cardiac signals during the “Sensing phase” that follows it.

Due to heart impedance that may reach 1000 ohms, switches must have low ON-resistance in order to handle currents up to 16 mA with low voltage drop (less than 100mV). Also low ON-resistance switches helps in reducing the time needed for the discharge phase.

Table 2 summarizes the values used in this simplified stimulation channel. [3]

Table 2-2: parameters of stimulation channel

PARAMETER	TYPICAL VALUE
TANK CAPACITOR, CTANK	10 - 30 μ F
SERIES CAPACITOR, CSERIES	10 - 30 μ F
SURFACE AREA OF CATHODE	10 MM ²
SURFACE AREA OF ANODE	50MM ²
RIN	600 Ω
RHEART	500 Ω
PULSE AMPLITUDE	0.2V – 8V
PULSE DURATION	0.1MS -2MS

2.3.1.2.1 Action Potential and Stimulation Threshold

Figure 2-6 shows the five phases (0 to 4) of an action potential waveform and how the membrane potential varies within each phase. The membrane potential has an initial value called resting membrane potential (RMP) of -90mV . In normal heart function, the natural electrical pulse generated at the SA node depolarizes the membrane till it reaches the threshold value. In artificial stimulation, the generated voltage pulse replaces the SA node in this task. Once the membrane potential reaches the threshold level, phase 0 starts and rapidly increase membrane potential till it reaches about $+30\text{ mV}$. Then early repolarization (phase 1) of membrane takes place, followed a plateau region (phase 2). In phase 3, the membrane continues its repolarization till it reaches the resting membrane potential in phase 4. Phases 1, 2 and the beginning of phase 3 forms the absolute refractory period (ARP) during which cardiac cells cannot be excited [12], i.e. the heart will not respond to another stimulation pulses applied in this period. Relative refractory period (RRP) follows the ARP. In this period the heart require high stimulation pulse to respond.

It is important that the cardiac pacemaker estimates this refractory period to prevent triggering further arrhythmias (mediated tachycardia). This period in pacemakers is called “Blanking” during which the pacemaker ignores any sensed events in order not to stimulate. This period is programmable and lasts for 300-400 milliseconds [13]

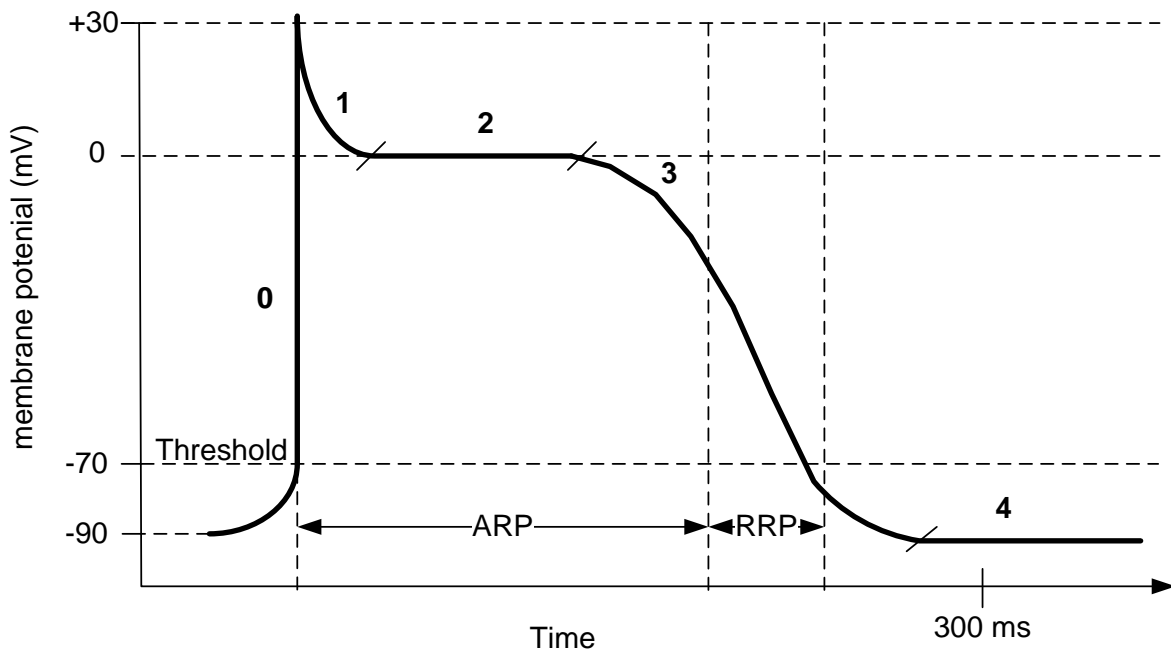


Figure 2-6: membrane potential during ventricular action potential

As the role of the pacemaker during stimulation is to transfer the membrane potential from its RMP to its threshold potential, this is achieved if the energy delivered to the tissues is sufficient. Stimulation energy depends on the strength and duration of the stimulation pulse. Figure 2-7 plots the stimulus strength (current or voltage) against its duration.

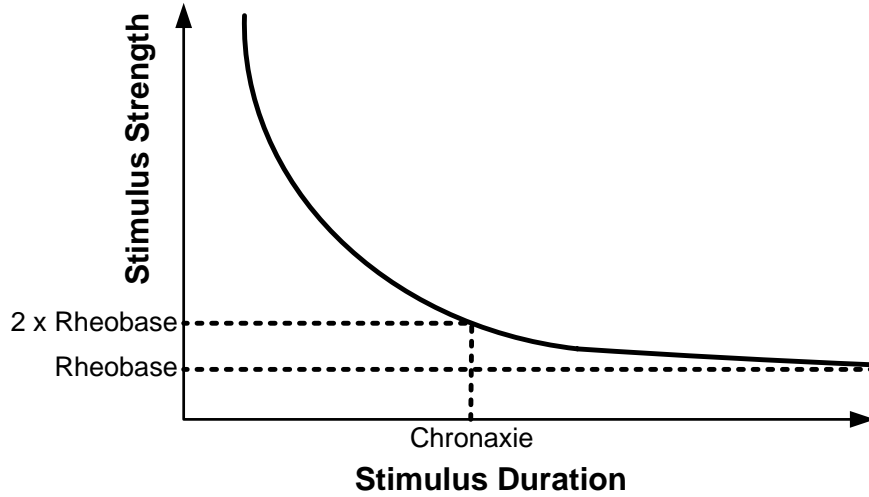


Figure 2-7: strength-duration curve

Rheobase (b) is the minimal strength (current or voltage) required to trigger an action potential at infinite duration. Chronaxie (c) is the pulse duration at which an action potential is triggered if the pulse strength is equal to double the Rheobase ($2b$). [12]

Equation (1) gives the needed strength of stimulation pulse as a function in Rheobase (b), Chronaxie (c) and pulse duration (d).

$$I = b \left(1 + \frac{c}{d} \right) \quad (1)$$

2.3.1.2.2 Electrode-Tissue interface

At the electrode-tissue interface, an electrochemical condenser (Helmholtz condenser) is formed due to the accumulation of charges of one sign on the electrode and charges of the opposite sign in the tissues (electrolyte) adjacent to the electrode [12]. The electrode-tissue interface has also a resistive component (R) that has to be taken in consideration while electrically modeling the interface. Helmholtz capacitance (C) depends on the nature of electrode's metal, electrode's surface area and the frequency (0.2 to $0.5 \mu\text{F}/\text{mm}^2$) [14]

Stimulation threshold is affected by this polarization impedance found at the electrode-tissue interface (fig. 2-8a). To estimate this influence, the electrode-tissue interface and the pacing circuit are simplified as shown in figure 2-8b. The lead impedance is assumed negligible. It can be noticed in figure 2-8c that the current pulse passing through the interface during constant voltage stimulation is not constant. In the beginning its value is equal to $\frac{V}{R}$ then it decays with an exponential function given in equation (2)

$$I_e = \frac{V}{R} \cdot e^{\frac{-t}{RC}} \quad (2)$$

Where t is the pulse width and the time constant is given by RC [14].

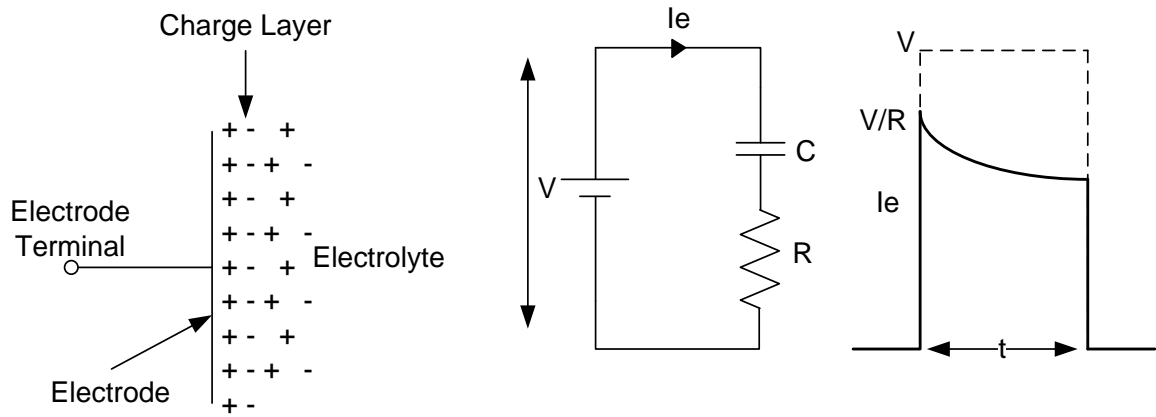


Figure 2-8: a) electrode-tissue interface b) interface equivalent circuit c) ideal and real stimulation pulse

2.3.1.3 Sensing Unit

Also known as the Sensing channel and its role is to amplify and filter cardiac signals (intraECG) then compare them with a threshold level in order to detect the presence or absence of spontaneous cardiac contraction. One sensing channel is connected per chamber (Atrium or Ventricle).

Sensing channel must be active for the major part of cardiac cycle, which requires a limitation in its power consumption. This is done through increasing input impedance that must be high ($>20K\Omega$) to limit the power consumption due to current consumption and to avoid excessively loading the tissues which may affect the measured signals. Also because of the low frequency range of heart signals, high impedance is used to adjust the band pass filter instead of using big capacitances.

Figure 2-9 shows the basic blocks that form a sensing channel which are discussed in this section.

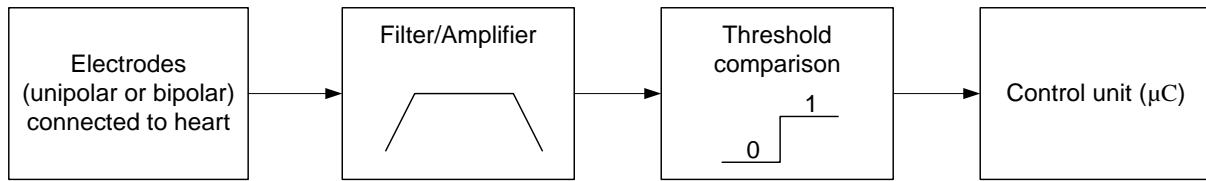


Figure 2-9: sensing channel block diagram

2.3.1.3.1 Unipolar and Bipolar sensing

It was shown by practice that bipolar sensing is better than unipolar one. A key difference between the two modes is that unipolar sensing with its wide dipole is more sensitive to electromagnetic and myopotential interference [15] (signals from neighboring chambers) which is better controlled in bipolar mode due to its smaller distance between electrodes.

2.3.1.3.2 Filter/Amplifier

A common source of interference is the network mains at 50 and 60 Hz. As these frequencies are near to the frequency components of cardiac signals, they have to be filtered out. In several generations of pacemakers, a frequency band pass of 70Hz to 200Hz has been proven to be efficient [11].

The studies of Furman et al. [16, 17] found that the amplitudes of the acute intraventricular electrograms ranged from 2.0 mV to 36.4 mV with a mean of 12.4 mV, while the amplitudes of intra-atrial electrograms were smaller with a mean value of 4.83 mV. With these amplitudes of cardiac signals, the gain of the amplification stage may reach to 700 [11] in order to provide the threshold comparator better amplitudes to detect correctly cardiac activity.

2.3.1.3.3 Threshold Comparator

The comparison threshold is a programmable parameter in pacemakers. This programmability enables it to adapt to differences in cardiac signals amplitudes among the different patients. In demand pacemakers which are the base for all modern pacemakers, the detection of cardiac signals superior than the programmed detection threshold, resets the internal timers and delays thereby the stimulation pulse.

2.3.1.4 Control unit

The control unit is responsible for the coordination of all the circuits (stimulation channel, sensing channel ...etc.) of the cardiac implant whether it is a pacemaker or a defibrillator. With its microcontroller (μC) driving a set of crystal oscillators of high precision, the control unit is able to set and define different delays such as the estimation of the refractory period, detection amplifiers blanking period, A-V delay and timer reset in the case of spontaneous cardiac activity is detected.

Blanking period means the masking of the inputs of sensing amplifiers in the two chambers (atrium and ventricle). This is needed during the stimulation and discharge phases (tens of milliseconds) to prevent saturation. The A-V delay is controlled in dual chamber stimulation mode to define the delay between atrial and ventricular stimulations.

For each stimulation demand, the control unit has to precise which chamber to stimulate and to define both amplitude and duration of the stimulus. These parameters are programmed by the doctor through telemetry circuits included in the control unit communicating with an external programmer unit. These telemetry circuits are also used to transfer collected information for diagnosis purposes [2].

Control unit is also equipped with a magnetic field detector which may be used to intentionally interrupt the pacing activity for test purposes. It also plays an important role in the case of magnetic interference by forcing an asynchronous (fixed rate) stimulation mode till the interference source is removed [7].

To summarize the coordination between the different units of the cardiac implant made by the control unit, figure 2-10 gives the main phases of cardiac cycle handled by the cardiac pacemaker. The cycle starts with the sensing phase in which the sensing channel is monitoring the cardiac activity. As long as spontaneous cardiac activity is detectable, the sensing phase continues. For this reason the period of the sensing channel is not precisely defined in figure 2-10. In case of absence of the spontaneous cardiac activity, the control unit commands the stimulation channel to deliver a stimulation pulse with the defined amplitude and duration to the concerned heart chamber. As the stimulation pulse duration is programmable (0.1ms to 2ms), in consequence the stimulation phase duration follows the pulse duration. The control unit modifies the connections inside the stimulation channel and configures it into the discharge mode. The discharge phase starts immediately after the stimulation phase and lasts for several milliseconds. As discussed before, the discharge phase is useful in clearing the residual charges on the electrode-tissue interface and the serial capacitor of the stimulation channel. During stimulation and discharge phases, the sensing amplifiers are masked to

avoid their saturation for the blanking period. At the end of discharge phase the sensing amplifiers are unmasked and another sensing phase begins to start a new cardiac cycle.

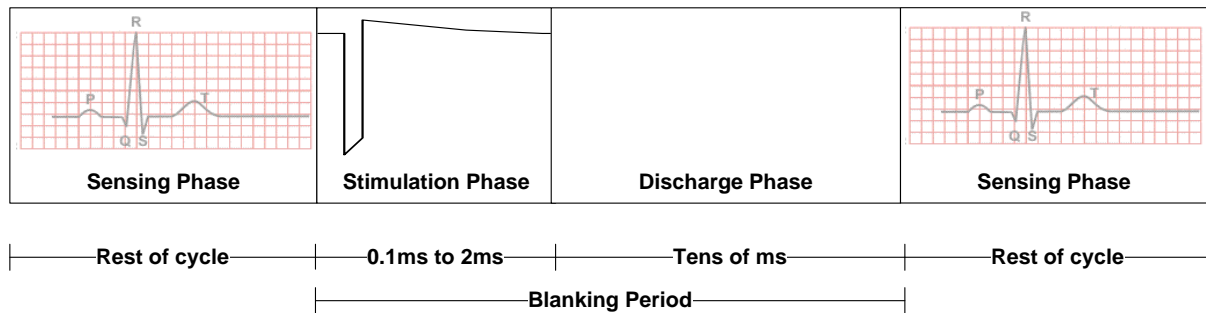


Figure 2-10: Main phases of pacing cycle in a cardiac pacemaker

2.3.2 Leads

The pulse generator (implant) is connected to the heart by leads (insulated wires) that reach the different heart chambers through veins. Leads ensure the monitoring of heart's rhythm and the delivery of needed therapies. Leads are classified into two types:

- **Endocardial leads:** the lead is passed transvenously and lodged in either the right atrium or right ventricle (fig. 2-11a).
- **Epicardial leads:** the lead is applied directly to the heart (epicardium) from outside (fig. 2-11b)



Figure 2-11: (a) endocardial leads [22] (b) Epicardial leads [23]

In order to conduct an electrical pulse to the heart tissues, at least two poles are needed; Anode and Cathode. Between Anode and Cathode, body tissues and fluids act as a part of the conduction path. Cathode is charged negatively when current flows and it is always in contact with the tissue. Anode is positively charged when current flows and it completes the return path of stimulation current. According to the way Anode and Cathode are distributed, two modes of stimulation exist: Unipolar and Bipolar.

2.3.2.1 Unipolar

In the unipolar mode of stimulation, the lead has only one electrode (Cathode) fixed to tissues. The stimulation pulse flows through the Cathode, stimulates the heart and returns through body fluids and tissues to the implanted pulse generator which acts as Anode. The unipolar stimulation mode is illustrated in figure 2-12.

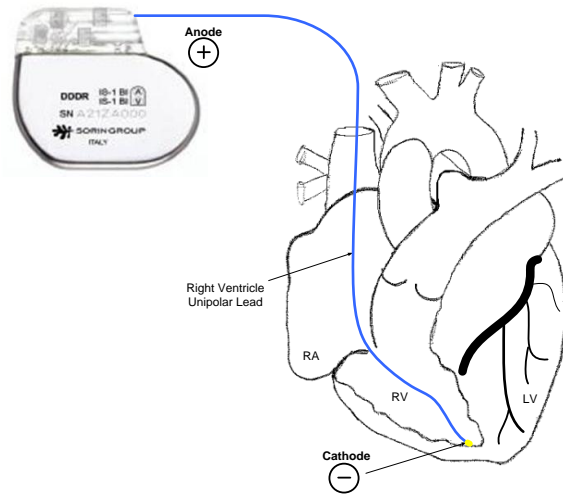


Figure 2-12: Illustration of unipolar stimulation/sensing

2.3.2.2 Bipolar

In bipolar stimulation mode, the lead has two electrodes. In reference to the implanted pulse generator position, the far electrode is called distal or tip electrode and acts as Cathode. The electrode nearer to the implanted pulse generator is called proximal or ring electrode and acts as Anode. The stimulation pulse flows through the Cathode, stimulates the heart and returns through the Anode. The bipolar stimulation mode is illustrated in figure 2-13.

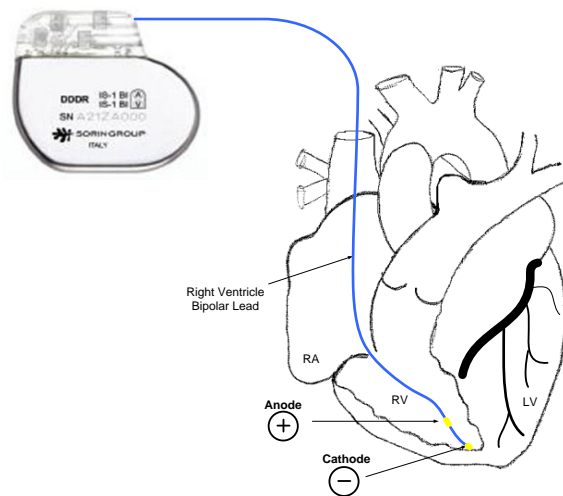


Figure 2-13: Illustration of bipolar stimulation/sensing

Dimensions of leads depend on whether they are unipolar or bipolar. Unipolar leads are thinner than bipolar leads due to the less number of cables inside. Nevertheless, bipolar leads are gaining more interest due to their better efficiency in sensing cardiac activity with less interference caused by signals in neighboring chambers. Today, very reliable and safe leads with $<4\text{mm}^2$ surface area electrodes and $>1000\ \Omega$ impedance have been introduced [19]

2.4 Cardiac Resynchronization Therapy (CRT)

Unsynchronized ventricular contraction is one of the main symptoms of heart failure. CRT device addresses this disorder through pacing the heart in both the right and the left ventricles in order to resynchronize their contraction and attempt to increase the cardiac output. This therapy is also referred to as “Biventricular pacing”.

In order to function properly, pacing leads must be placed in the right atrium, the right ventricle, and the left ventricle. As shown in figure 2-14, right atrium lead and right ventricle lead are fixed inside the chambers. But the case is different for the left ventricular lead in which it has to be fixed outside the chamber. The lead is advanced through one of the ventricular veins to the vicinity of the left ventricular external wall (free wall). Once the left ventricular free wall has been accessed, a stable lead position must be obtained with the best cardiac response for stimulation.

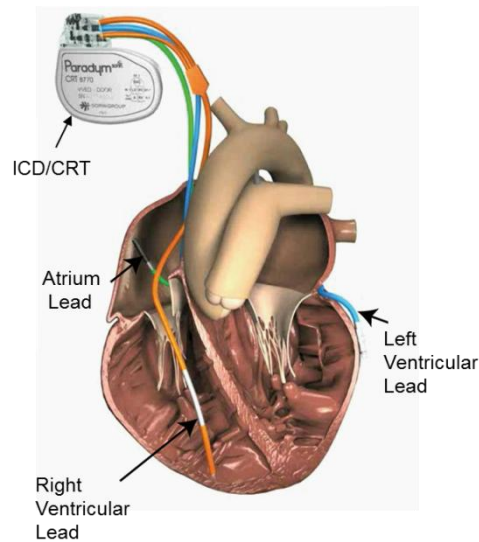


Figure 2-14: CRT pacemaker with three stimulation leads connected

Beside this complicated procedure to navigate with the lead till finding the best stimulation site, left ventricular stimulation is experiencing a number of difficulties such as:

2.4.1 Phrenic nerve stimulation

One of the most difficult problems to troubleshoot is when after careful manipulation of a left ventricular lead into what seems to be an ideal lateral wall location with excellent pacing thresholds, high output stimulation results in phrenic or diaphragmatic stimulation. This erroneous stimulation may cause hiccups and abdominal cramps [21] for the patient.

The best way to avoid phrenic nerve stimulation is to place the lead in another vein. If this is not possible, some studies have found that this can be avoided by changing the inter-electrode distance in the lead [20]. However with bipolar electrode leads, changing the inter-electrode distance is not possible, the only solution is to insert a new lead which evidently increases the complexity manifold.

2.4.2 Limited choice of stimulation site

The task is already difficult for the physician facing the decreasing diameter of the vein which obliges him to fix the lead at a certain point and choose the best stimulation site available. The employment of limited number of electrodes inside the bipolar lead further limits the physician choice inside the left ventricular veins.

2.4.3 Lead displacement

In some patients after a successful implantation for the left ventricular leads, an inhibition of cardiac response to stimulation may be noticed. This may be caused due to lead displacement inside the veins. In this case, another surgical intervention similar to the first one is needed to reposition the left ventricular lead. This kind of complication is inevitable using the ordinary bipolar leads which does not offer a non-invasive solution to the problem.

2.5 Conclusion

In this chapter we presented the structure of human heart as well as disorders and diseases that may affect it. We saw how cardiac implants continued their evolution to better treat patients suffering from cardiovascular diseases. We explored the building blocks of cardiac implants and how they interact with cardiac tissues to analyze the patient's state and deliver the adequate treatment.

We terminated the chapter with a presentation of the importance of biventricular pacing (CRT) and the enumerated some limitations of bipolar leads used in left ventricular stimulation.

In the next chapter we will present the design process of a multi-electrode pacing system that alleviates the limitations of left ventricular stimulation.

References

- [1] Mond, H. G. 1983. The cardiac pacemaker, function and malfunction: 1st Ed. New York: Grune and Stratton.
- [2] John G. Webster, Design of Pacemakers, IEEE Press 1995, chapter 5
- [3] John G. Webster, Design of Pacemakers, IEEE Press 1995, chapter 6
- [4] WebMD.com
- [5] L. Sherwood "Fundamentals of Human Physiology" Cengage Learning, 2011
- [6] David Prutchi, Michael Norris "Design and development of medical electronic instrumentation" John Wiley and Sons, 2005 - 461 pages
- [7] S. A.P. Haddad, R.P.M. Houben and W. A. Serdijn "The Evolution of Pacemakers" IEEE EMB Magazine, Vol. 25, No. 3, May/June 2006, pp38 – 48.
- [8] S. S. Barold, R. X. Stroobandt, A. F. Sinnaeve "Cardiac Pacemakers step by step" Blackwell publishing 2004.
- [9] National Heart Lung Blood Institute. <http://www.nhlbi.nih.gov>
- [10] CRT/ICD patient booklet of Sorin Group
- [11] Fernando Silveira, Denis Flandre « Low power analog CMOS for cardiac pacemakers" Springer 2004.
- [12] W. A. Tacker and L. A. Geddes "The laws of electrical stimulation of cardiac tissues" Proceedings of the IEEE, vol. 84, No. 3, March 1996
- [13] G. Alec Rooke "Pacemaker Review" Professor of Anesthesiology, University of Washington, Seattle, WA
- [14] A. Ripart and J. Mugica "Electrode-Heart Interface: Definition of the Ideal Electrode" Pacing and Clinical Electrophysiology, Wiley Volume 6, Issue 2, pages 410–421, March 1983
- [15] A. P. Nielsen, W. R. Cashion, W. H. Spencer, H. J. Norton, G. W. Divine , T. D. Schuenemeyer, J. C. Griffin "Long-Term Assessment of Unipolar and Bipolar Stimulation and Sensing Thresholds Using a Lead Configuration Programmable Pacemaker" JACC 1985
- [16] Furman, S., Hurzeler, P., and DeCaprio, V. 1977a. The ventricular endocardial electrogram and pacemaker sensing. J. Cardiovascular and Thoracic Surg. 73: 258–266.
- [17] Furman, S., Hurzeler, P., and DeCaprio, V. 1977b. Cardiac pacing and pacemakers III. Sensing the cardiac electrogram. Am. Heart J. 93:794–801.
- [18] L. A. Geddes and L. E. Baker, Principles of Applied Biomedical Instrumentation, 1st and 3rd edition New York: Wiley, 1968, 1989.

- [19] Harry G. Mond, “Recent Advances in Pacemaker Lead Technology”, Cardiac Electrophysiology Review 1999
- [20] Samuel J Asirvatham “Implanting a Left Ventricular Pacemaker Lead” Indian Heart J 2007; 59: 197–204
- [21] A. K. Tadakamalla et al. “Phrenic Nerve Stimulation: An Unexpected Complication of Implantable Cardioverter Defibrillator (ICD)” E-Journal of cardiology 2011 vol 1, N 1
- [22] Sorin Group Data
- [23] Medtronic, Inc. stimulation lead photo

Chapter 3

Multi-electrode System for Left Ventricular Stimulation: Design and Implementation

3. Multi-electrode System for Left Ventricular Stimulation: Design and Implementation

3.1 Introduction

Modern cardiac pacemakers treat congestive heart failure using biventricular pacing. Biventricular pacing, as the name suggests, is pacing (stimulating) both right and left ventricles in order to resynchronize the heart rhythm [1]. Unlike, the other chambers of heart, for pacing left ventricle, the LV lead is inserted inside one of the veins on the external wall of the chamber [2]. The employment of bipolar leads, had limitations which were discussed in the section 2.3 of chapter 2. These limitations can be briefly summarized as follows:

- Phrenic nerve stimulation
- Limited choice of stimulation site
- Lead displacement

This chapter presents a multi-electrode lead system to address the above limitations. In this chapter we will show, how the multi-electrode system offers physicians more flexibility in choosing the best stimulation site for their patients, thereby enabling better management of phrenic nerve stimulation. Furthermore we will also see that multi electrode system considerably reduces the probability of the undesirable post-implantation surgery which is required to reposition the lead. Thus the multi-electrode lead allows better therapy and cardiac disease management.

Figure 3-1a depicts the conventional bipolar lead and Figure 3-1b the multi-electrode lead. As can be seen from the figure, the multi-electrode lead has multiple sites of stimulation as compared to the bipolar one. The positioning of the left ventricular multi-electrode lead in the coronary sinus can also be seen in the figure. Table 3-1 compares the multi-electrode approach to the conventional bipolar approach.

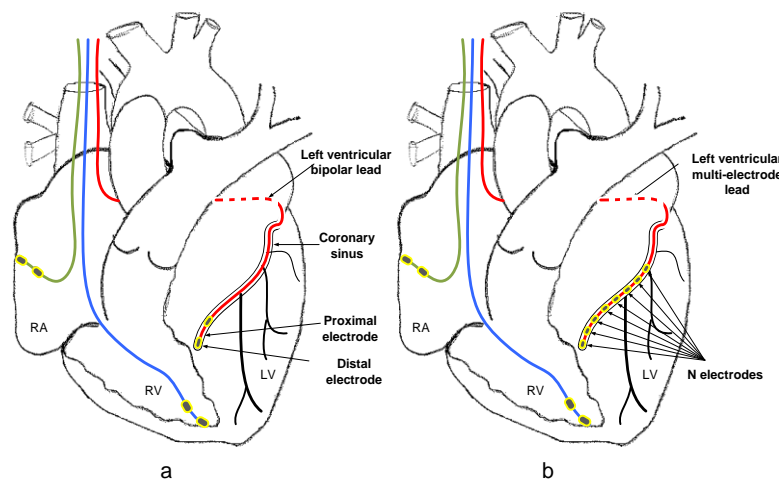


Figure 3-1 : (a) illustration for the positions of bipolar leads in the different heart chambers, (b) multi-electrode lead replaces the bipolar left ventricular lead of figure (a)

Table 3-1: Bipolar lead vs. Multi-electrode lead

	Bipolar lead (fig. 3-1a)	Multi-electrode lead (fig. 3-1b)
Number of electrodes	2	several
Inter-electrode distance	Fixed	Programmable
Electrode polarity	Fixed	Programmable
Stimulation location	Fixed	Programmable
Stimulation failure	Surgery needed	Non-invasive reprogramming
Phrenic nerve stimulation by error	Change lead	Program new inter-electrode distance

3.2 Multi-electrode System: Principle & Constraints

Figure 3-2 shows the multi-electrode system and its components. Similar to conventional cardiac stimulation systems, the multi-electrode system is composed of an implant (pacemaker), the multi-electrode lead and electrodes. Owing to the multiplicity of electrodes meant to be selectively activated, an additional electrode-controller unit is needed to define the activity and polarity of each electrode in the multi-electrode lead individually

It is imperative that we understand the constraints which we have to deal with in such a multi-electrode system. These constraints come not only from the specifications/performance criterion laid out for medical devices but also from the inherent nature of a multi-electrode system. We now discuss the most important constraints: compliance with standards, powering and communication.

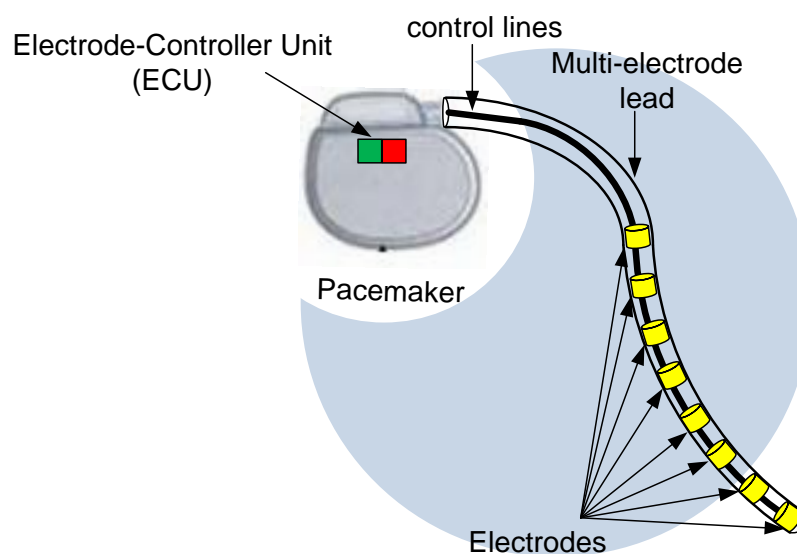


Figure 3-2: Multi-electrode system components. The number of control lines equals the number of electrodes in the lead

3.1.1 Compliance with standards

One of the simplest ways to design such a multi-electrode system, where we select/deselect/configure each electrode individually is to use a dedicated wire for each electrode (fig. 3-2). This of course means that the number of control lines for these electrodes would be equal to the number of electrodes. While feasible, this approach is practically impossible since it would increase the number of control wires emanating from the pacemaker connector (interface). The medical standard bodies stipulate that the pacemaker connector can support only up to 3-4 wires.

To resolve this constraint, the Electrode controller unit has to be divided into two parts. The first part resides in the implant (Implant Electrode Controller - IEC) and the second part is transferred to the lead (Lead Electrode Controller - LEC) as shown in figure 3-3. Both IEC and LEC mutually communicate through the standard pacemaker interface using 2 or 3 control lines. Here the LEC plays a de-multiplexing role between IEC and the electrodes.

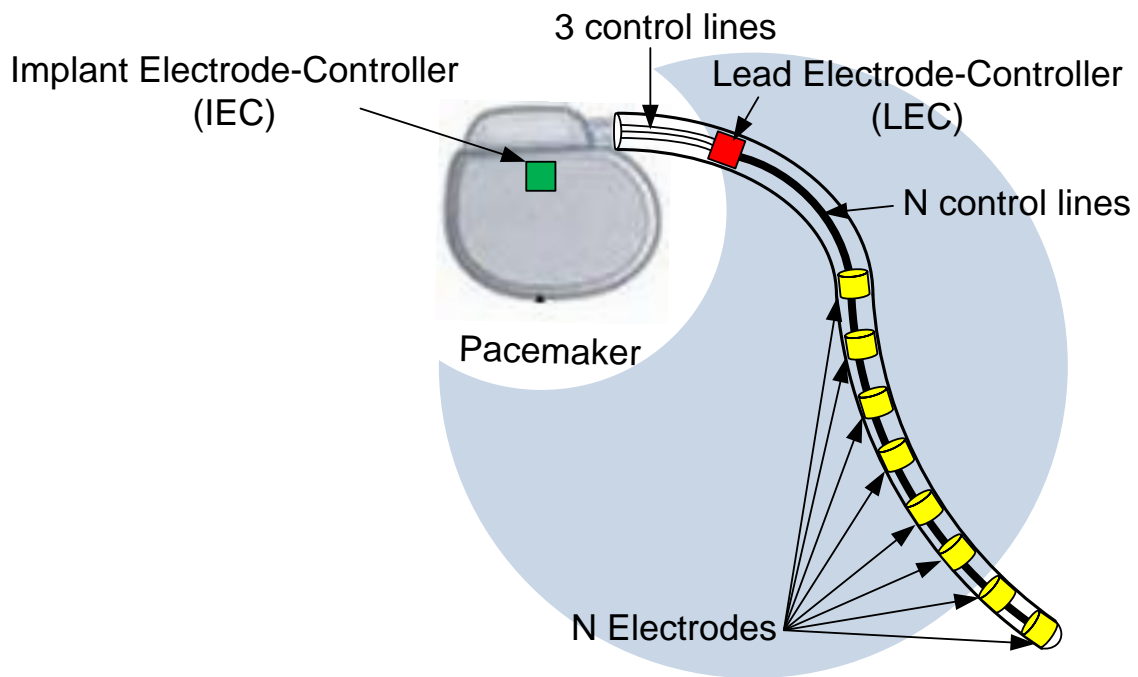


Figure 3-3: Illustration of multi-electrode system with its two control units in the implant and inside the lead (norm compliant)

3.1.2 *Communication protocol: Power and Configuration*

Having chosen to employ a separate electrode-controller inside the lead to manage the multiple-electrodes, we now face the obvious challenge of powering this electrode controller (LEC). Since this LEC has to be placed inside a lead, the dimensions of this LEC have to be very small. Size constraints therefore make it impossible to have on-board battery. We therefore chose to supply power to this LEC by the pacemaker via a dedicated power line.

Since the IEC in the implant should control the LEC in order to configure/manage the electrodes, a communication protocol is needed between the LEC and IEC.

Furthermore in order to minimize the number of wires, we chose to re-use the same wire (line) which we had used for powering. The communication protocol adopted for our system will be discussed in detail in section 3.4.3 of this chapter, but first we present the state of the art of such multi-electrode systems.

3.3 State of the Art

The multi-electrode lead solution is under active research, with several pacemaker manufacturers investigating different possibilities. Unfortunately most of the research exists as propriety intellectual property.

By exploring the patents in the field of multi-electrode systems for cardiac pacemakers, we were able to distinguish three different strategies followed for the implementation of IEC and LEC in order to circumvent the aforementioned constraints. In this section we will summarize these three strategies named: centralized structure, distributed structure and direct structure.

3.3.1 Implementation Strategies for LEC

3.3.1.1 Centralized Structure

In this structure, one electrode-controller unit is inserted at the proximal end (near the implant) of the lead to control all the electrodes (figure 3-4). This LEC acts as a de-multiplexer connected from one side to the implant through two or three control lines, and from the other side connected to the electrodes through a number of control lines equal to the number of electrodes.

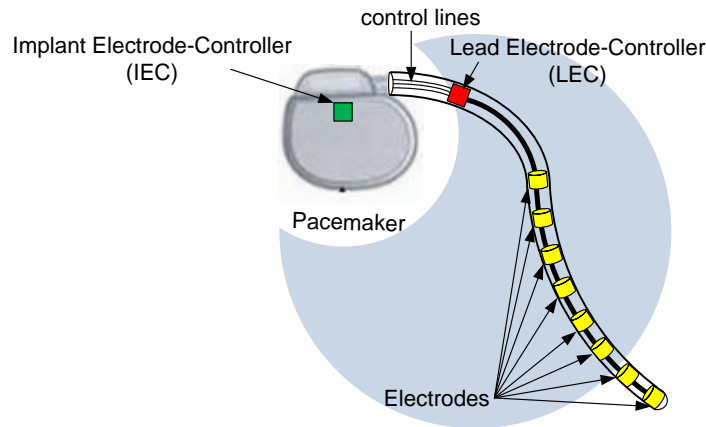


Figure 3-4: Centralized structure for the multi-electrode system

This structure was presented in Sorin Group patent filed by R. Dal Molin et al. [5] where the electrode-controller chip is inserted inside the lead. Two control lines connecting the LEC to the pacemaker while ten wires emanate from the LEC toward the ten electrodes of the lead. The two control lines carry stimulation pulses, configuration bits and power to the LEC according to an implemented protocol. Placing stimulation pulses destined to the heart with other configuration pulses on the same two control lines, may risk triggering cardiac disorders for the patient. That's why the patent suggests means for rapid opening of output switches in the LEC to prevent this risk.

Medtronic Inc. Patent filed by Jelen, Jeff et al. [8] gives another example where the electrode controller had the form of a separate encasement connected to the pacemaker's connector to de-multiplex the control signals toward the electrodes.

The centralized structure offers a reliable multi-electrode solution with less complexity compared to the distributed structure. The inconvenient of this structure may appear in the number of control lines running inside the lead. As the number of control lines between the LEC and the electrodes increase with the number of electrodes in the lead, a big number of lines may decrease the elasticity of the lead which is a key feature for leads.

3.3.1.2 Distributed Structure

In this structure, the LEC is divided into smaller controllers in which each electrode has its associated controller. The number of control lines is the same along the lead regardless of the number of electrodes (figure 3-5).

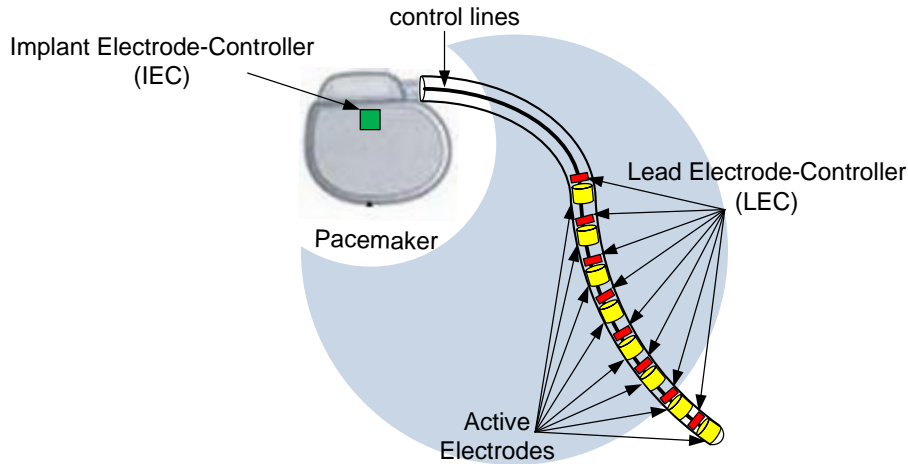


Figure 3-5: Distributed structure for the multi-electrode system

The concept of this structure is adopted in many patents with certain differences in implementation. For instance, Proteus Biomedical, Inc. patent filed by Zdeblick et al [3] presents a distributed structure in which two control lines running along the lead connected to four electrodes. An electrode-controller of unique address is associated to each electrode. The two control lines of the lead carry power, configuration and stimulation pulses to the electrode-controllers. A complex communication protocol based on Phase Shift Keying (PSK) is used to combine all these different patterns present on the two control lines.

Another example is given in the Medtronic, Inc patent filed by R.S. Schallhorn et al [4] but this time with three control lines running along the lead. Two lines (Anode and Cathode) are dedicated for stimulation and power pulses. The third line is dedicated for configuration bits. This patent takes a step further in avoiding the risk of leaking signals other than stimulation to patient's heart. It did that by isolating the transfer of data bits on a separate control line. Despite this step, the risk of DC current transmission to the heart is always present due to power pulses that share the two control lines with stimulation pulses. Cardiac stimulation standards specify that the total average current transmitted to the heart must not exceed 100nA during the whole cardiac cycle. The patent depends on the implemented protocol to minimize this risk.

3.3.1.3 Direct Structure

An exception was made by Saint Jude Medical in their quadripolar (4 electrodes) lead [9] where they used a special 4-wire connector and directly controlled the lead electrodes by an IEC inside the implant. In their solution the number of electrodes in the lead is constrained by the number of wires that can be passed through the pacemaker connector.

3.4 System Design & Implementation

3.4.1 Adopted Strategy

Under our research project we wanted to test two strategies (Centralized and Distributed) in order to adopt the best among them in terms of reliability and treatment efficiency. So we implemented the LEC in the centralized structure with eight outputs to control eight electrodes in the lead. Nevertheless, it can be used in a distributed structure by employing several LEC chips and activating the unique address in the logic of each LEC chip. LEC logic is designed to switch between the centralized and distributed modes through programming.

The support for dual mode functionality impacts the total size of the chip. Of course if the chip is to be used in the distributed structure, there will be no need for eight outputs for the electrodes. But only one output is sufficient to control one electrode in this case.

In order to avoid completely the risk of leaking electrical pulses to the heart other than the stimulation pulses, we made the choice of using a 3-wire interface between the pacemaker connector and the LEC. 2 wires (Anode and Cathode) are used exclusively for stimulation delivery and the acquisition of cardiac signals. The third line is dedicated for the communication protocol between the pacemaker (master) and the LEC (slave). This communication protocol carries power and configuration bits needed for the LEC functionality. The advantage of this method that neither power nor data are shared with the stimulation lines like the case of some patents cited before.

Moreover, we have committed ourselves to ensure the compatibility of our multi-electrode lead with any pacemaker of the market, whether it supports the control of multi-electrode leads or not. We took this further step by implementing an auxiliary switching unit in our LEC which has the role of guarding an active connection between pacemaker and the patient's heart through at least two electrodes without any power consumption. This auxiliary unit permits also low power consumption for the whole system as will be shown in section 3.4.2.6 of this chapter.

3. Multi-electrode System for Left Ventricular Stimulation: Design and Implementation

We also included an additional feature named double stimulation. It consists of the delivery of two consecutive stimulation pulses either on the same electrode configuration or different configuration. This feature opens a new clinical research point which can show its utility in cardiac pacing enhancement. We will further discuss this in section 3.4.3.4 of this chapter.

In this section we will describe in details the important design considerations taken into account during the implementation of the multi-electrode system. In order to minimize the possible confusion during the explanation, we would rather refer in our description to the centralized structure for the multi-electrode system. At the end of this chapter we will highlight the main additional design features made for the distributed structure.

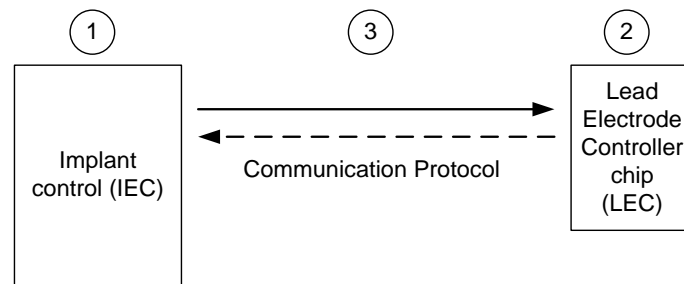


Figure 3-6: Abstraction of the main parts of the system implementation

Multi-electrode system can be abstracted into three components as shown in figure 3-6; implant control (IEC), LEC and the communication protocol linking both sides together. Communication protocol is presented in the figure as a bidirectional path with a dashed return path (LEC \rightarrow IEC). The initial specification was made for a bidirectional communication, but in the implementation of our system's test chip we decided to prove the concept using unidirectional communication. Bidirectional communication is to be implemented in future versions of this system.

3.4.2 *Implant and lead electrode controller (IEC & LEC)*

A conventional control unit inside an implant (pacemaker) manages the sequence of actions and events within the pacing cycle. Pacing cycle is the time between two ventricular or two atrial beats [1]. This pacing cycle consists of three phases: Sensing, Stimulation and Discharge (figure 3-7a).

- During the sensing phase, the pacemaker's sensing channel (section 2.2.1.3) filters and analyzes acquired cardiac signals searching any disorders in the patient's heart activity.
- In case of detected cardiac disorder, a stimulation demand is generated which triggers the output circuit (section 2.2.1.2) to start the stimulation phase and deliver electrical stimulus to the heart on the configured electrodes.

3. Multi-electrode System for Left Ventricular Stimulation: Design and Implementation

- Discharge phase then follows to eliminate residual charges from the electrode-tissue interface as well as the stimulation/sensing path.

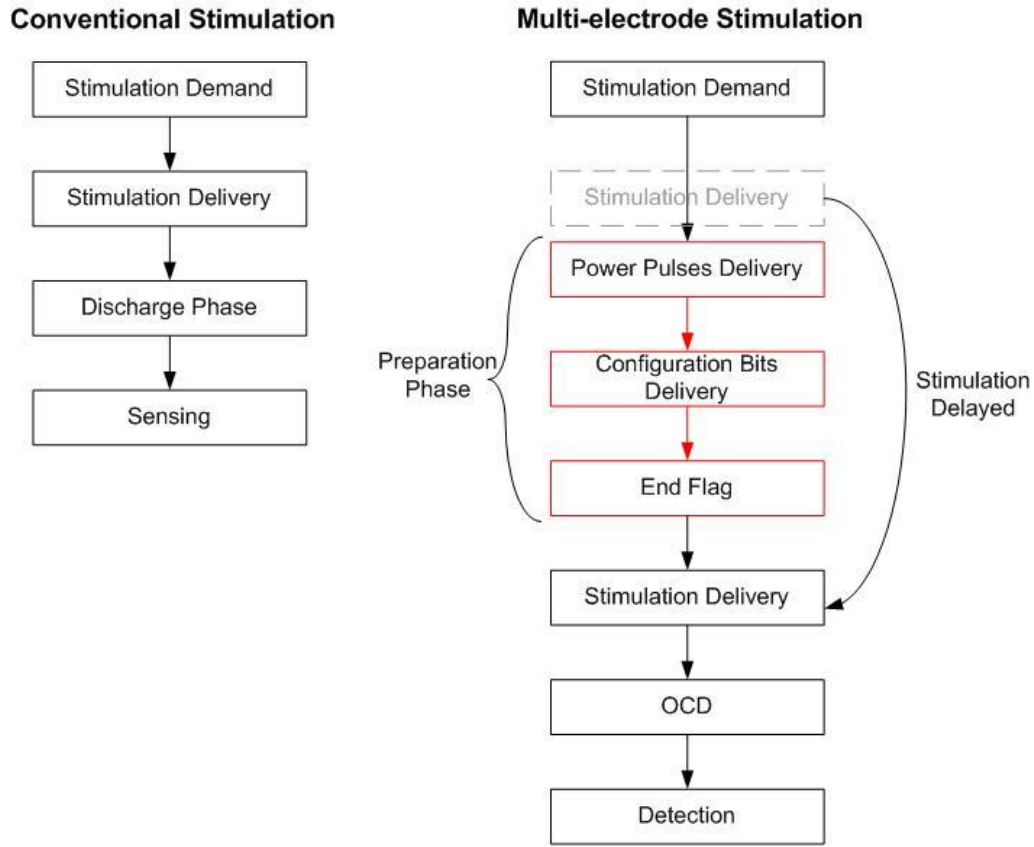


Figure 3-7: (a) phases of conventional pacing cycle (b) pacing cycle after the insertion of the multi-electrode preparation phase

In our multi-electrode system, an additional phase is needed to be inserted between the stimulation demand and the delivery of the stimulus. This phase is named in figure 3-7.b as preparation phase and it has the role of providing the LEC in the lead with needed power and electrodes configuration. However, this additional phase delays the stimulation delivery. Therefore it is crucial to minimize the time of this phase. To do that, high transmission rate is required at the pacemaker as well as high decoding speed at LEC. In section 3.4.3 will discuss in detail how the communication protocol was designed to minimize this preparation delay.

We designed the LEC in the form of a miniaturized ASIC (Application-Specific Integrated Circuit) to be inserted inside the lead as illustrated in figure 3-8. In the centralized strategy of multi-electrode system introduced earlier in this chapter, one LEC controls all the electrodes of the lead according to the configuration received from the implant. Here we give a glance at the main blocks of this LEC chip.

3.4.2.1 Power Storage Unit

Since this LEC has to be placed inside the stimulation lead, the size is very limited and this rules out on-board battery. The alternative solution is to store power pulses sent by the implant on the P&C line (power and configuration line) on a capacitor integrated in the LEC process. As power pulses and configuration bits are multiplexed on the P&C line, the connection between the storage capacitance and the P&C line has to be governed by controllable switches in order to prevent leakage of stored charges during the transfer of configuration bits.

Power storage unit is the only power source for LEC that ensures its functionality during a full cardiac cycle, a capacitor with a considerable size would be needed to maintain sufficient energy for the chip circuitry. Thanks to the implemented protocol, several power pulses are planned to enable the reduction of the storage capacitor size and rather recharge it in a regular basis. This will be more clarified with the explanation of the communication protocol in section 3.4.3 of this chapter.

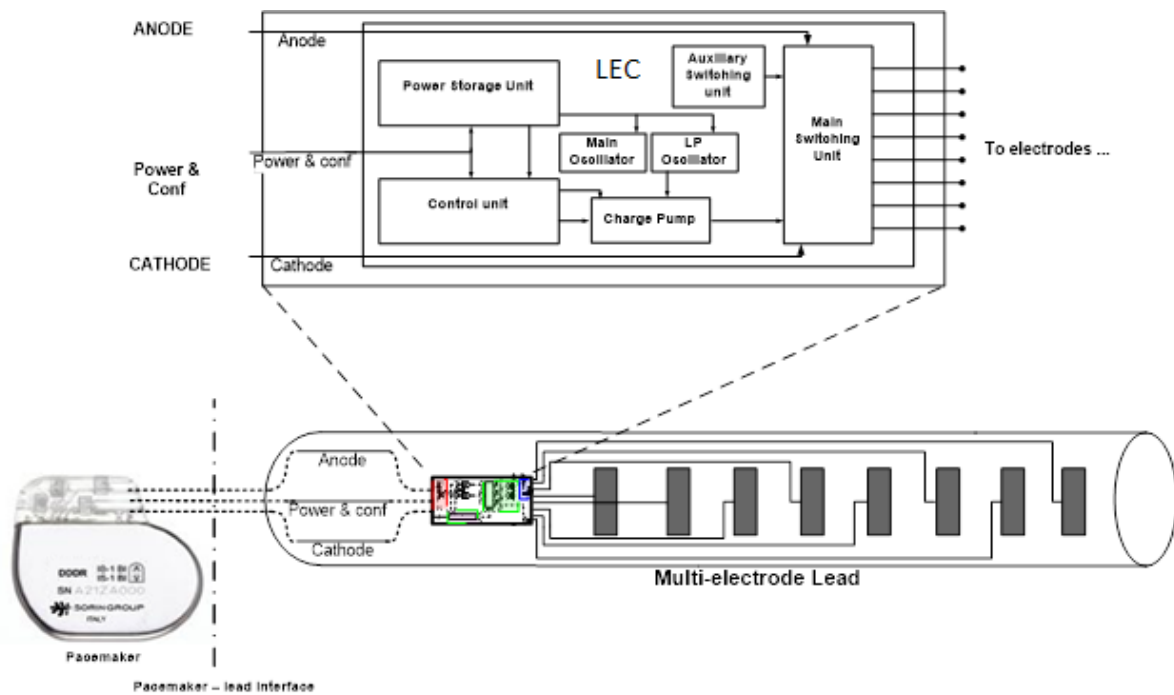


Figure 3-8: block diagram of the LEC (centralized structure)

3.4.2.2 Control Unit

LEC control unit is a custom-designed digital logic in which the communication protocol is implemented. The first and essential role of this unit is to differentiate between power pulses and configuration bits found on the P&C line. The control unit then routes power pulses to the power storage unit, and internally decodes the configuration data bits. Control unit relies on local oscillators to decode the timed digital configuration bits as well as the calculation of different delays used within the communication protocol.

Moreover, the control unit activates both main and auxiliary switching units at precise moments according to the decoded configuration data that indicate the desired state and polarity of each electrode in the lead.

3.4.2.3 Oscillators

As we chose to implement a unidirectional communication protocol between the pacemaker (IEC) and the LEC, the IEC does not receive any acknowledgements or resend demands from the LEC in case of transmission errors. Therefore, timings have to be highly respected in order to ensure correct functionality of the system. Oscillators are used to estimate the needed delays. But as the LEC has a limited power source, the tradeoff between frequency precision and power consumption had to be compromised. We chose local oscillators of $\pm 5\%$ tolerance. This tolerance increases the challenge facing the communication protocol to take in account differences in frequency between master and slave. Two local oscillators of different frequencies one of high and another of low frequency are used in the LEC chip as follows:

Main Oscillator: runs at 1MHz frequency and used for rapid decoding of configuration bits. The faster the decoding, the shorter the preparation phase inside the LEC that results in shorter delay between stimulation demand and stimulation delivery as discussed earlier. It is also used in the estimation of short delays in the communication protocol.

This high frequency oscillator is of considerable power consumption. Therefore it is disabled by the end of the decoding phase. The low power oscillator continues to work till the end of the functional cycle.

Low Power oscillator: runs at 32 KHz which has lower power consumption when compared to the main oscillator. This oscillator is used at the end of the cardiac cycle to estimate the long delay needed for the Discharge phase (13ms). This permits the LEC to function in a lower power mode till the end of the cardiac cycle. Another block plays an important role in lowering the power consumption of the LEC. This block is named auxiliary switching circuit and will be explained later in this section.

3.4.2.4 OTP Memory

OTP or One Time Programmable memory is used to store trimming codes that correspond to the most precise value for the oscillators' frequency. These trimming codes are validated during the test phase of the chip. Once validated, the codes are burned inside the OTP to ensure the stability of the oscillators' frequency.

3.4.2.5 Main Switching Unit

The "Main switching unit" defines the path of stimulation from the pacemaker to the heart, and it is composed mainly of high voltage MOS switches in order to support the voltages (tens of volts) and currents (tens of mA) of stimulation pulses delivered to the heart. The choice of a high-voltage manufacturing technology was compulsory to support stimulation voltages and currents.

The path between the pacemaker and the configured electrodes has to be maintained by keeping the configured MOS switches active. The control unit maintains this during stimulation and discharge phases. During the sensing phase, the auxiliary switching unit takes over this role to transmit cardiac signals to the pacemaker.

3.4.2.6 Auxiliary Switching Unit

By the end of the multi-electrode preparation phase, the LEC has performed its job in preparing the stimulation path according to configuration chosen by the pacemaker. This is achieved after correctly decoding configuration bits and activating correspondingly concerned electrodes through the switching unit (HV MOS switches). LEC's role extends beyond the preparation phase in order to ensure the stability of configuration on its electrodes through maintaining the power on its switching unit till the end of the pacing cycle.

An auxiliary switching unit is activated in the LEC when power level drops. This unit is able to maintain the connection between electrodes and pacemaker without any power supply. In a first implementation we used JFET switches. JFET switches are normally active while to disconnect them a power is needed to force the inactive state. This auxiliary switching unit keeps the connection between pacemaker and electrodes even when the LEC power vanishes. This is the case during the sensing phase. It is difficult to estimate a fixed duration for this phase in order to size the storage capacitance according to it.

Another advantage of using such an auxiliary switching unit is **to ensure a compatibility with any pacemaker implant found in the market**. The fact that this auxiliary switching unit is connected without power source, it ensures a minimal connection in the multi-electrode lead in order

3. Multi-electrode System for Left Ventricular Stimulation: Design and Implementation

to act as a simple bipolar lead. This connection is independent of any specific communication protocol that may exist in any multi-electrode system. This is an additional advantage for our system over the other multi-electrode solutions.

In chapter 4 we will present another way to better implement the auxiliary switching unit or as we will call it (Default Connection Unit).

3.4.2.7 Charge Pump

For driving the HV MOS switches inside the main switching unit, a charge pump (DC-DC converter) is needed to up-convert the stored energy on our on board capacitor (Power storage unit) into the control voltage levels needed to maintain the pass/blocked states of the HV switches interfacing with the heart.

3.4.3 Communication Protocol

The communication protocol between IEC and LEC was first specified as a bidirectional to ensure the correctness of configuration reception at the LEC. This preliminary specification was made in collaboration between Sorin and CEA Leti and it was made for a 2-wire interface between pacemaker and the lead. In this first protocol, power pulses and configuration bits shared the same 2 wires in the lead with the stimulation pulses. Due to the risk of leaking configuration bits and power pulses to the patient's heart, we decided to define a new specification for the communication between the IEC and LEC.

In our implementation of these test chips (IEC & LEC) we were constrained specially in the IEC by the analog resources available on the conventional implant (pacemaker) chips. We were only allowed to modify the existing blocks and adapt them to our new multi-electrode functionality without adding new analog blocks. Therefore the only way was to implement our multi-electrode solution (IEC) digitally inside the implant with the least analog modifications. Another constraint was dictated by the clinical need for ensuring the possibility of delivering double stimulation (successive stimulation pulses with minimal separation delay) with different or same electrode configurations as will be discussed later in section 3.4.3.4. Adding this double stimulation feature led to an increase in number of bits required to configure the electrodes twice, and required a specific management of the implant's limited resources to be taken into consideration in the communication protocol. These constraints pushed us in the direction of defining our own communication protocol in which the power pulses and configuration bits are isolated from the patient's heart on a third dedicated wire. The above mentioned aspects also precluded the use of any standard communication protocol.

3. Multi-electrode System for Left Ventricular Stimulation: Design and Implementation

As introduced in Fig. 3-7, the preparation phase has to be as short as possible so as not to delay the stimulation delivery. Therefore, the transmission of configuration bits ($\text{IEC} \rightarrow \text{LEC}$) as well as acknowledgement transmission ($\text{LEC} \rightarrow \text{IEC}$) had to be made as fast as possible. In the same time, the tradeoff between rapid transmission rate and power consumption has to be well managed through the choice of the oscillators' frequency.

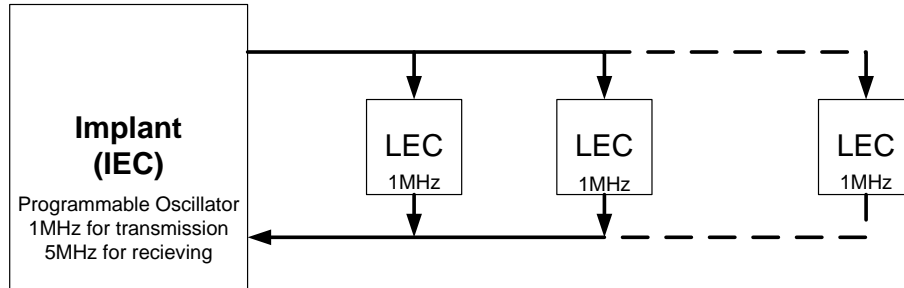


Figure 3-9: example for bidirectional communication between IEC and LEC

We now discuss an example of this tradeoff management. Figure 3-9 illustrates the implant communicating with several LEC units and vice versa. Due to the limited power resources in LEC, we fixed its frequency at 1MHz. at the implant side re-used its programmable oscillator (1MHz – 5MHz). Based on the oversampling concept, the receiving unit should work at a frequency faster than that of the sending unit. Therefore during $\text{IEC} \rightarrow \text{LEC}$ transmission, IEC uses its 1MHz frequency and construct each bit over 4 clk cycles (about 250 KHz transmission rate). On the other side the LEC will sample at its fixed 1MHz frequency, therefore its sampling frequency appears to be faster than the sending one.

During $\text{LEC} \rightarrow \text{IEC}$ transmission, LEC uses its fixed 1MHz frequency. On the other side the IEC samples at its highest frequency of 5MHz, therefore its sampling frequency also appears faster than that of the sending unit. By this strategy we reached a good compromise between fast transmission and lower power consumption at the LEC.

In our implementation of this test-chip, we kept only the IEC-LEC part to make a unidirectional communication protocol and kept the implant CLK frequency at 1MHz. This added another challenge for the LEC to correctly decode the sent configuration in one shot as there will not be any data resend from the IEC. We will show in this section how the communication protocol resolved all these difficulties.

3. Multi-electrode System for Left Ventricular Stimulation: Design and Implementation

We custom-designed our communication protocol at both ends: pacemaker and LEC. Pacemaker plays the role of master in this protocol as it initiates the communication and provides power and data. In return the LEC plays the role of slave and is required to manage power and to process received data.

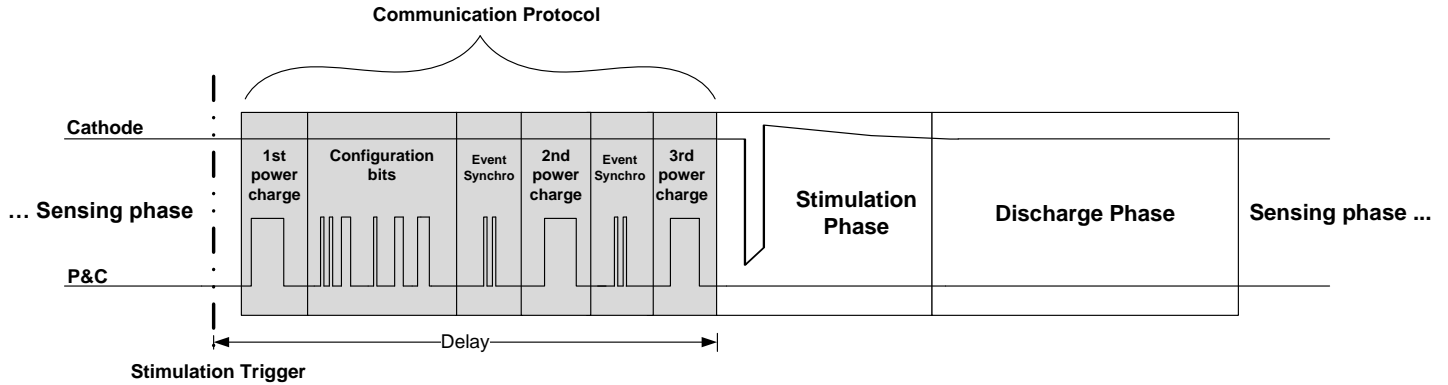


Figure 3-10: the different phases of the communication protocol

Firstly the pacemaker sends a first powering phase (fig. 3-10) to wake-up the LEC and activates its circuitry. Once the LEC is activated, the pacemaker sends the configuration bits which informs the LEC about the set of electrodes to be activated and their polarities. LEC decodes configuration bits to extract this information then waits for pacemaker's order (Event Synchronization) to activate selected electrodes according to this configuration.

These "Event Synchronization" phases are planned with specific timing to synchronize the LEC actions with events taking place in the pacemaker. Once the electrodes have been activated, the stimulation is delivered to the cardiac tissues. We note here that these activated electrodes have to maintain their configuration till the end of pacing cycle. Therefore additional power phases are also planned to ensure sufficient power level in the LEC to maintain its configured state till the end of the pacing cycle.

High transmission rate is required at pacemaker as well as high decoding speed at LEC. Two independent local oscillators (LO) running at 1MHz are implemented, one at pacemaker and the other at LEC. At such high frequency, the consumption in a power limited chip such as LEC is considerable. We save power by deactivating the LEC's 1MHz LO after the transmission of configuration bits ends. Another low power oscillator in the LEC takes over till the end of pacing cycle.

The communication bits can be classified into three types as follows:

3.4.3.1 Power pulses

The first phase of power pulses sent by the pacemaker on the P&C line serves as a wake up for the LEC. This phase would have been sufficient for the whole activity of the LEC if a big capacitor could be used inside its power storage unit. But as the size of capacitor significantly affects the overall size of the LEC, we chose to reduce the capacitor's size and repeat several power phases over the activity duration as shown in figure 3-10. The power charging phases were placed before every power consuming activity planned for the LEC circuits to accomplish. Besides waking up the LEC, this first phase ensures that there is sufficient power for the configuration phase. The second power phase precedes the switching unit's activity of applying the chosen configuration on its MOS switches. The last power phase is placed just before the stimulation phase to make sure that the switching unit has sufficient energy to maintain the state of configured electrodes during the stimulation phase and the discharge phase following it.

3.4.3.2 Event Synchronization bits

Event synchronization bits are inserted before the actions expected to be done by the LEC at a specific moment. An example of these time specific actions is the enabling/disabling of the circuitry in the LEC responsible for connecting the P&C line to the power storage unit. In order to charge the power storage unit, we have to connect the P&C line to it and then once the powering phase is over we have to immediately disconnect it from the P&C to avoid discharge via leakage. Moreover these event synchronization bits help the LEC control unit to differentiate between communication bits and power pulses

3.4.3.3 Configuration bits

Configuration bits carry the information of activity and polarity of each electrode along the multi-electrode lead. This information is named here "data bits". Other types of bits such as "calibration" and "sync" are inserted and organized as shown in (fig. 3-11) to complete the structure of the configuration bits.

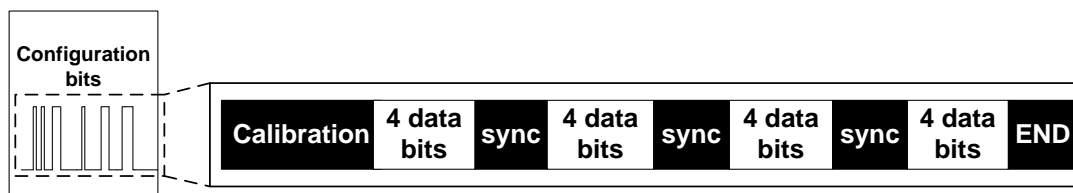


Figure 3-11: different types of bits that compose the configuration train

3. Multi-electrode System for Left Ventricular Stimulation: Design and Implementation

Data bits are written by the pacemaker at a clock frequency equivalent to 250 KHz (bit length = four clock cycles of 1MHz). The LEC at its end decodes using a 1 MHz clock. This method ensures correct decoding at the LEC despite the fact that both pacemaker and LEC oscillators run at 1MHz.

Data decoding is based on counting clock cycles per bit in order to acquire its value near its middle. Due to activation/deactivation of the LEC's LO for power management purposes, LEC's LO is not in phase with that of PACEMAKER and not highly precise, which can erroneously estimate the bit length at LEC side. To avoid this, we implement three mechanisms:

- Calibration: this mechanism estimates the number of clock cycles that make up a bit according to the LEC's LO.
- Data synchronization: within the frame, one "sync bit" is added after each 4 data bits. This helps us avoid the propagation of errors within the frame. This approach is similar to the asynchronous start-stop data communication used in character synchronization in ASCII [6].
- Frame Synchronization: Each frame is time-shifted so as to be synchronized with the LEC clock. This ensures that the decoder counts correctly the length of each bit based uniquely in complete clock cycles. (In number of clock cycles).

3.4.3.3.1 Calibration

Calibration phase allows the LEC to estimate the length of a bit using its local oscillator. In the beginning we chose to make the calibration by adding an extra bit of the same length as a data bit, in the beginning of configuration train. As an example, figure 3-12a illustrates the calibration bit written on the P&C line, as well as the two clocks of pacemaker and LEC. Assuming LEC clock frequency is 5% less than pacemaker frequency due to imprecision in LEC's LO, the LEC may estimate the length of a 4-cycles bit to be sometimes $r=3$ and others $r=4$, where (r) is the number of clock rising edges used to estimate the bit length. This imprecise estimation cannot be accepted. Therefore we decided to improve the precision by adding two calibration bits instead of one (fig. 3-12b). The estimation may also give two different values for the bit length, either $r=7$ or $r=8$. So we decided to include the number of clock falling edges (f) in the count to further improve the precision of estimation.

Hence, the estimation (cal) of one single bit length is calculated using (3)

$$cal = \frac{r+f}{4} \quad (3)$$

3. Multi-electrode System for Left Ventricular Stimulation: Design and Implementation

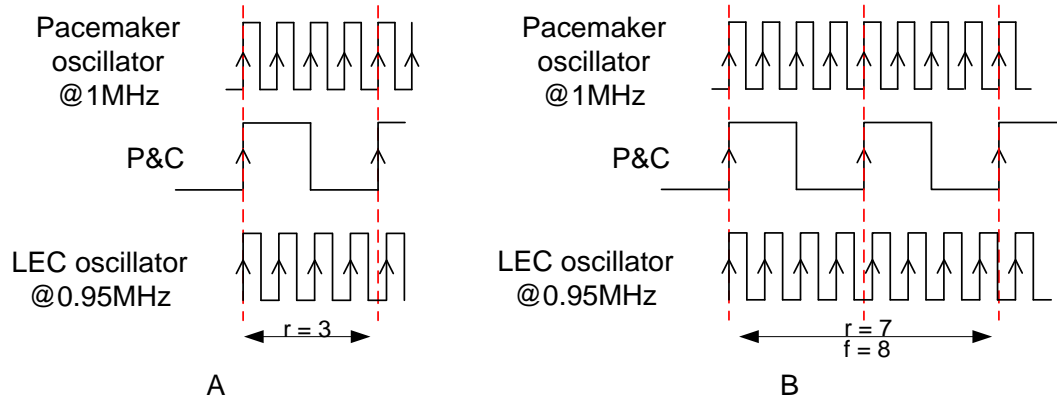


Figure 3-12: Example of error in estimation during calibration phase. (LEC; Lead-Electrode Controller)

(Cal) will not always be a whole number, so depending on the value (D) after the decimal point calculated using (4), decoding strategy will change as shown in (5).

$$D = \text{cal} - \text{foot cal} \times 100 \quad (4)$$

$$\text{count} = \begin{cases} \text{foot cal} , & D < 50 \\ \text{ceiling cal} , & D \geq 50 \text{ and } i = \text{odd} \\ \text{foot cal} , & D \geq 50 \text{ and } i = \text{even} \end{cases} \quad (5)$$

Where “i” is the bit number in a nibble of four data bits, it varies from 1 to 4. Equations (3), (4), (5) are used to solve uncertainty in estimating the bit length during the calibration phase.

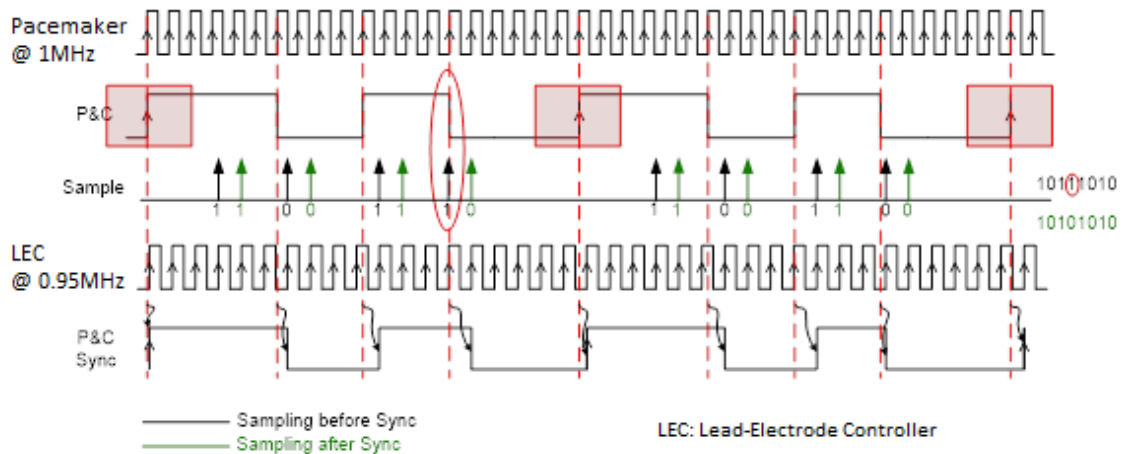


Figure 3-13: Example of error in data decoding due to frequency difference

3.4.3.3.2 Data Synchronization (Sync bits)

A Sync bit is a kind of delimiter inserted periodically every 4 data bits. Its form is always a low-to-high transition (rising edge). Its role is to limit the propagation of any decoding error to the rest of data. When the LEC's control unit finishes decoding the first four data bits, it uses this sync bit to reset the bit counter and starts counting to acquire the next 4 data bits.

To guarantee the maximum reliability of the decoding, a sync bit should be inserted after each data bit. But it is impractical if the number of bits is big as it doubles the time required for transmission. The choice of the insertion frequency of sync bits in the configuration train was made in function of the number of data bits in the train, data bit length and the time available for transmission.

3.4.3.3.3 Frame synchronization

After showing the importance of Calibration phase and Data Synchronization in ensuring correct decoding, a third method has to be added (Frame synchronization). To understand its role we would give an example in reference to (fig.3-13)

The upper signal (PACEMAKER@1MHz) represents the pacemaker's clock running at 1MHz. (LEC@0.95Mhz) signal represents the LEC's clock running at 0.95MHz to represent a frequency difference of (-5%) in comparison with pacemaker's clock frequency

(P&C) signal here shows a part of the configuration bits on the P&C line with three Sync bits marked with red rectangles, and 4 data bits between each pair of Sync bits. According to calculations made in (3) and (4), Calibration showed that bit length estimation is ($cal = 3.75$), therefore $D = 75$. According to (5) the decoding strategy will be as follows: Starting from the rising edge of the 1st sync bit, the decoder counts 4 clock cycles to acquire the value of the 1st data bit, then count 3 clock cycles to acquire the value of the 2nd data bit, then count 4 clock cycles to acquire the value of the 3rd data bit and finally counts 3 clock cycles to acquire the value of the 4th data bit. (i.e. counted 4 for odd "i" and 3 for even "i"). The same sequence is repeated for the next four data bits after the 2nd sync bit and so on till the end of data. Black arrows mark the positions where the values of data bits are captured using the explained strategy. The error is caused by the dephasing between LEC's clock and pacemaker's clock which resulted in counting an incomplete clock cycle as one. Added to this the difference in frequencies, the error was propagated and appeared in the last bit in the first nibble (circled in red).

3. Multi-electrode System for Left Ventricular Stimulation: Design and Implementation

To avoid counting incomplete cycles we decided to shift the configuration bits after the calibration phase on the LEC's clock (P&C sync in fig. 3-13). The green arrows show the positions where the values of data bits are captured on the original P&C signal using the explained strategy.

In conclusion, combining these three mechanisms together enables the LEC's control unit to correctly decode the received data.

3.4.3.4 Double Stimulation

Another advantage of our system is the double stimulation. This is the possibility of delivering two successive stimulation pulses in less than $5\mu\text{s}$. These pulses are delivered either on the same or different electrodes with same or different polarity. This feature opens a new clinical research point which can show its utility in cardiac pacing enhancement.

Another utility of this double stimulation is the biphasic stimulation option. If for the first stimulation pulse, electrodes were configured to a first polarity then it is inverted for the second pulse, we obtain a biphasic pulse as shown in figure 3-14. Biphasic pulses can effectively reduce the discharge phase time.

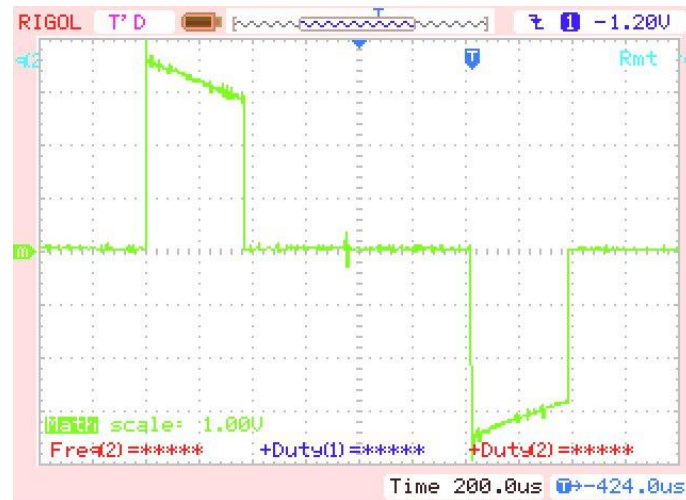


Figure 3-14: Biphasic stimulation pulses as an example of double stimulation mode

3. Multi-electrode System for Left Ventricular Stimulation: Design and Implementation

3.4.4 Comparison

In this section we summarize the key features of our multi-electrode system and compare it with other multi-electrode systems found in patents as shown in Table 3-2.

Table 3-2: comparison of our solution with other multi-electrode systems found in patents

		Distributed Structure		Centralized Structure	Direct Control Structure
	Our Work	Proteus Medical [3]	Medtronic [4]	Sorin Group [5]	St Jude Medical [9]
Number of LEC units	1	Several	several	1	0
Connector Interface	3	2	3	2	4
Number of lines in the lead	N	2	3	2	4
Lead Compatibility with other pacemakers (without multi-electrode support)	Yes	Not mentioned	Not Mentioned	Not Mentioned	Not Mentioned
Double Stimulation	Yes	Not mentioned	Not Mentioned	Not Mentioned	Not Mentioned
Power transfer	Dedicated P&C line	Shares stimulation lines	Shares stimulation lines	Shares stimulation lines	-
Configuration transfer	Dedicated P&C line	Shares stimulation lines	Dedicated line	Shares stimulation lines	-
Power supply availability	Not always	Always	Always	Always	Always

3.5 Distributed Structure

In order to test the possibility of implementing the multi-electrode system in the distributed structure, we designed our control unit in a way that permits the LEC chip to be used in both modes. The details of implementation discussed in section 4 apply completely to the distributed structure mode. Figure 3-15 shows the distribution of LEC chips along the lead and their association to electrodes.

A first difference between centralized and distributed modes is the number of LEC chips used. Now the pacemaker communicates with several slaves (LEC chips) in the lead. This requires a differentiation between these slaves. Inside each LEC chip, a unique address is burned into its OTP memory. According to the address sent by the pacemaker, only the concerned chips respond and are activated.

3. Multi-electrode System for Left Ventricular Stimulation: Design and Implementation

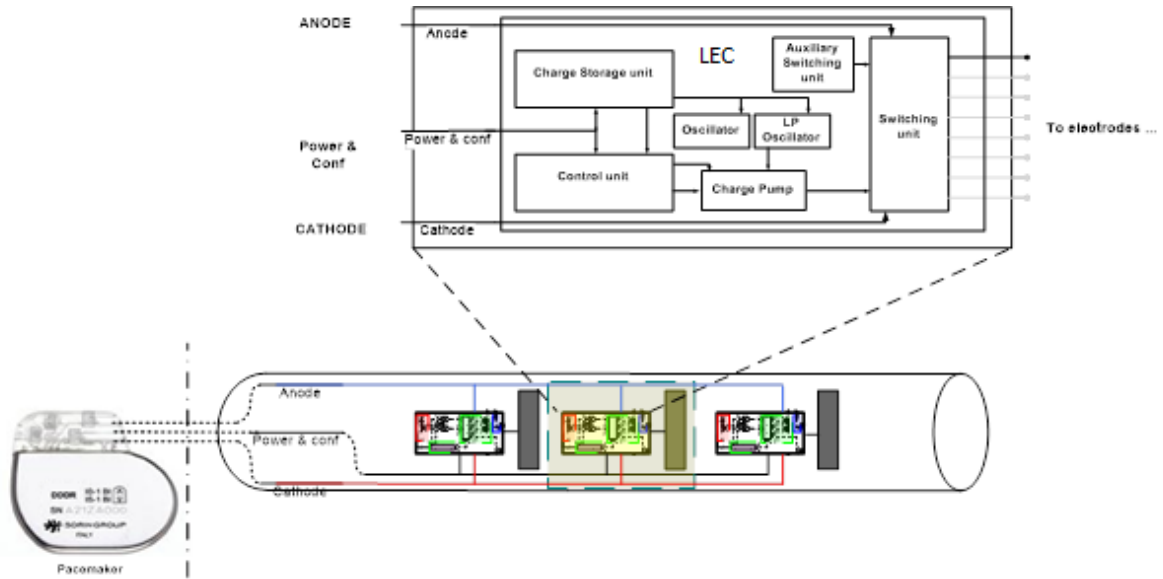


Figure 3-15: Block diagram of multi-electrode system (distributed structure)

A second difference between centralized and distributed modes is the number of electrodes controlled by the LEC chip. In the distributed mode, only one electrode is to be controlled by each LEC chip. This means that in our implementation that 7 LEC outputs are deactivated as shown in figure 3-15.

The distributed mode's first target is to reduce the size of the electrode controller chip. We can imagine how much we can gain only by decreasing the number of output pads from 8 for example to one. This was not explicitly showed in our implementation due to the dual mode functionality ensured by our system. This dual mode may justify the non-optimal size for our LEC chip.

3.6 Measurement Results

The full solution LEC chip was taped out in $0.18\mu\text{m}$ technology. This technology is suitable for high voltage presented in the stimulation pulse and has a very low leakage profile. Table 3-3 summarizes the chip features.

On fig. 3-16, we see that the capacitor takes up a sizeable portion of the total area. For future work we aim to further improve size of system so that it can be fitted to standard 6 French (2 mm) diameter pacemaker lead.

3. Multi-electrode System for Left Ventricular Stimulation: Design and Implementation

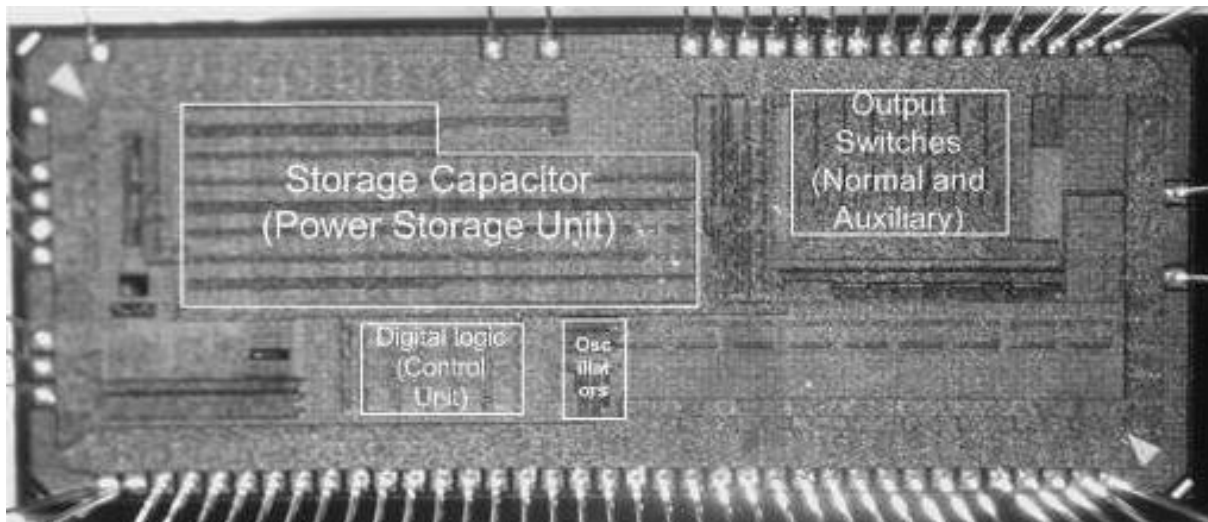


Figure 3-16: LEC chip microphotograph

Table 3-3: Chip Summary

Technology	0.18 μm
Area	2.25x5.35 mm ²
Average consumed current per cardiac cycle	206.3 nA
Time for configuration	2 ms
Clock frequency	1 MHz
Operating voltage	1.8V
Clock frequency tolerance	-20% to 40%

Our new chip consumes 206nA per pacing cycle. This additional consumption is negligible compared to the overall pacemaker consumption of few micro Amps [7].

Our system takes 2 ms to respond to a stimulation demand requested by the pacemaker. Conventional systems without multi-electrode management, take about 500 μs to respond to such a demand. The delay caused by configuration phase is negligible in our system and justified for all the advantages provided.

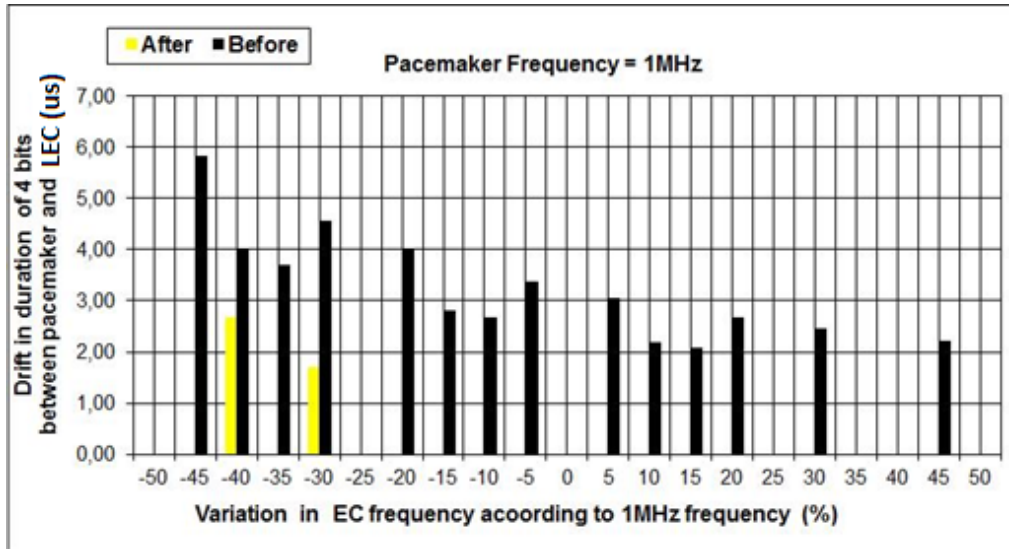


Figure 3-17: Errors in decoding before and after the application of our communication protocol

Our implemented communication protocol tolerates difference in oscillator frequency whether it is in the increasing or decreasing direction, thanks to calibration phase and the accompanying calculations which helped in refining the estimation of bit's length. The chart in fig. 3-17 compares decoding error rate between an older version of our communication protocol marked in red, and our latest version explained in detail in section IV, marked in green. In this test we fixed pacemaker's frequency at 1MHz and kept varying the LEC's frequency from 0.55MHz (-45%) up to 1.45MHz (+45%) with a step of 50 KHz. The frequency range tolerance was observed to be from - 20% to +40% as it appears in the chart.

Fig. 3-18 shows the P&C signal (yellow) comprising communication and power as observed during chip validation.

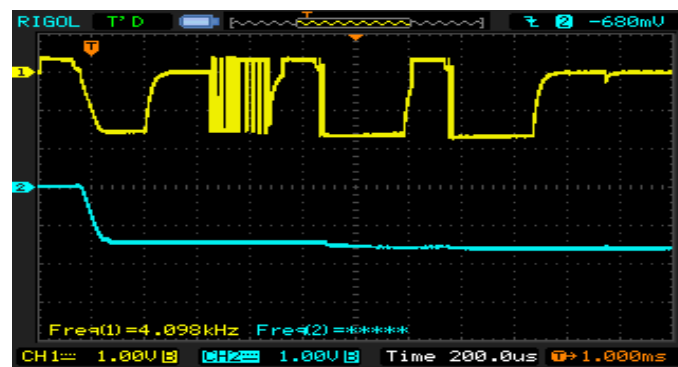


Figure 3-18: signal on P&C line as observed during chip validation

3.7 Conclusion

In this chapter we presented the different design aspects for our multi-electrode system in its two structures (centralized and distributed). We showed how we modified the implant's control in order to drive our custom-designed electrode-controller inserted inside the lead. The system helps in overriding the limitations of left ventricular stimulation by adding more flexibility for the choice of stimulation sites through its selective control of up to 8 electrodes with the possibility of interchangeable polarity for each. The re-configurability of lead electrodes suppresses the need for post-implant surgery in case of inhibition of patient response to stimulation caused by lead displacement.

We implemented a one-wire communication protocol that tolerates difference in oscillator frequencies between the implant and the electrode-controller. According to this protocol, power pulses and configuration bits shared the same line, leaving Anode and Cathode lines for stimulation and sensing purposes. This enabled the isolation of patient's heart from data and power pulses. Moreover it resulted in a norm-compliant 3-wire connector interface.

Our system is distinguished by ensuring compatibility of our multi-electrode lead with any pacemaker in the market thanks its auxiliary switching unit. The concept was proved using discrete JFET switches. In chapter 4 we will present a better solution named "Default Connection Unit" to be integrated within the electrode-controller chip process.

Another notable feature in our system is its capability of delivering two consecutive stimulation pulses of same or different polarities as configured. This feature enables biphasic stimulation which may reduce the discharge period that follows the stimulation phase.

Publications

1. I. Seoudi, K. Amara, F. Gayral, A. Amara, R. Dal Molin “Multi-electrode system for pacemaker applications” IEEE ICECS 2011
http://ieeexplore.ieee.org/xpl/freeabs_all.jsp?arnumber=6122230
2. I. Seoudi, K. Amara, F. Gayral, A. Amara, R. Dal Molin “Innovative Multi-electrode Communication Scheme for Cardiac Pacemakers” TBME 2012 (submitted – under review)

References

- [1] K. A. Ellenbogen MD and M. A. Wood MD “Cardiac Pacing and ICDs” fifth edition, Blackwell Publishing 2008.
- [2] S. J. Asirvatham “Implanting a left ventricular pacemaker lead” Indian Heart J. 2007 Mar-Apr;59(2):197-204.
- [3] Zdeblick “Implantable satellite effectors” US patent: US7640060B2
- [4] R.S. Schallhorn, G.W. King, G.A. Hrdlicka “Selective activation of electrodes within an implantable lead” US patent: US6473653B1
- [5] R. Dal Molin, A. Ripart “Circuit for controlled commutation of multiplexed electrodes for an active implantable medical device” US patent: US2008/0177343A1
- [6] R. Horak “Telecommunications and data communications handbook” Wiley 2007
- [7] F. Silveira, D. Flandre “Low power analog CMOS for cardiac pacemakers: design and optimization in Bulk and SOI technologies” Springer 2004
- [8] US Patent 7254443 B2 of Medtronic
- [9] Quartet™ Quadripolar, Left-ventricular Pacing Lead.
<http://www.sjmprofessional.com/Products/Intl/Pacing-Systems/Quartet-Quadripolar-Left-ventricular-Pacing-Lead.aspx>

4. Default Connection Unit

Chapter 4

Default Connection Unit

4. Default Connection Unit

4.1 Introduction

In the previous chapter we described the multi-electrode solution which allows programmable multi-site stimulation. The multi-electrode solution needed specialized electronics in the pacemaker and also in the lead to enable its operation. While the multi-electrode systems is indeed a much needed advancement in cardiac therapy, especially in the biventricular stimulation, which we discussed at length in the preceding chapters; the multi-electrode system necessitates the presence of mutually compatible controllers in the lead and the pacemaker (the LEC and IEC). In the previous chapter we described our own implementation of these two controllers, however in the real world, situations might arise which limit the operation of such a solution. One such situation, which frequently occurs, is the replacement of the pacemaker system. Due to depletion of battery, or general malfunctioning of the pacemakers, physicians often replace the implanted pacemakers with new pacemakers.

However, since the multi-electrode implementation is proprietary, the multi-electrode lead cannot be used with a new pacemaker not explicitly designed to control it. As the cardiac pacemakers have limited lifetime (5 to 7 years), after which it must be replaced, lead compatibility is crucial, indeed leads are not necessarily replaced during this operation as their lifetime is normally superior to 10 years and their replacement is much more complicated than the pacemaker replacement.

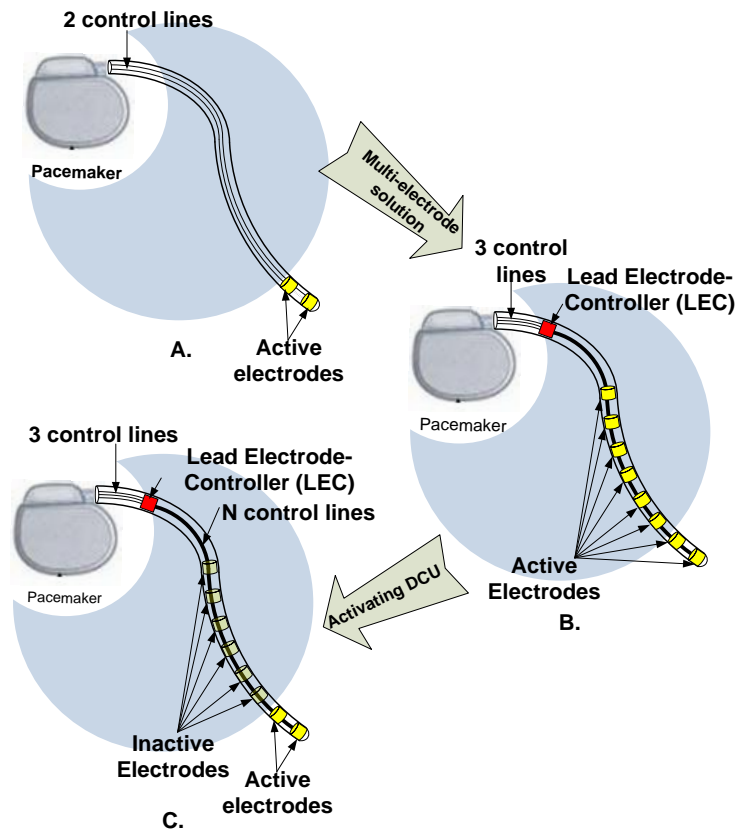


Figure 4-1: (a) Simple bipolar stimulation lead, (b) Multi-electrode stimulation lead with an electrode-controller LEC, (c) Multi-electrode stimulation lead with the DCU activated resulting in a bipolar lead

In the multi-electrode solution presented in chapter 3, several electrodes were inserted along the stimulation lead connected to an electrode-controller (LEC) at one end of the lead. The LEC configures the multi-electrode lead, by selectively enabling the appropriate electrodes and choosing their polarity (cathode or anode). Since LEC inside the lead obtains this configuration information from the pacemaker, the LEC effectively acts as an interface between the Pacemaker and the electrodes (Fig. 4-1b). A specific power and communication protocol was implemented partially in the LEC and partially in the pacemaker.

In this chapter we present a solution to solve the lead compatibility problem by adding a switching structure to the existing LEC. This switching structure, called DCU (Default Connection Unit), *allows the multi-electrode lead to function as a standard bipolar lead (fig. 4-1c) without the need for additional configuration or power supply. DCU is designed to be autonomous and independent of any communication protocols between pacemaker and LEC.*

The key features of the DCU can be resumed in three points:

- a) “Normally-ON” switch,
- b) Low R_{on} resistance,
- c) Can be disabled (turned off) when needed.

We first addressed the lead compatibility problem by using the auxiliary switching unit as presented in chapter 3. JFET switches were used as discrete components in the auxiliary switching unit to prove the concept. Even though some of the features brought by the DCU can be fulfilled by alternate technologies such as JFET, depleted MOS, etc., these technologies are generally not available in process technologies used by medical device industry (pacemakers etc.)

Our DCU structure can be adapted to any process as it is based on ordinary MOS transistors and therefore presents a versatile solution. Other solutions on the other hand were only available as discrete components and hence were unviable owing to size constraints of the LEC chip.

4.2 Design Challenges and Choices

Figure 4-2 shows the block diagram of the LEC which houses the DCU and its interfaces with pacemaker and electrodes. In the dedicated stimulation lead, since the needed energy for LEC chip could not be recovered from the anode and cathode only, power is supplied to the LEC chip by using an additional cable (P&C line in fig. 4-2 to transfer power pulses and configuration bits [1]. This transfer is done using a specific protocol between LEC and pacemaker which is then decoded by the

4. Default Connection Unit

LEC's control unit [1]. The anode and cathode lines carry the stimulation energy from pacemaker to the electrodes.

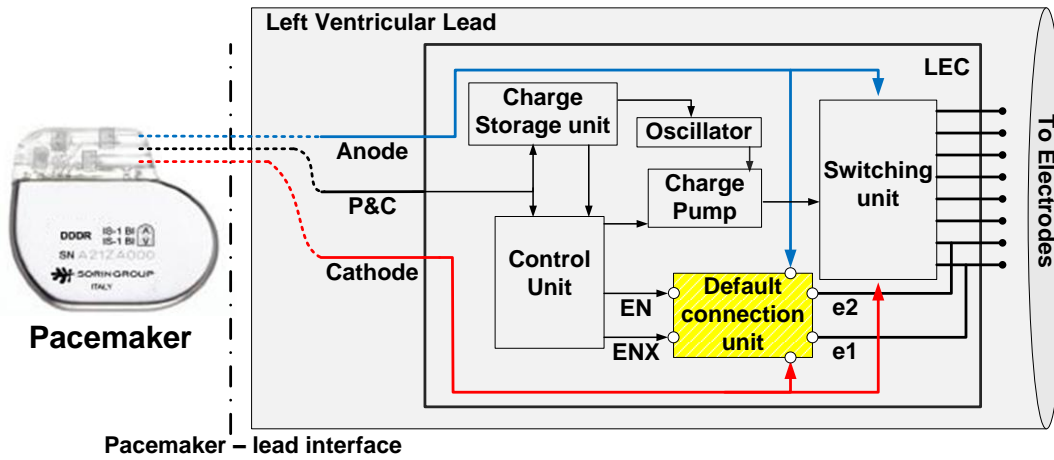


Figure 4-2: Lead Electrode Controller blockdiagram including the DCU

Despite the fact that the DCU is integrated inside the LEC, they function alternatively as described in table 4-1. Since the P&C line is also used for communication besides powering, a specific protocol had to be devised to that effect. Furthermore since DCU is active when LEC is inactive, it renders the DCU transparent to any such protocol mechanism between LEC and pacemaker. Therefore, P&C line cannot be used to provide the DCU with needed power as it is the case with LEC. Hence, the DCU was designed to use available energy on Anode and Cathode to power itself.

Table 4-1: Operation modes

	LEC	DCU
Multi-electrode mode (Fig. 4-1b)	Active	Inactive
Default mode (Fig. 4-1c)	Inactive	Active

The amount of energy available on the Anode and Cathode varies in each phase of the pacemaker's pacing cycle. Pacing cycle consists of three phases named "Stimulation", "Discharge" and "Sensing" [1]. During the "Stimulation" phase Anode & Cathode carry the stimulation pulse from the pacemaker to the selected electrodes. This stimulation pulse has amplitude that varies from -2V to -8V for a maximum duration of 1ms. During the "Discharge" phase, residual charges on the electrode-tissue interface is drained through Anode & Cathode. This discharge voltage reaches approximately +1V for a duration of tens of milliseconds. During the "Sensing" phase, Anode & Cathode carry the sensed cardiac signals from selected electrodes back to the pacemaker in order to enable the monitoring of the patient's state. Cardiac signals have amplitude of tens of millivolts which is very weak compared to the stimulation amplitude. The "Sensing" phase duration can vary from several seconds to several minutes, depending on the patient's need for stimulation.

The energy source is available exclusively during the “Stimulation” phase, which lasts for a maximum of 1ms, while the DCU must function for seconds or even minutes depending on the duration of “Discharge” and “Sensing” phases. As we will show in section 3, the DCU was designed to use this limited power source and function reliably for the entire pacing cycle.

4.3 DCU Operation Principle

As described in table 4-1, DCU operates in the default mode when LEC is inactive. Figure 4-2 illustrates the position of DCU inside the LEC chip. DCU has four inputs (Anode, Cathode, EN and ENX) and two outputs (e1 and e2). EN & ENX are control signals generated by the LEC’s control unit in order to activate/deactivate the DCU. The outputs e1 and e2 are connected to two of the electrodes in the multi-electrode lead. These two electrodes are named hereafter (default electrodes). These default electrodes are shared between the LEC’s switching unit and the DCU. Note that when DCU is active, it takes full control of the default electrodes (LEC is inactive). Despite the fact that the LEC is inactive along with its control unit responsible for EN & ENX generation, these signals are set to values that enable DCU through a power-on-reset circuit which detects the presence of power on Anode and Cathode during stimulation phase.

4.4 System Implementation

The DCU when activated creates two connections between its inputs and its outputs. One between Anode & E1 and the other between Cathode & E2. These connections are marked in (fig. 4-3) as “Path1” and “Path2”. Both paths have to be maintained during the three phases of the pacing cycle described before. When the DCU is deactivated, it has to cut the connections of both path1 and path2. We now describe the DCU circuitry implemented to achieve this function

4.4.1 *Architecture*

We will start by describing the DCU behavior in its active state during the different phases of pacing cycle. “Path 1” is formed by two PMOS transistors M1 and M2, connected back-to-back. Similarly, “Path 2” is formed by two NMOS transistors M4 and M5, connected back-to-back. Transistors of both paths are sized for low R_{ON} , to meet the specification of switches conventionally used for similar purposes in pacemakers. As we remarked that Cathode & Anode inputs may change their polarities or fluctuate during the different phases of the pacing cycle, therefore, “relative voltage difference” between them is needed to drive the transistors

4. Default Connection Unit

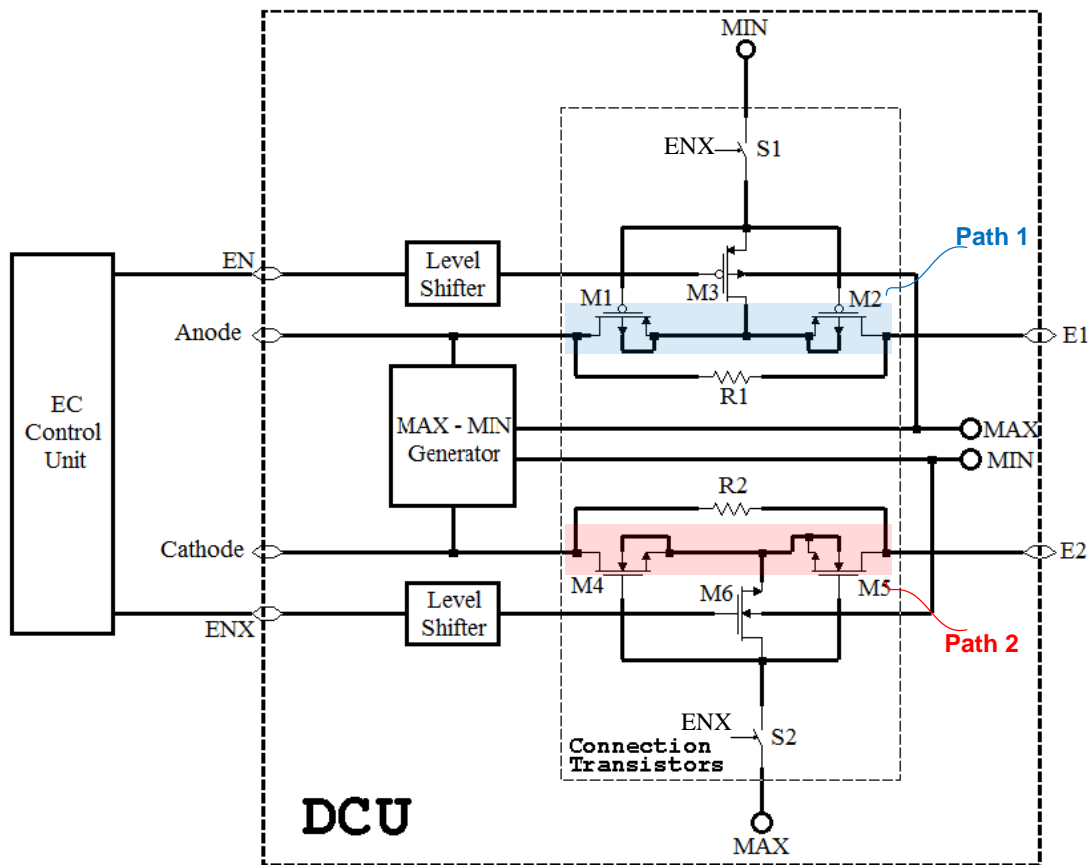


Figure 4-3: DCU circuit

This is achieved through the MIN–MAX generator (fig. 4-3). The MIN–MAX generator as the name suggests, does a relative comparison of cathode & anode inputs and produces the maximum (MAX) and minimum (MIN) of these as outputs. The circuit of MAX-MIN generator is given in figure 4-4. M7 and M8 PMOS are connected as such to generate the maximum voltage found between Anode and Cathode. Similarly M9 and M10 NMOS generate the minimum voltage found between Anode and Cathode.

4. Default Connection Unit

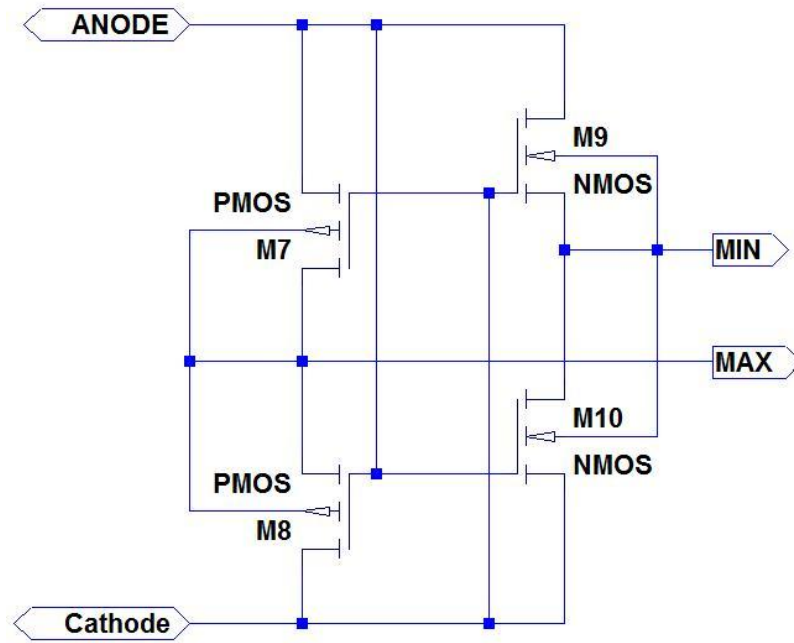


Figure 4-4: MAX-MIN generator circuit

During the “Stimulation” phase, once the energy is present between Anode and Cathode, MAX-MIN generator produces MAX and MIN signals. Switches S1 and S2 are closed in order to drive the gates of transistors in “path1” and “path2”. Circuits of S1 and S2 are given in figures 4-5 and 4-6 respectively.

S1 connects or not the MIN voltage to the MOS gates of “path 1”. It is composed of an analog switch controlled by ENX signal and its inverse (output of inverter fig. 4-5). A Diode D is added to prevent leakage of charges stored in the gate capacitances when the switch is off. All the MOS

4. Default Connection Unit

transistors have their bulk polarized by MAX and MIN according to their type (NMOS or

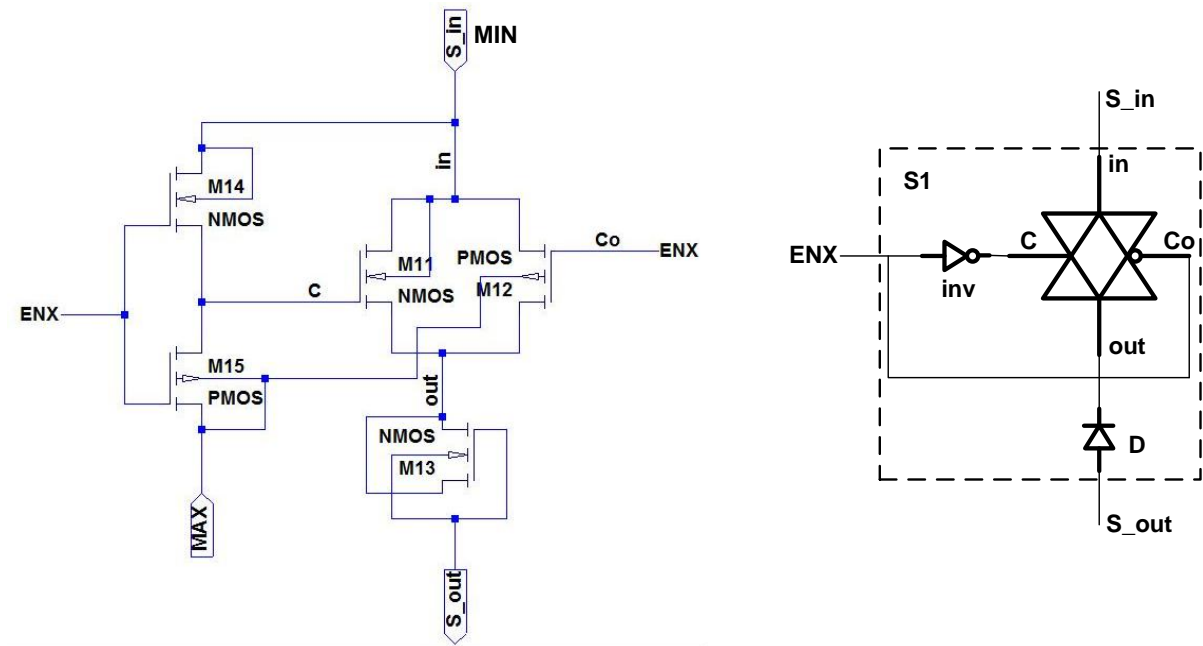


Figure 4-5: circuit and symbol of S1 switch

Similarly, S2 connects or not the MAX voltage to the MOS gates of “path 2.” S2 is also controlled by ENX to ensure the coherence functionality with S1.

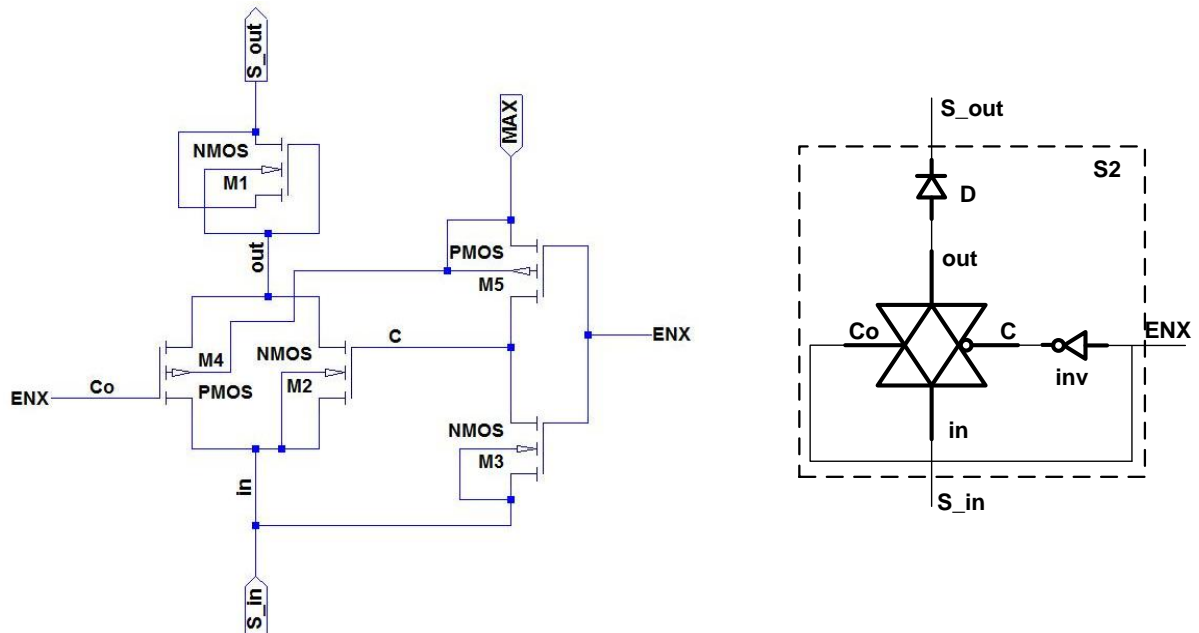


Figure 4-6: Circuit and symbol of S2 switch

EN and ENX control signals are generated from the LEC's power-on-reset unit triggered by the presence of energy between Anode and Cathode. EN and ENX disables M3 and M6 to preserve the voltage drop between gates and sources of transistors in “path1” and “path2”. This is how a part of

4. Default Connection Unit

the stimulation energy was used to turn ON “Path1” and “Path2”, thereby eliminating the need for an external power source.

During “Discharge” phase, the DCU must retain its connected state in order to allow the discharge of residual charges through a high conductance path; otherwise the discharging takes considerable duration. However since during the “Discharge” phase, there is no voltage difference between the anode and cathode lines, unlike during the “Stimulation” phase, we need to find a way to keep the transistors in the ON state. We did so by using the gate capacitances present in M1-M2 and M4-M5 to store energy during the stimulation and maintain it during the limited duration of the “Discharge” phase. We discuss the sizing issues connected to gate capacitances in the following subsection. In order to avoid the leakage of charge stored in the gate capacitances, S1 and S2 are automatically opened immediately after the “Stimulation” phase.

During the “Sensing” phase, DCU must retain a connected path to transfer cardiac signals from electrodes to the pacemaker. As discussed in section II, the duration of the “Sensing” phase is unpredictable and depends on the patient’s need. Since capacitances cannot be sized for unpredictable retention durations it is not feasible to use the technique employed in the “Discharge” phase. In this case we chose to ensure this connection by using resistors (R1, R2) of the order of $k\Omega$ (fig. 4-4). The resistance values were judiciously chosen to prevent the passage of electrical signals during “Stimulation” and “Discharge” phases while ensuring the passage of cardiac signals. R1 and R2 have to be large compared to cardiac muscle resistance between electrodes (300 ohms typically) and small compared to sensing channel input resistance (100 kilo-ohm typically).

Finally, DCU can be deactivated when the LEC is active. This is done by activating M3 and M6 (fig. 4-4) through the control of EN and ENX signals. These two transistors when activated, short circuit the gates and sources of M1-M2 and M4-M5, and block the connection between “default electrodes” and pacemaker. The back-to-back connection between each couple of transistors M1-M2 and M4-M5 enhances the DCU OFF state. This justifies the choice of using two transistors per path and not just one.

4.4.2 MOS Sizing

For the DCU to meet the specification of switches used normally in the stimulation path of cardiac pacemakers, its transistors M1, M2, M4 and M5 have to be sized to have low R_{on} . We based our sizing calculations on a 1st order model, which is a simplified version of Shichman-Hodges model [3] represented by (6), where W and L are width and length of MOS, K_P is given in (7).

$$\frac{W}{L} = \frac{1}{R_{ON} K_P (V_{GS} - V_T - V_{DS})} \quad (6)$$

$$K_P = \mu_p C_{OX} \quad (7)$$

This model was sufficient to calculate the initial size of MOS we then used simulations to refine the sizing.

The target for this MOS sizing is to reach a total R_{ON} of $20\ \Omega$ for the two main paths together. Since there are two MOS switches per path, each MOS switch is sized to have $R_{ON} = 5\ \Omega$. As the range of functionality is between $-2V$ and $-8V$, we based our sizing on the worst case @ $-2V$. Table 4-2 gives an example for the obtained size.

Table 4-2: example for MOS sizing

	PMOS (M1, M2)	NMOS (M4, M5)
Target R_{ON}	$5\ \Omega$	$5\ \Omega$
K_P	$7.2e-6$	$25e-6$
V_{GS}	$2V$	$2V$
V_T	$0.9V$	$0.9V$
W	$26.56881\ \mu m$	$10.861\ \mu m$
L	$1.56\ \mu m$	$1.76\ \mu m$

As can be seen from table 4-2, the size of the MOS switches is quite big. It will be shown in the next section how this big size turned to be an advantage for our application rather than considering it as a high price to pay to match electrical specifications.

4.4.3 Gate capacitance sizing

As mentioned before, in order to retain the state of the DCU to its ON state after the “Stimulation” phase, the stimulation energy has to be stored in a capacitor which is sized according to the duration during which the state must be retained. The leakage current must be considered in M3 and M6 as it impacts the final size of the needed capacitor. Equation (8) shows the dependency of retention time (ΔT) to the leakage current (I_{Leakage}) and capacitance (C). ΔV represents the voltage difference between the voltage level at the end of the stimulation pulse and the MOS threshold voltage V_T .

$$\Delta T = C \frac{\Delta V}{I_{\text{leakage}}} \quad (8)$$

As the MOS transistors were sized to have small R_{ON} , these transistors have large W . From (9) we can see that gate capacitance is directly proportional to W . The gate capacitance for these MOS transistors was calculated using this equation. By comparing the calculated capacitance needed to retain the DCU state during the “Discharge” phase with the gate capacitance of our sized MOS transistors, we found that we have already a bigger capacitance than needed and calculated in (8); therefore no additional capacitors were needed

$$C_{GS} = \epsilon_0 \epsilon_R \frac{W.L}{T_{OX}} \quad (9)$$

C_{GS} is the MOS gate capacitance; ϵ_0 is the vacuum permittivity, ϵ_R is the permittivity of SiO_2 and T_{OX} is the oxide thickness.

Table 4-3 gives an example for sizing of the gate capacitance needed to retain the MOS switches state during at least the discharge duration ($\Delta T = 13\text{ms}$) and compare it to available gate capacitance found due to the big MOS size as was presented in the last section.

Table 4-3: example of capacitance sizing

	Path 1 (M1, M2)		Path 2 (M4, M5)	
Total leakage current	5.6189e-11 A		6.0722e-11 A	
Total voltage drop ΔV	6V		6V	
Targeted Retention Time ΔT	13 ms		13 ms	
Capacitance	needed	available	needed	available
	0.1217 pF	47.7 pF	0.1315 pF	22 pF

From table 4-3 we can see that the available gate capacitance is more than enough to retain the MOS state. Therefore no extra capacitance was needed to be used.

4.4.4 Noise

Since cardiac signals are very feeble (few mV), it's important to consider the effect of noise which our DCU might present. To do so we model heart as a voltage source generating the cardiac signals (V_c) with internal resistance of approximately 500 ohms in series with our DCU circuit. The maximum frequency of cardiac signal is of the order of 30-100 Hz [4]. We carried out a thermal noise analysis at body temperature. The noise was found to be negligible (nano volts) compared to cardiac signals.

4.5 Results

The DCU chip was taped-out in 0.18 μm process. Table 4-4, summarizes the DCU chip features and gives the power consumption of its sub blocks.

Table 4-4: Chip Summary

Technology	0.18 μm	
Functional voltage	-2V to -8V	
Area	2.2 x 1.75 mm^2	
Power consumption	Connection Transistors	17.4 nW
	Level shifter	119 nW

Figure 4-7 shows the simulation results of the DCU in its **active** state. Waveform (1) represents the variation of voltage difference between DCU inputs (Cathode and Anode) plotted against time. The period (STIMULATION) indicates the presence of stimulation energy between Anode and Cathode. Waveform (2) shows the voltage difference between DCU outputs (E2 and E1). When the DCU is active it takes full control of the default electrodes (E2 and E1) and the stimulation pulse is transmitted with minimal loss (fig. 4-7). A slight rise in the positive direction followed by decay in both waveforms (1) & (2) can be remarked just after the stimulation pulse (polarity inversion region in fig. 4-7). This is due to the change of polarities in anode and cathode during “Discharge” phase as explained in section 2. Waveforms (3) & (4) show MAX and MIN internal signals and their variation during pacing cycle. Finally, waveforms (5) & (6) present the control signals ENX & EN used to activate/deactivate DCU.

4. Default Connection Unit

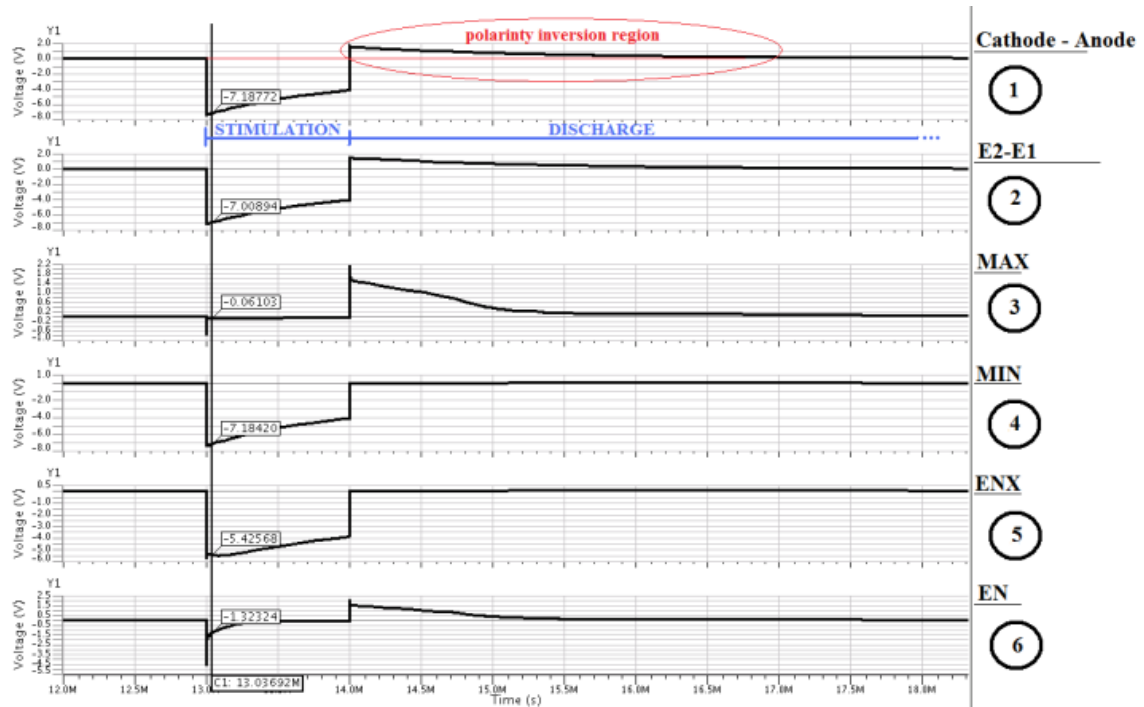


Figure 4-7: Simulation results of DCU in its active state

Figure 4-8 shows the simulation results of the DCU in its **inactive** state. The DCU here is simulated in isolation from the LEC to show its efficiency in inhibiting the stimulation pulse. Note that during the stimulation phase, the DCU outputs (E1 and E2) retain their existing potential unlike (fig. 4-7). This indicates the blocking of the path between pacemaker and electrodes. It can be remarked here that during the discharge phase, waveforms (1) & (2) are kept at zero. This shows that no charge was delivered to the electrodes to be discharged.

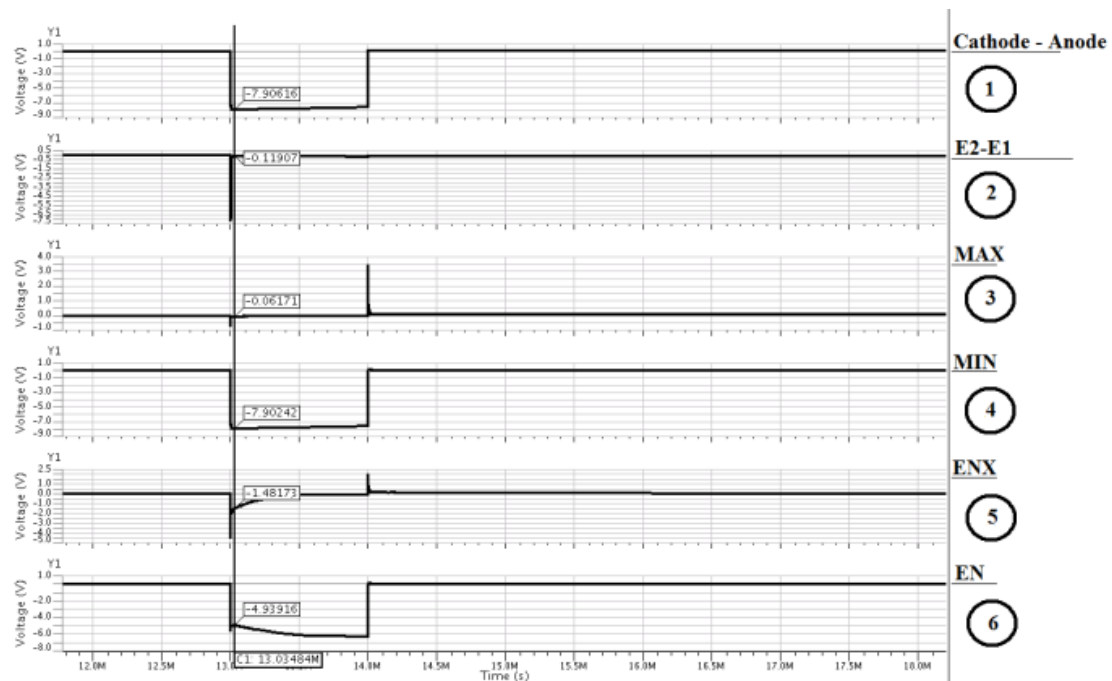


Figure 4-8: Simulation results of DCU in its inactive state

4. Default Connection Unit

The DCU chip layout is shown in Fig. 4-9. In order to facilitate the validation of the chip apart from the electrode-controller unit, we duplicated the Anode and Cathode cells (Path1 and Path2 of fig.4-3) in their active and inactive states. Like that it is enough to apply a stimulation pulse between Anode and Cathode then observe the state of the two electrodes of each cell. This first run of the chip has to be further improved to optimize its size

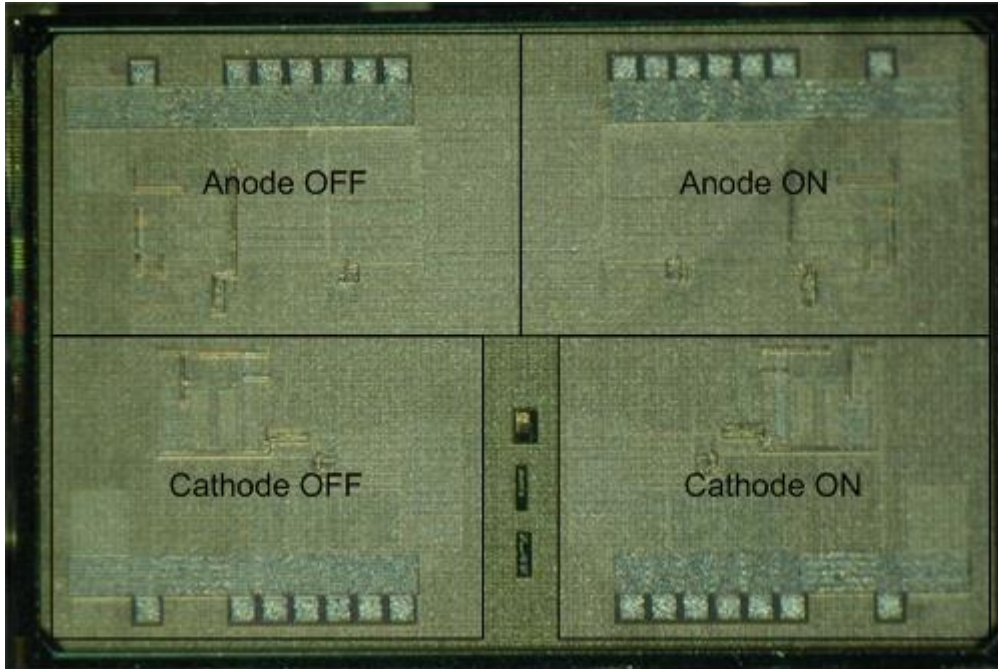


Figure 4-9: DCU chip microphotograph

4.6 Conclusion

In this chapter we addressed the problem of multi-electrode lead compatibility with any pacemaker device in the market. The presented DCU (Default Connection Unit) alleviates this challenge by transforming the multi-electrode lead into a standard bipolar lead through the activation of two electrodes that it shares their control with the main switching unit found in the electrode-controller chip.

We showed how the DCU was designed to use the available stimulation energy to activate its paths between Anode, Cathode and default electrodes without the need for a power source (battery). It also stores a part of this energy in order to retain its state for a period that at least covers the discharge phase duration. DCU paths are equipped with resistances that enable it to continue ensuring the connection between electrodes and the pacemaker during the duration of the sensing phase which depends on each patient.

DCU distinguishes our multi-electrode system and takes a step forward compared to the auxiliary switching unit presented in section 3.4.3.6 of chapter 3 as it is integrated in the technology process used in the electrode-controller chip.

As the DCU is assigned to only two electrodes in the multi-electrode lead, this may show some limitations to the site of stimulation for the new pacemaker connected to the lead. In chapter 5 we will introduce a new solution to address this issue. We will show how nonvolatile memories and its underlying implementation technologies offer us ways to maintain the last configured stimulation site and thereby allowing us to circumvent the fixed site limitation imposed by the DCU.

Publications

I. Seoudi, J-F. Debroux, M. Laflutte, A. Makdissi, K. Amara, A. Amara, R. Dal Molin “Default connection in multi-electrode leads for cardiac pacemakers” accepted in NEWCAS 17-20 June 2012

References

- [1] Islam Seoudi et al. “Multi-electrode system for pacemaker applications”, ICECS 2011
- [2] Samuel J Asirvatham “Implanting a left ventricular pacemaker lead” Indian Heart J. 2007 Mar-Apr; 59(2):197-204.
- [3] A. F. Schwarz, “Computer aided design of microelectronic circuits and systems”, Academic Press, 1987.
- [4] Mark W. Kroll, Micheal H. Lehmann “Implantable cardioverter defibrillator therapy” Springer 1996

4. Default Connection Unit

Chapter 5

Enhanced Multi-Electrode Lead Using Non-Volatile Memory Technologies

5.1 Introduction

In chapter 3 we presented a multi-electrode system capable of multisite stimulation. We also presented the design challenges and constraints of such a system. In chapter 4 we furthered our contribution by adding to the multi-electrode lead a default connection unit (DCU) which enables compatibility of a multi-electrode lead with any other pacemaker not specifically designed to control it. However while the DCU solution does solve the compatibility problem, as we discussed at length in chapter 4, it does so by somewhat restricting the lead i.e. by transforming the multi-electrode lead to standard bipolar lead. This approach, in effect not only reduces the inherent functional advantage of a multi-electrode lead (by transforming it to a two electrode lead), but it also limits the therapeutic advantage of such a solution. In a multi-electrode system the physician would have chosen the ideal site/polarity of the electrodes for pacing thereby enhancing the effectiveness of the therapy, but in the “DCU active” version of such a lead, such therapeutic advantages cannot be availed.

In this chapter, we build on the experience gained to address these limitations. We will explore the technologies which can improve the multi-electrode lead such that the lead not only retains all the functional features of lead as discussed in chapter 3 but enhances it by drastically bringing down the power consumption and size. Additionally, the solution presented will also allow the lead to incorporate within itself the DCU functionality, thus ensuring the absence of any compatibility issues should the need of any pacemaker replacement arises. To do so we will leverage new technologies which go beyond frontiers of standard CMOS and CMOS processes. We now discuss the key ideas underlying the improvements to the multi-electrode lead.

5.2 Enhancements to the Multi-Electrode

In section 3.2 and 3.3 when we discussed the requirements of multi-electrode solution, we remarked that size and power consumption are the key issues governing the design choices. The importance of power consumption is two-fold, firstly the solution has to consume extremely low power (because pacemakers run on batteries for several years), secondly since the LEC has to reside inside the lead, the space restrictions rule out any onboard battery, therefore the LEC has to effectively operate on power supplied by the pacemaker. The solution presented in Chapter 3 was based on this approach, where before each stimulation, the pacemaker would send the power pulses to the LEC and also configure the LEC for multi-site stimulation. This solution therefore needed configuration each pacing cycle (therefore also power). Furthermore the time spent in configuration added to the delay between the stimulation demand and stimulation delivery. Note that the need for configuration stems from the fact that after the stimulation and discharge, the electrode configuration is lost and

therefore each demand for stimulation necessitate the need for reprogramming the multi-electrode system.

Note that if we can somehow retain the last configured state of the multi-electrode system, it would avoid the repetitive need for reprogramming the system. This would not only lead to reduction in power consumption (a key design goal) but also eliminate latency (caused due to programming) and last but not the least, the pacemaker replacement would not lead to incompatibility issues. Thus state retention would lead us to a win-win solution, where we will address all our design issues and compatibility problems.

In this and the following sections we explore the most important technologies which offer us the possibility of state retention: non-volatile memories. We will explore several candidates of non-volatile memory technologies and show the possibility of their integration in our electrode-controller unit to completely replace its main switching unit and its default connection unit with a new Non-volatile switching unit as illustrated in figure 5-1.

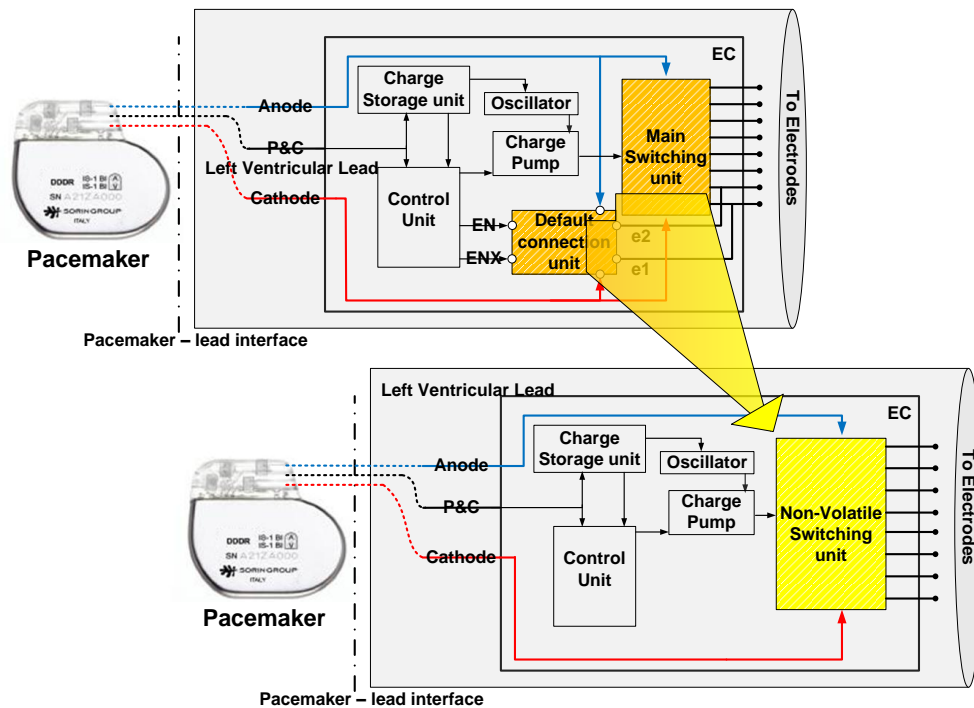


Figure 5-1: Replacement of main switching unit and default connection unit by the new non-volatile switching unit inside the lead electrode-controller unit

The new non-volatile based switching unit will primarily reduce the size of the electrode-controller as it replaces two switching units by one. Moreover the size of the non-volatile switching cells is far smaller than CMOS transistors. Non-volatile switching unit solves the compatibility problem with other pacemakers in a smarter and more flexible way. In the case that the multi-electrode pacemaker is replaced by another pacemaker in the market, the non-volatile switching unit enables the multi-electrode lead to retain its last configured electrodes no matter their number and polarities were

unlike the case with DCU which was assigned to specific electrodes to be activated no matter the last configured electrodes was for the patient.

Table 5-1 resumes the requirements of switching unit as already discussed in chapter 3 and 4.

Table 5-1: switching unit specification for cardiac stimulation

Supported Voltage Range	-1V to -8V
Supported Current Range	Tens of mA
ON Resistance	10 Ω - 20 Ω
State Retention	Stable without power source

We now explore three key memory technologies namely NRAM, RRAM and Flash

5.3 Advanced Non-Volatile Memory Technologies

5.3.1 Nanotube RAM (NRAM)

Carbon nanotubes are molecules known for its high electrical conductivity, its high mechanical strength and its wide range of sheet resistance (1 K Ω/\square - 1 M Ω/\square) [22]. Beside these interesting properties, its dimensions are in the nanometers scale as shown in figure 5-2.

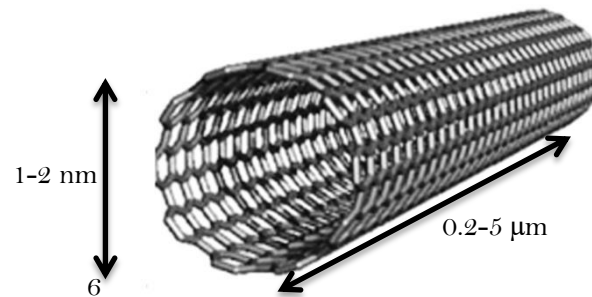


Figure 5-2: single walled carbon nanotube [18]

“Nantero” a company specialized in non-volatile memories, took the lead in using carbon nanotubes in memory cells. They invented a switching element using carbon nanotubes as the conduction path. This switching element forms the base of their memory architecture named NRAM (non-volatile or nanotube RAM).

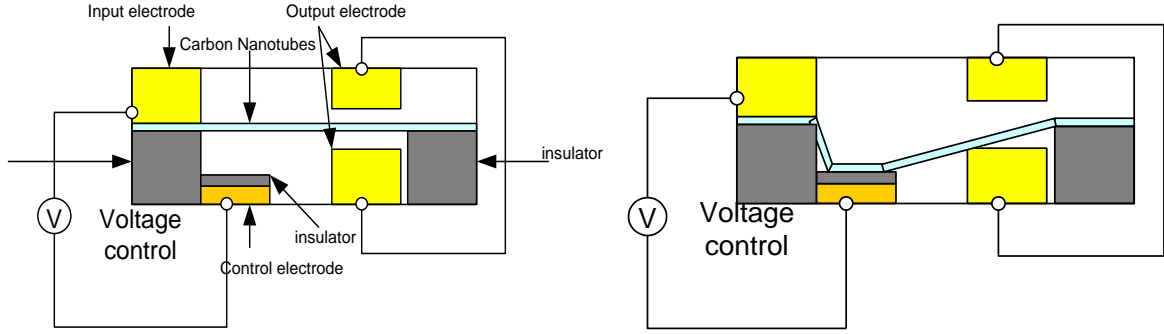


Figure 5-3: NRAM cell in erased state (left) Programmed state (right) [24]

Figure 5-3 illustrates an example of the NRAM cell as described in one of Nantero's patents. The cell is composed of input and output conducting electrodes between which is suspended a bundle of carbon nanotubes. The input electrode is in permanent connection with the nanotubes. A control electrode is used to establish electrical connection between the input and output electrodes due to the deflection of nanotubes towards the control electrode in response to a first voltage applied between the control and input electrodes. This connection makes the ON state of this cell. At a second voltage this effect is reversed and the nanotubes deflect back to cut off the connection between input and output electrodes creating the OFF state of the cell. These two states are stable and non-volatile thanks to Van Der Waal force present between nanotubes and the output electrode.

At this nanoscopic scale, several forces work together to give the NRAM cells its bi-stability [17]. The relation between these forces is given in equation (10)

$$F_T = F_{vdw} + F_{elastic} + F_{electrostatic} \quad (10)$$

Where F_{vdw} is the Van der Waal force maintaining the deflection of nanotubes against the elastic force $F_{elastic}$ which tends to mechanically return the nanotubes to their initial position. $F_{electrostatic}$ is the electrostatic force responsible for repulsion or attraction between nanotubes in response to an applied field. This interaction between nanotubes is one of the reasons explaining the deflection of a nanotube bundle which is the key feature of this NRAM cell.

All these forces and the functionality of the NRAM cell are strongly dependent on its geometry [17]. This dependence gives this cell an advantage of being adaptable to different applications with different ranges of voltages and currents. Such nanotubes can be tuned to have a resistance between 0.2 – 100 KOhm/square or in some cases from 100KOhm/square to 1 GOhm/square as shown in figure 5-4a. Figure 5-4b gives an example of measured values for input voltage and output current during the ON and OFF states of the cell.

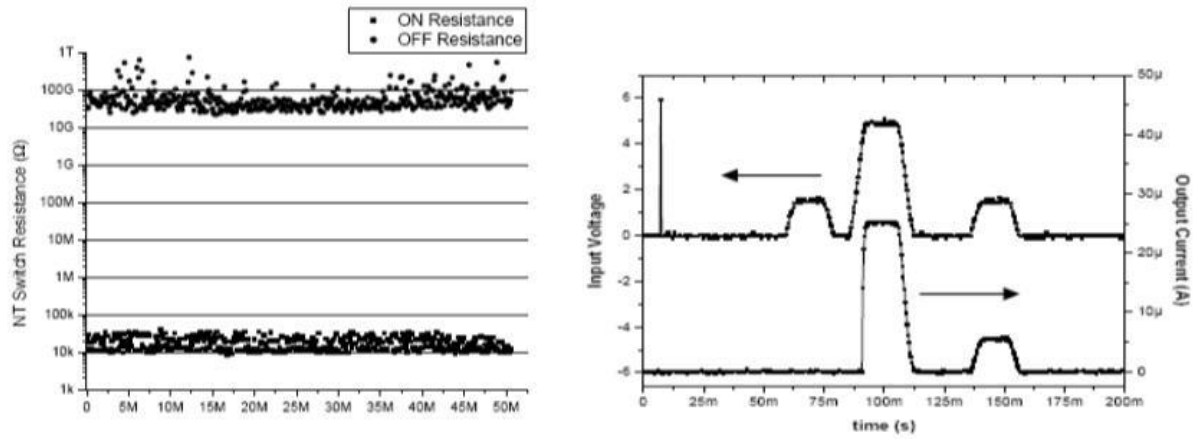


Figure 5-4: measured values for ON/OFF resistances (left), measured voltages and currents (right) [16]

NRAM showed distinguishing features among all other technologies used in memories. ON and OFF states don't leak as in the case of memories based on charge storage. The fact that states are based on mechanical deflection of nanotubes gives them more stability and can be retained for many years. Table 8 summarises the key features of NRAM that made it the best candidate for our application in cardiac stimulators.

Table 5-2: NRAM features summary [19, 22]

Feature	Value
ON Resistance	K-ohm
OFF Resistance	G-ohm
Switching speed	<3ns
Read/write cycle	<10ns
Erase Voltage	6V
Write Voltage	< 5V
Write current	~25μA
Active area of device	22nm x 22nm
Endurance	50 million cycles
Read stress test	145 million cycles

As shown in table 5-2, the resistance difference between NRAM states is in the order of mega ohms. These distinguished states make it an ideal solution for switching applications especially with its high switching speed.

These features were extracted from a specific cell of area $22 \times 22 \text{ nm}^2$. Consequently, the write and erase voltages corresponding to this geometry were around the 5V. The strength of this technology is that these values can be adapted to other applications by modifying the geometry of the cell. NRAM shows very good endurance and strong resistance to stress tests as shown in table 8.

In view of all these extraordinary features of NRAM that one can imagine it is too good to be true. A novel technique has been developed allowing carbon nanotube based devices to be fabricated directly on existing CMOS $0.18 \mu\text{m}$ process with only one mask of overhead.

5.3.1.1 NRAM Application for Multi-Electrode Switching Unit

A theoretical example for the integration of the NRAM cell in our cardiac stimulation system is illustrated in figure 5-5. Two NRAM cells are associated with each electrode to control its connection to Anode or Cathode. Only one NRAM cell is activated at a time to polarize the electrode either to Anode or to Cathode, but never both together.

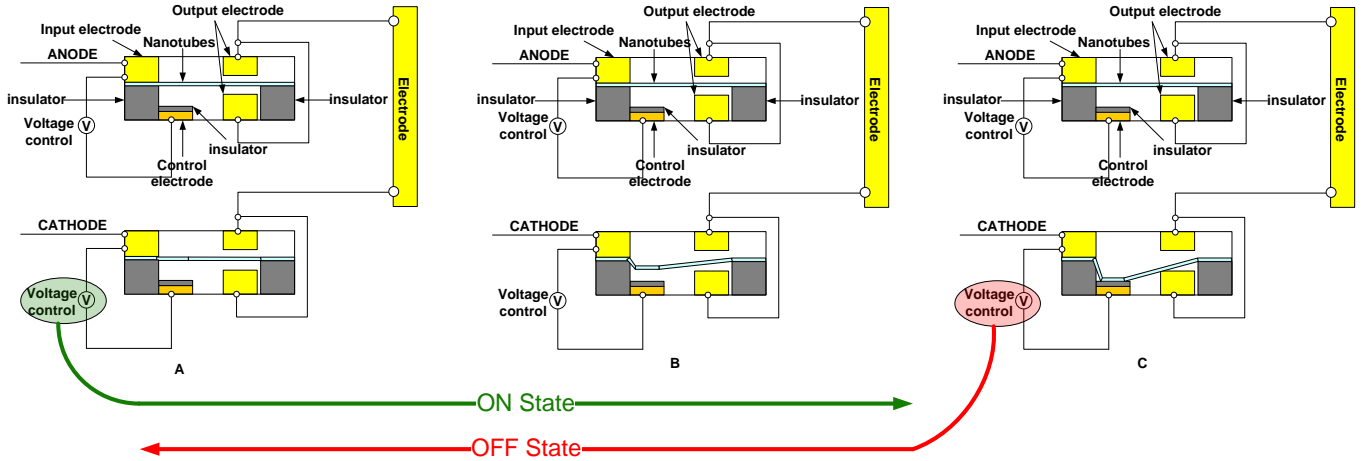


Figure 5-5: An example for the non-volatile switching unit in the multi-electrode system

When the write voltage is applied to the NRAM cell associated to Cathode (marked in green in fig. 5-5a), the nanotube bundle start progressively to deflect (fig. 5-5b) toward the control electrode creating a direct connection between input and output electrodes of the cell (fig. 5-5c). In conclusion, the electrode now is connected to Cathode only, without any connection to Anode. The same sequence can be independently applied to another electrode in the lead, but to connect it to Anode. Once a stable connection is established in any two electrodes of the lead, stimulation pulses can be sent to the heart as well as sensing cardiac signals.

By applying the erase voltage to the NRAM cell as marked in red in figure 5-5c, the nanotube bundle deflect back to its initial position cutting off the connection between input and output electrodes.

The stability of NRAM states and its immunity against bit failure caused by charge leakage, magnetic field or even alpha particles makes it very reliable technology specially in medical applications. Adding to that its miniaturized size and its speed switching makes it the best technology to be adopted for our application.

But the existing NRAM cells with their actual targeted applications in the non-volatile memory applications, are not adapted to our specifications which requires the support of important amount of currents (tens milliamps) and voltages (tens of Volts) during the stimulation phase. We investigated with the technology inventor (Nantero) the feasibility of enhancing the cell features in order to match our system's specification. They confirmed the feasibility but it would require further research and studies to be invested in this direction in future.

One intermediate solution for the existing NRAM cells (without geometrical modification) to support stimulation currents in our system could be achieved by employing several NRAM cells mounted parallel to each other. By that the stimulation current is divided into the parallel cells preserving each of them from being damaged.

At this point, our goal was to prove the concept which is more or less theoretically reached. We decided to take a further step and to try another technology in the non-volatile memory field. In the next section we will explore two technologies (MRAM and Memristance) that we believe they can be grouped under the same family of resistive RAM as will be revealed later in this chapter.

5.3.2 Resistive RAM family

Several memory technologies can be grouped together under the Resistive Ram family. Technologies like MRAM and Memristance were different when they emerged but they evolved to reach a nearly common structure with more common features. Here will take these two examples of the resistive RAM technologies and see how they evolved and whether their features enable us to integrate them within the cardiac implants or not.

5.3.1.1 Magnetic Tunnel Junction (MTJ)

Magnetic Tunnel Junction (MTJ) is composed of two ferromagnetic layers separated by a thin insulating barrier (a few nanometers or less). One of these ferromagnetic layers has a fixed (pinned) orientation of magnetization and is considered as the reference layer. The other ferromagnetic layer has free magnetization, switchable between two stable states and acts as storage layer [1]. According to the relative orientation of magnetization between storage and reference layers, MTJ forms two stable resistive states. Low resistive state (R_{min}) is obtained with parallel (P) orientation while High resistive state (R_{max}) is obtained with Antiparallel (AP) orientation of layers as shown in figure 5-6.

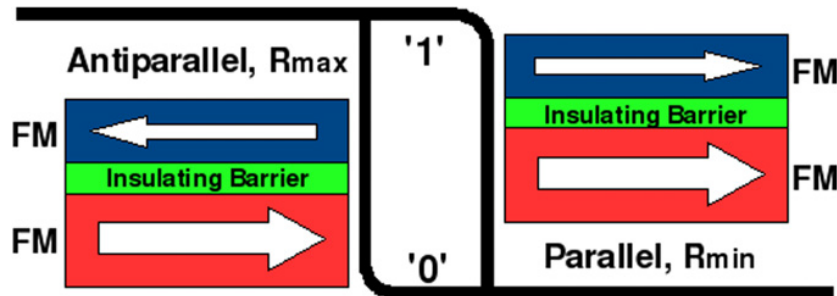


Figure 5-6: MTJ states [2]

Electrons can tunnel through the thin barrier when a bias voltage is applied between the two layers of the cell. The tunneling current depends on the relative orientation of magnetization in the two ferromagnetic layers. This dependence is governed by the ratio between parallel and antiparallel orientation given by the parameter TMR (Tunneling Magneto Resistance). TMR ratio is described in equation (11) where R_{AP} is the MTJ resistance when the storage layer is oriented antiparallel to the reference layer. And R_P is the MTJ resistance when the storage layer is oriented parallel to the reference layer [2].

$$TMR = \frac{R_{AP} - R_P}{R_P} \quad (11)$$

AP and P are two stable nonvolatile states of the MTJ cell that can be used to represent logical states 0 or 1. Data storage in MTJ cell is nonvolatile and does not leak because data are no longer

stored as electrical charges but as resistive change in this magnetic nanostructure. Switching between MTJ states differs according to the type of MTJ cell as will be explained in the following sections. These types differ in the write/erase sequences and methods. Rather than the memory architecture in which the MTJ cell is integrated

5.3.1.1.1 Field Induced Magnetic Switching (FIMS)

In the FIMS architecture of MRAM, the MTJ cell is located at the intersection of two perpendicular lines; word line WL and bit line BL. Synchronized current pulses are applied on WL and BL during write phase to generate a magnetic field only on the addressed MTJ memory cell as shown in figure 5-7b [13]. During the read phase, a control transistor is switched on and current is passed through the MTJ cell. According to the measured resistance, the state of the cell is determined to be 0 (AP) or 1 (P).

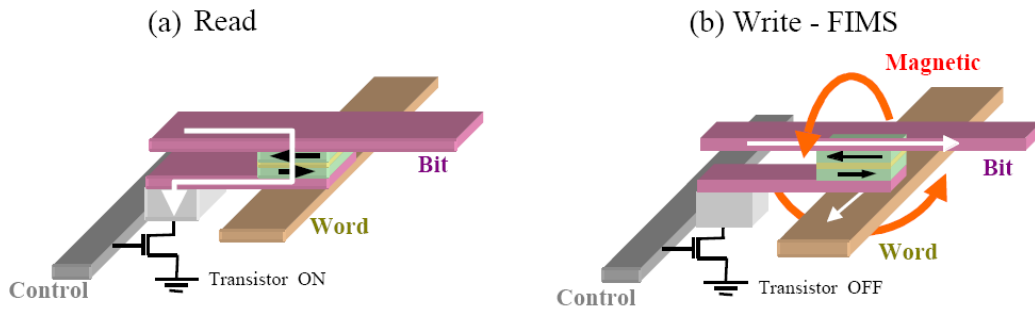


Figure 5-7: FIMS cell (a) read phase (b) write phase [13]

In this MRAM technology three major issues are identified:

1. low resistance discrimination between “0” and “1” states (*i.e.* small sensing margin);
2. high sensitivity to disturb during writing (“bit fails”);
3. high switching current ($>10\text{mA}$) required for magnetization reversal [4]

5.3.1.1.2 Toggle Cell

“Toggle” means that the MTJ cell will switch its state to the opposite state every time a unique pulse sequence is applied [14]. The MRAM architecture used with Toggle cell as shown in figure 5-8 is similar to the FIMS architecture but the difference lies in the Toggle MTJ cell. In Toggle cell the two ferromagnetic layers of MTJ are replaced by enhanced SAF layers (Synthetic Anti Ferromagnet) separated by a tunnelling barrier. Similar to conventional MTJ cell, Toggle cell has one reference SAF layer with fixed magnetic moments and one storage SAF layer with switchable magnetic moments. The storage SAF is composed of two magnetic layers separated by an anti-ferromagnetic layer. The moments of these two magnetic layers are always oriented anti-parallel to each other giving a resultant moment in one direction as shown in figures 5-8b and 5-8c.

The State of the toggle cell is defined by the storage SAF resultant moment direction in comparison to that of reference SAF resultant moment, whether it is parallel (low resistance) or antiparallel (high resistance) [15].

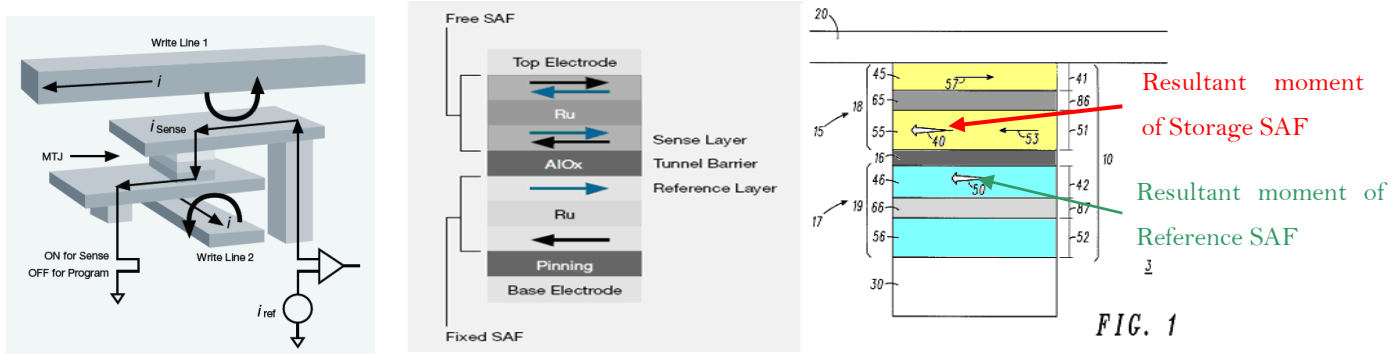


Figure 5-8: toggle cell anatomy - SAF layers [17, 18]

Toggling currents sequence:

The arrows represent the magnetic moment of the two sub layers in the SAF storage layer. In this example, the darker arrow is the layer that is adjacent to the tunnel barrier and is therefore the information storage layer that determines the resistance. To toggle the bit from an initial “0” to a final “1,” the currents are pulsed with timed sequence that results in magnetic fields as shown in figure 5-9.

The main rule of state switching is that the SAF responds by orienting its moments orthogonal to the applied magnetic field. Starting from an initial state at t_0 , current is applied on write line 1 during t_1 . The moments will be oriented orthogonally to field H_1 . At t_2 a second current is applied on write line 2 generating a second field H_2 . The SAF moments will be shifted only 45° between the two active fields. At t_3 H_1 is deactivated resulting into the relaxation of moments in the orthogonal direction to H_2 . Finally at t_4 the field H_2 is deactivated and the SAF moments are oriented along the bit easy axis with the darker arrow pointing 180° from its initial state. Hence, the bit has been switched from “0” to “1”. Due to symmetry if this process is repeated with the same polarity pulses, the bit will toggle again to the opposite state [14].

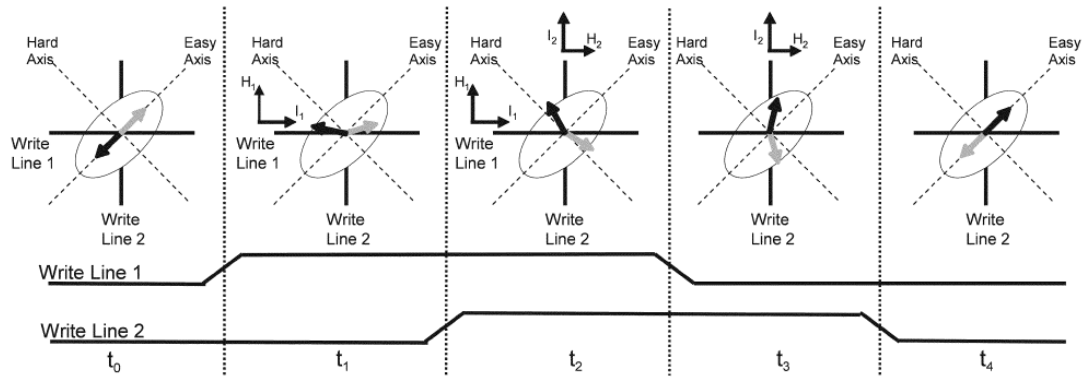


Figure 5-9: toggle sequence

Electrical specifications and features [12]

- Supply voltage : -0.5V to 4V
- Temperature range: -40 to 105 °C
- Read/write access time : 35 ns
- CMOS standby current : 9 – 12 mA

Extra Features

- Full non-volatile operation with 20 years minimum data retention
- Data immunity against exposure to external magnetic fields with a maximum specification of 2000 A/m during write operations and 8000 A/m when reading or inactive. [11]
- The magnetic polarization does not leak away with time like charge does, so the information is stored even when the power is turned off.
- Switching the magnetic polarization between the two states does not involve actual movement of electrons or atoms, and thus no known wear-out mechanism exists
- Program lines are physically separated from the MTJ, which reduces the parasitic delay

5.3.1.1.3 Thermally Assisted Switching (TAS)

Similar to toggle MRAM, magnetic fields generated by current sequences are used in switching. The exception for TAS MRAM that the target bit is selected by heating it to certain temperature which decreases the field needed for switching. [21]

TAS MRAM brings the following benefits:

1. shrinking the memory cell size with only one metal line to produce magnetic field
2. reducing the power consumption ($>1\text{mA}$) thanks to limited writing current compared to FIMS [4]
3. Improving bit fails immunity.

Despite those benefits, the heating introduces new challenges and reliability problems which are currently under research.

5.3.1.1.4 Spin Torque Transfer (STT)

In the first generation MRAM the high programming current has constrained the scaling capability. STT architecture was developed mainly to overcome scaling barriers. A new writing approach is adopted in STT architecture in which the magnetization of the storage layer can be reversed by applying a current density (J) higher than certain critical current density (J_c) of the cell [4]. The direction of the injected current determines whether the final state of magnetization is P or AP as shown in figure 5-10 [2]

Critical switching current I_{C0} is defined as the current value above which the device switches from AP to P or vice versa [4]. STT cell shows hysteresis property in which critical switching currents are not always identical for the two different states. It is easier to switch from AP to P because the other direction takes more current [3].

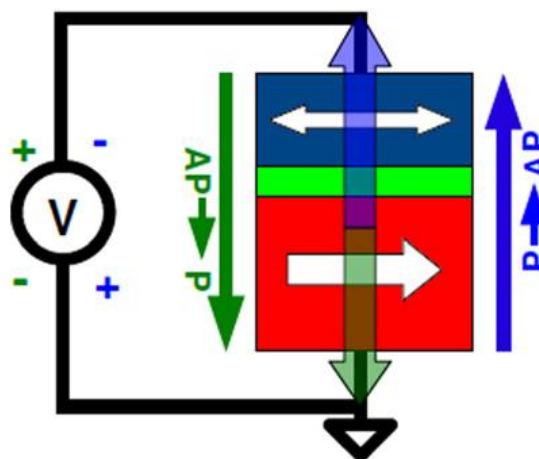


Figure 5-10: STT structure [2]

Since no magnetic field is needed during the writing phase, only bipolar voltage is applied between BL and SL to inject a top-down or bottom-up current enabling magnetization switching. Hence the

STT architecture is said to consume less power compared to conventional MRAM cells. Also it improved bit selectivity and helped scaling down the memory cell to reach $6\text{--}9\text{ F}^2$ ($2\text{--}3\text{ nm}^2$) [1]

The basic features of STT cell are grouped in table 13 as found in the literature [2,3,5]:

Table 5-3: STT features

Feature	Value
Faster write operation	<100ns
High endurance	$>10^{14}$ cycles
Better scaling	Ex: $240 \times 80\text{ nm}^2$
Bias voltage amplitude	+/- 0.79V
Current to switch P to AP	-883uA
Current to switch AP to P	581uA
Current density P to AP	-11.1 mA.cm ⁻²
Current density AP to P	7.3 mA.cm ⁻²

Despite the advancement brought by the STT cell, still it has some drawbacks that may need improvements. The first issue is known as self-read disturbance caused by reading currents across the cell. Even that reading currents are far below switching critical currents, switching can always occur because of thermal fluctuations. The second issue is concerning the dependence of writing time on the device area which is an undesired effect.

All MRAM manufacturers converge toward STT architecture because of its interesting features compared to other architecture. For this reason we chose to investigate the integration of MRAM memory cell in our system represented in the STT architecture.

By looking on the STT cell and comparing it with other types of resistive RAM cells, a lot of similarities can be found, especially in its two stable nonvolatile states obtained through two different resistive states. STT is also a two pin cell and switch its state depending on the direction of current passing through the cell. This similarity will be further clear after looking on a second type of RRAM family such as Memristance cell.

5.3.1.2 Memristance

Memristance is a shorter name of memory resistor given by Leon Chua in 1971 to be the 4th fundamental circuit element that defines a relation between flux and charge. Chua proved theoretically this relationship through symmetry of relationships describing each of the three fundamental circuit elements [5].

$$\text{Resistor} \quad dv = R di$$

$$\text{Capacitor} \quad dq = C dv$$

$$\text{Inductor} \quad d\phi = L di$$

Therefore the Memristance completes the symmetry and define the missing relationship between flux and charge

$$\text{Memristance} \quad d\phi = M dq$$

In 2008 researchers from HP lab built a nanoscale Memristor switch – 50nm x 50nm – by sandwiching a semiconductor material (Titanium oxide) of thickness D between two nanowires as shown in figure 5-11. As charge q is the time integral of current, and flux is the time integral of voltage according to faraday's law, therefore the memristance ($M(q)$) can be modelled in terms of nonlinear resistance. The total resistance of the device is determined by two variable resistors connected in series. The doped region of the semiconductor represents a low resistance R_{ON} while the undoped region of the semiconductor represents a high resistance R_{OFF} . The barrier between these two regions moves in the same direction as electric current generated by the applied bias voltage across the device [6]. The barrier position is presented by the state variable w that varies between 0 (undoped R_{OFF} state) and full length D (doped R_{ON} state).

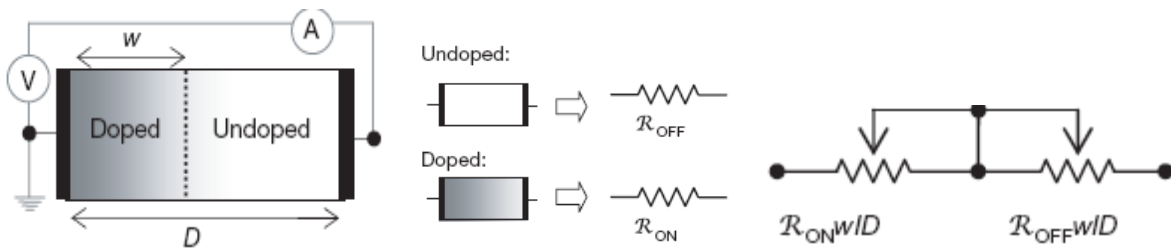


Figure 5-11: Memristance model

The characteristic equation of the memristance model is given by equation (12)

$$v(t) = R_{ON} \frac{w(t)}{D} + R_{OFF} \left(1 - \frac{w(t)}{D}\right) i(t) \quad (12)$$

And the state variable is given by

$$w(t) = \mu_V \frac{R_{ON}}{D} q(t) \quad (13)$$

Where μ_V is the average ion mobility

And by the assumption that $R_{on} \ll R_{off}$, the memristance $M(q)$ is simplified as follows

$$M(q) = R_{OFF} \left(1 - \frac{\mu_V R_{ON}}{D^2} q(t) \right) \quad (14)$$

Memristance has hysteresis properties that appear in response to symmetrical alternating-current voltage bias. The V-I response is a double loop hysteresis at low frequencies (fig. 5-12). As the frequency of the input signal increases, the double loop tends to collapse into linear straight line similar to linear resistance characteristic curve.

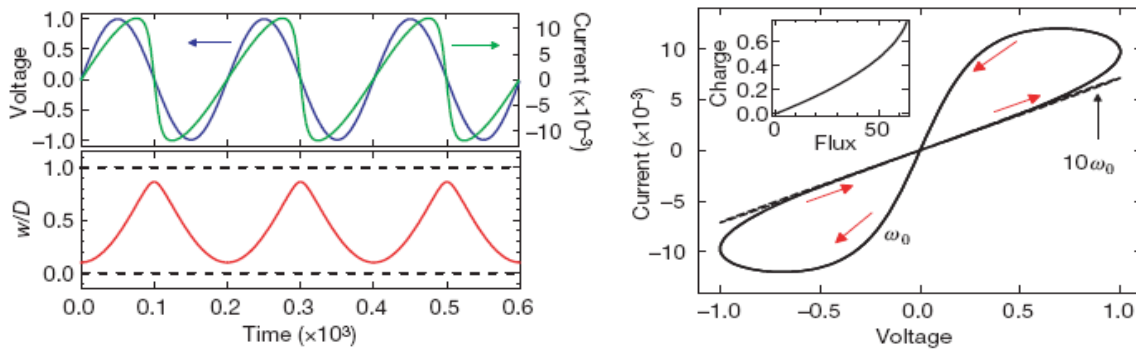


Figure 5-12: Memristance Voltage and current curves

To summarize the precedent description, Memristance is a *variable resistor* which *memorizes* its value reached in response to the last applied bias voltage. It tends to behave as a linear resistor at infinite frequency [7]. Its resistance which is a function of the semiconductor length D between its terminals can be large enough to represent two states for switching applications [8]. An example of this full range resistance difference is given in [10] for a cell of $D=10\text{nm}$. The minimum resistance value R_{MIN} was $100\ \Omega$ while the maximum resistance value R_{MAX} was $20\ \text{K}\Omega$.

Although Memristance and STT MRAM are different technologies with different concepts, but from our application point of view they have in common the following features:

- ON and OFF states are represented by two distinct resistance values
- Change in state is dependent of the direction of current across the cell
- Support limited amounts of currents
- High voltages risk damaging the cell
- Read signals may affect the states stability (bit failure)
- Low R_{on} - R_{off} ratio

Therefore we assumed that we can verify the integration of both technologies in our system if we used one model of any of these technologies. We chose a memristance SPICE model found in the literature in order to test how a cell initially designed for memory applications can be adapted to match the specifications of our system.

5.3.1.3 Memristance Behavioral Model

Batas *and* Fiedler [19] made a behavioral model of Memristance cell using discrete active circuit elements as shown in figure 5-13.

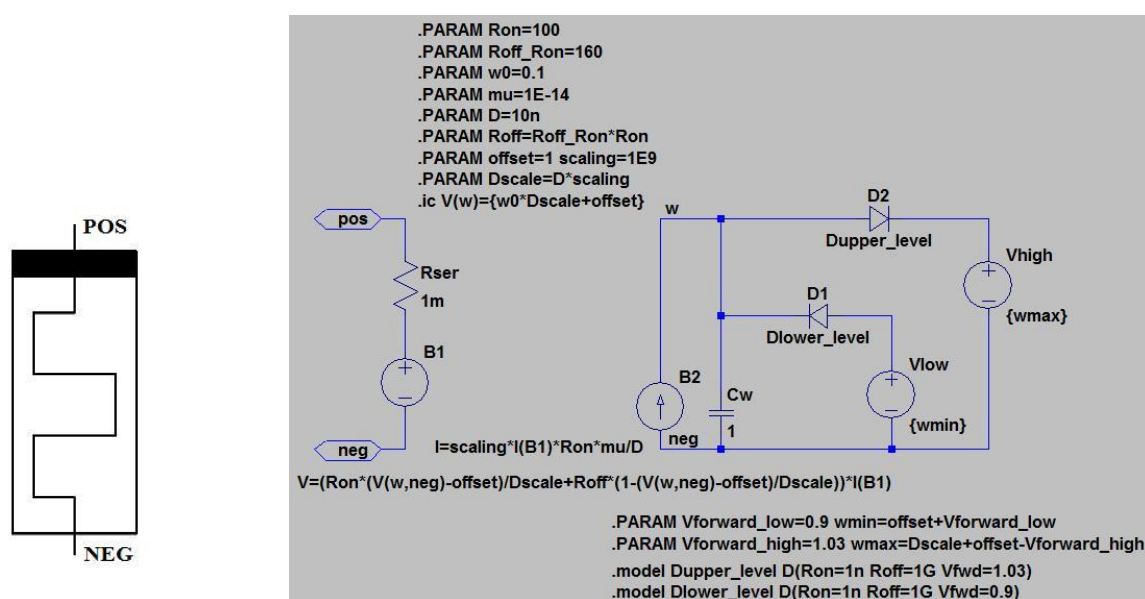


Figure 5-13: (a) memristance symbol (b) behavioral model circuit in LT Spice

In order to make sure that the model behaves as the original memristance cell described by HP team in their paper [5], an input sine wave of 1V amplitude and 0.5Hz frequency is applied between the memristance terminals POS and NEG. figure 5-14 shows in the upper pane the input sine wave and the measured current across the cell. The lower pane shows the state variable (w) that represents the motion of the barrier separating doped and un-doped regions of the memristance. We can see how (w) is varying between its two extremities $[0, D]$ in response to the input voltage. The response current signal is plotted across the input voltage signal giving the known double hysteresis curve as shown in figure 5-15.

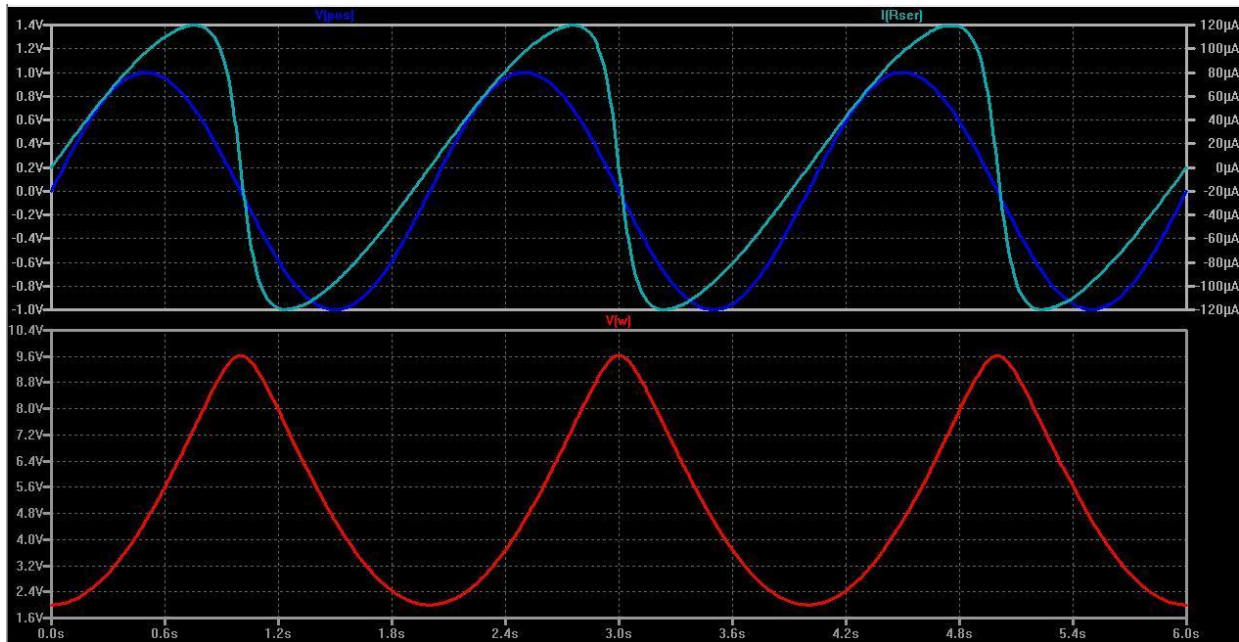


Figure 5-14: (upper pane) input voltage sine wave of amplitude 1V and 0.5 Hz frequency against the measured current across the cell. (lower pane) the variation of state variable w with the input voltage

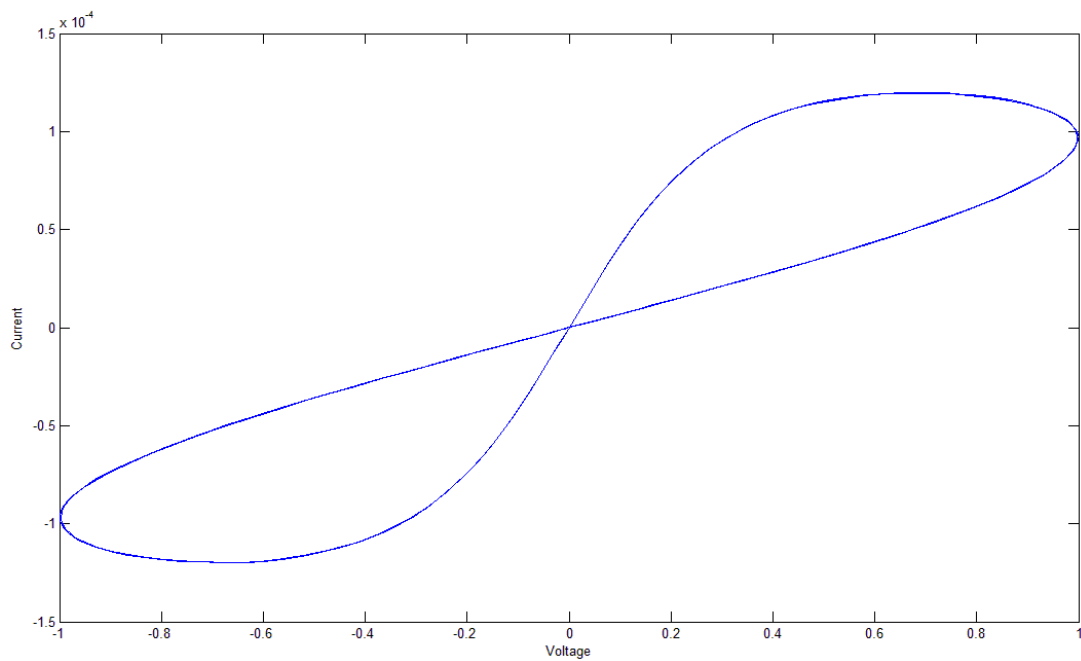


Figure 5-15: plot of voltage against current presented in the upper pane of fig. 5-14. The result is the double hysteresis curve

Table 5-4 summarizes the parameters of the memristance model.

Table 5-4: Memristance model parameters [19]

Feature	Symbol	Value
Minimum Resistance (ON State)	R_{on}	$100 \, \Omega$
Maximum Resistance (OFF State)	R_{off}	$16 \, K \, \Omega$
Full length of the cell	D	$10 \, nm$
Ion mobility	μ	$1e-14$
Initial state variable	W_o	0.1
Voltage range	V	$+/-1V$
Current range	I	$+/-120 \, \mu A$

For the memristance cell with such electrical and geometrical parameters (table 5-4), the maximum input voltage that can be applied across the cell's terminals corresponds to its full length D . During simulations, it was observed that if the input signal exceeds $1V$ the state variable reaches its maximum value and saturation is reached.

5.3.1.4 Adapting Memristance Cell for Cardiac Stimulation applications

In our application of cardiac implants, stimulation signals can reach up to $8V$. So we studied the possibility of increasing the voltage range that can be supported by the cell by increasing the cell's full length D . theoretically this would prevents the cell from entering into the saturation condition. Simulation results are shown in figure 5-16 for an input voltage of $8V$ and different values for D parameter. We found that the minimum D value at which the cell responses correctly was at $28 \, nm$.

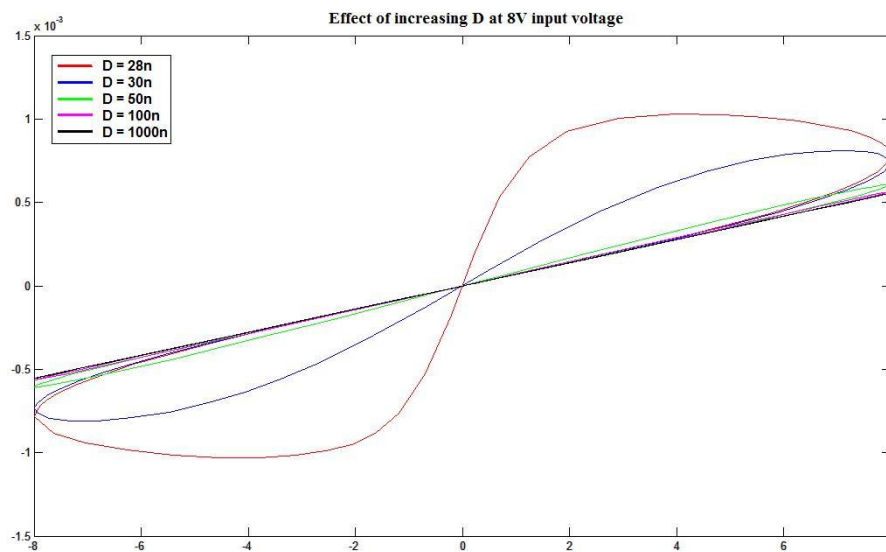


Figure 5-16: effect of increasing the full length D of the model on the double hysteresis curve (behavior)

As a first step, we increased D from 10nm to 28nm to work at 8 volts input voltage. To check if changing D does not affect negatively the cell's behavior at less voltage levels, we simulated the cell again at different input voltages and we obtain correct behavior as shown in figure 5-17.

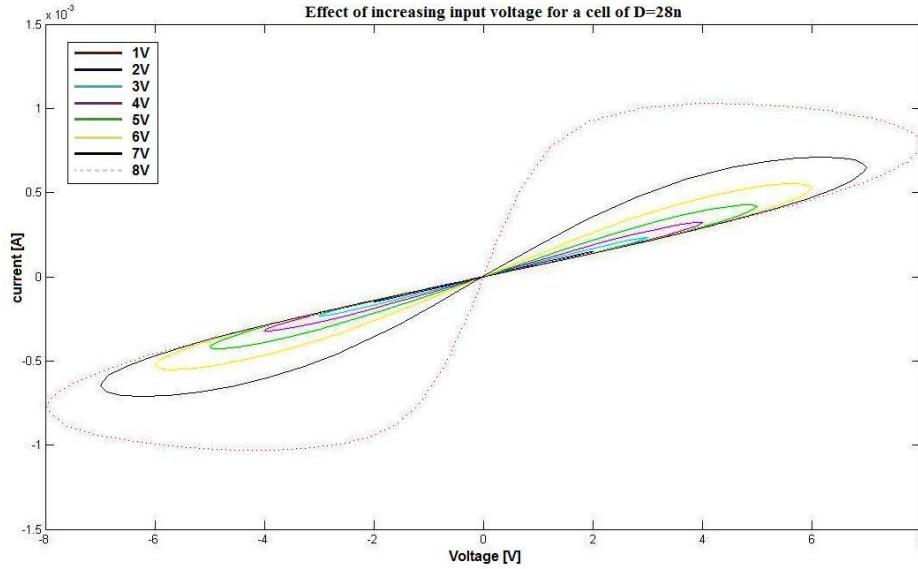


Figure 5-17: recheck of model correct behavior at all the voltage range after increasing D to 28nm

As a second step, we tested the evolution of the cell's resistance with the applied voltage. In figure 5-18 we applied a positive ramp signal covering the full voltage range from -8V to +8V. As the initial value of the state variable (W_0) was set to 0.1 (table 5-4), it can be remarked that the resistance value starts at 14K Ω and increases till it reaches its maximum value 16K Ω . The resistance value remains stable at its maximum as long as the applied voltage is negative.

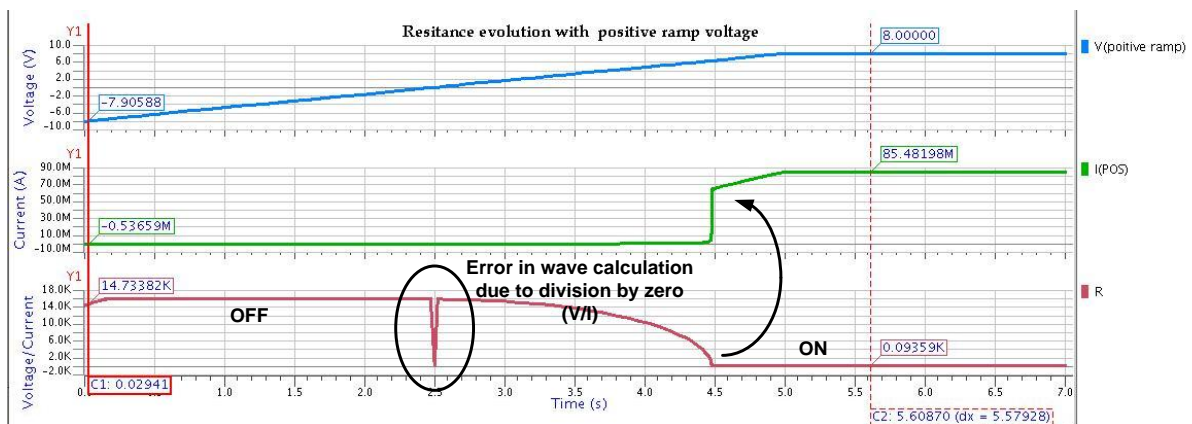


Figure 5-18: model's resistance evolution with an applied positive ramp voltage signal.

Note: At 0V we observe a glitch on the resistance waveform. This is caused by the division by zero calculation error when the voltage signal is divided by the current signal (0 mA at this instance) to give the resistance value.

When the applied voltage becomes positive, the cell's resistance starts to decrease gradually with the increase of positive voltage value. After a while, the minimum resistance value (100Ω) is reached and a switching is observed through the sudden increase in current passing across the cell as marked in the figure 5-18.

In figure 5-19, we applied a negative ramp voltage signal that covers the full voltage range from +8V to -8V. The resistance value starts to decrease from its initial state till it reaches its minimum value (100Ω). At this moment, the switching is observed on the current signal. The current signal then decreases because of the continuous decrease of voltage input while the resistance is constant.

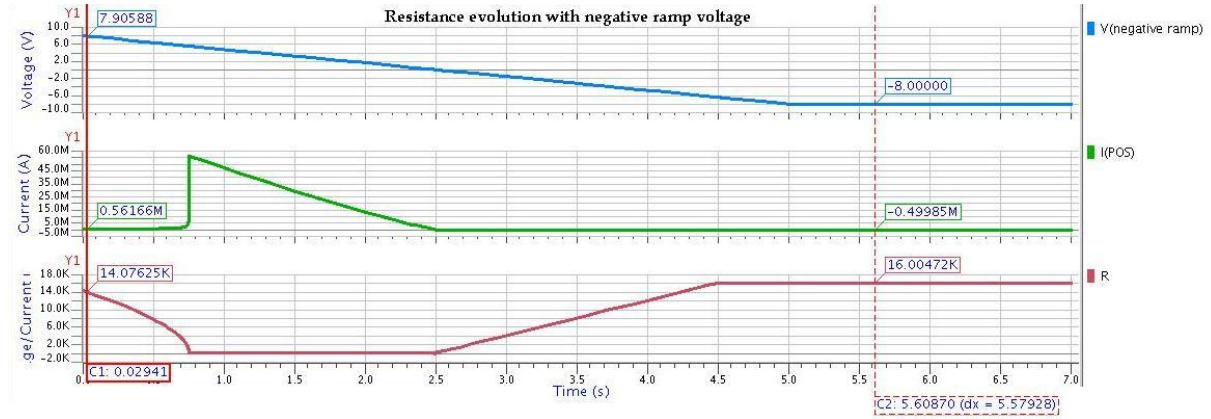


Figure 5-19: model's resistance evolution with an applied negative ramp voltage signal.

When the input voltage polarity is inversed to negative, the resistance started to increase gradually till it reaches its maximum value ($16K\Omega$).

The resistance evolution with applied voltage experiment of figures 5-18 and 5-19 showed that the memristance cell has certain switching delay. This delay is a normal behavior due to the change in dopants concentration along the semiconductor film caused by the applied bias voltage. But in order to better evaluate this delay in relation to the applied voltage we ran another experiment.

In this experiment we applied constant voltage signals rather than ramp voltage signals. Given that the initial state of the memristance cell model is OFF, we applied positive voltage signals to observe the switching of the state. Figure 5-20 shows the current values across the memristance cell in response to the eight different voltage signals applied $[1V - 8V]$.

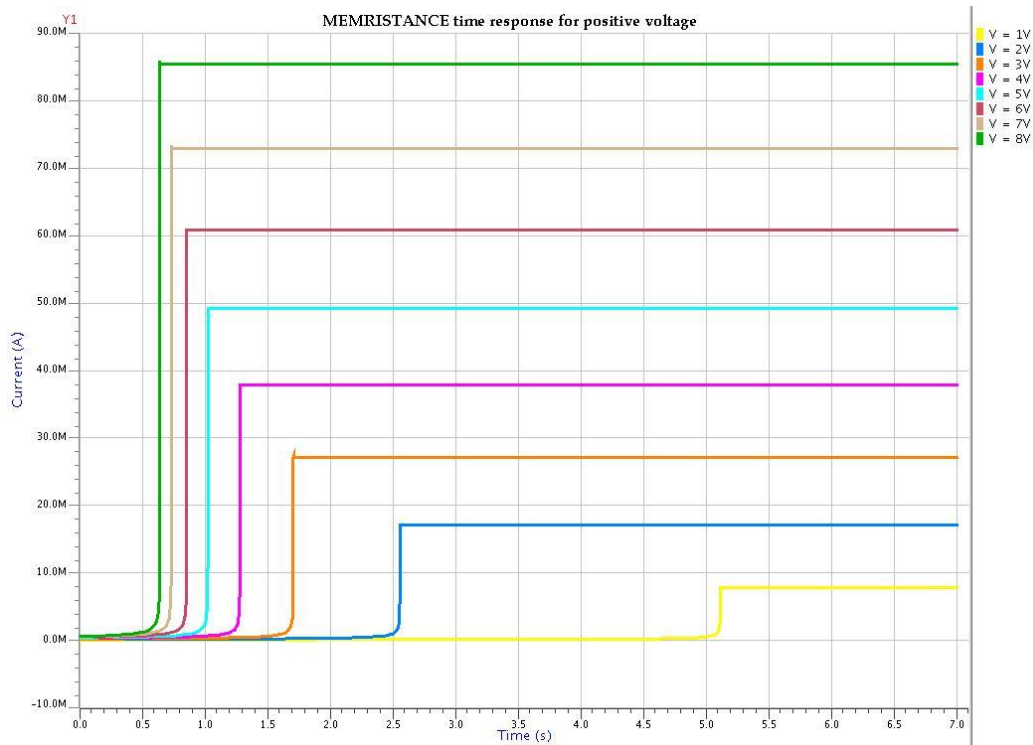


Figure 5-20: Memristance model switching delay for different positive voltage applied across the cell

It is clear from figure 5-20 that as the voltage increases, the switching delay decreases. But the surprise here was the very long switching delay observed. At 8V where we expected the shortest switching delay, it was observed at 0.6 sec. while at 1V the switching delay was tremendously long of 5 seconds.

Even that this model does not reflect precisely the physical properties of the memristance cell, the observed switching delays during this experiment predicts certain trend for the impact of the increase in the cell's full length D . **This amount of switching delays cannot be tolerated in systems like cardiac stimulators and is considered as a blocking point for the integration of this technology within the system.**

Another blocking point for this technology was observed during an experiment to test the stability of the memristance states facing conditions near to that of our application. First, the resistance value for ON and OFF states were set to 1K and 160K respectively. As in the cardiac stimulation systems, the stimulation signal is in the form of pulses that repeats every cardiac cycle (ex: 1 second), we applied a series of positive pulses at 8V to pass through the memristance cell (upper pane of fig.5-21). The cell is initially set to OFF state. Therefore we expected that the applied voltage signal would be blocked.

In the beginning the memristance blocked the input signal, but rapidly the situation was changed. With every positive pulse in the input sequence, the cell's resistance (blue signal in the upper pane of fig. 5-21) is decreased while during the inter-pulse duration the memristance retained its last resistance reached thanks to its memory effect. The resistive state kept decreasing till it reached its minimum value and switched from OFF to ON as shown in figure 5-21.

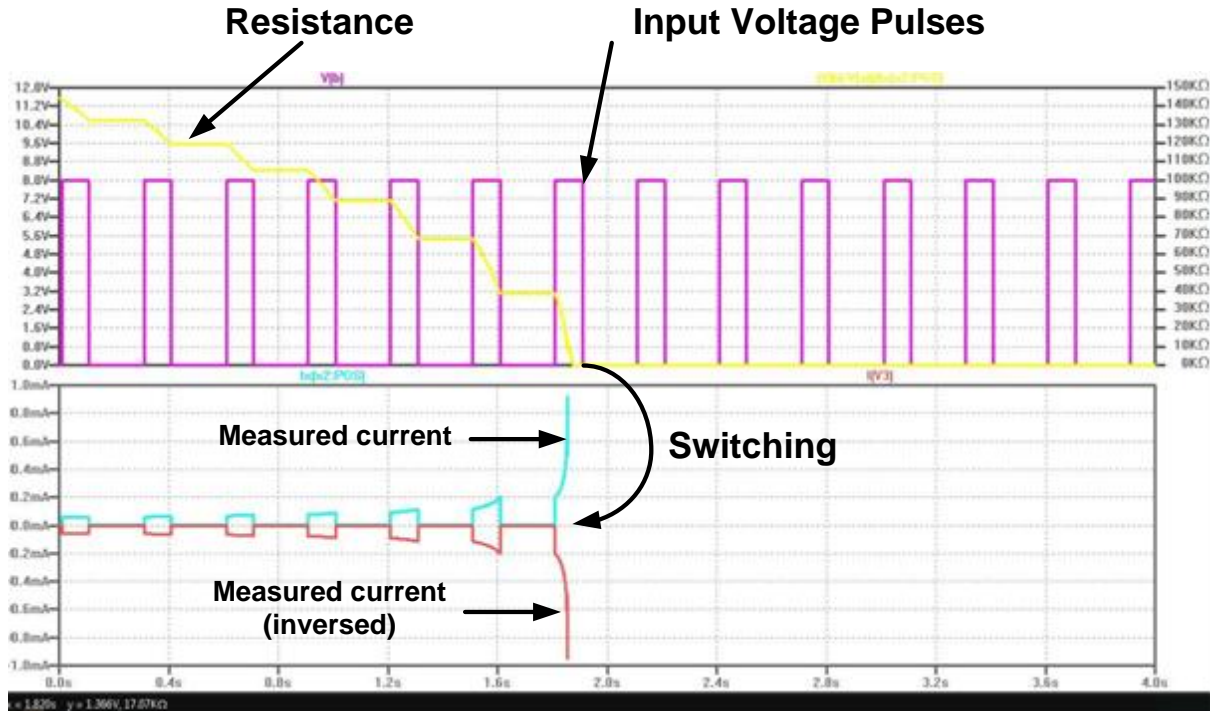


Figure 5-21: (upper pane) applied positive voltage pulse sequence and the memristance cell resistance is plotted. (lower pane) the measured current across the cell in the two directions. The missing part of the current waveform signifies a stable current value

This behavior observed during this experiment is a fatal drawback for this technology to be used in our application. It reflects instability in the memristance states to pass signals through them. This instability was mentioned as well in a published paper [9]. They returned the cause of this instability to nonzero net flux generated by read signals after several read cycles.

In conclusion for the study of resistive RAM family represented in memristance and MRAM, we found these technologies are not suitable for our application. Nevertheless, other emerging resistive RAM technologies such as CBRAM and OxRAM could be investigated in the future to be adapted to our cardiac implant systems.

5.2 Conventional Non-Volatile Memory Technology: Flash Memory

5.2.1 Theoretical background

A flash memory cell is composed of a single Floating Gate (FG) transistor. As showed in figure 5-22, the FG transistor has one control gate and one floating gate. The floating gate is situated between substrate and the control gate. The floating gate acts as potential well in which the forced charges stay trapped until an external force is applied to liberate them [23].

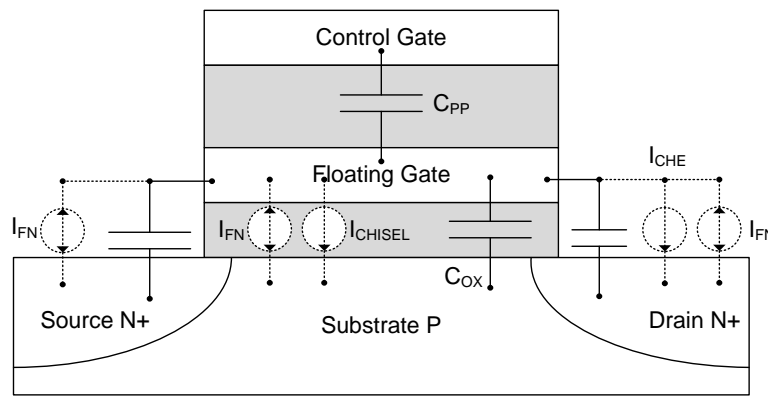


Figure 5-22: Flash memory cell showing the structure of its floating gate transistor [20]

The quantity of charges that can be trapped in the floating gate modifies the threshold voltage of the transistor. Two different quantities of charges correspond to two different states of the flash cell. We here follow the terminology which defines the ON state when the cell is erased, and OFF state when the cell is programmed as shown in figure 5-23.

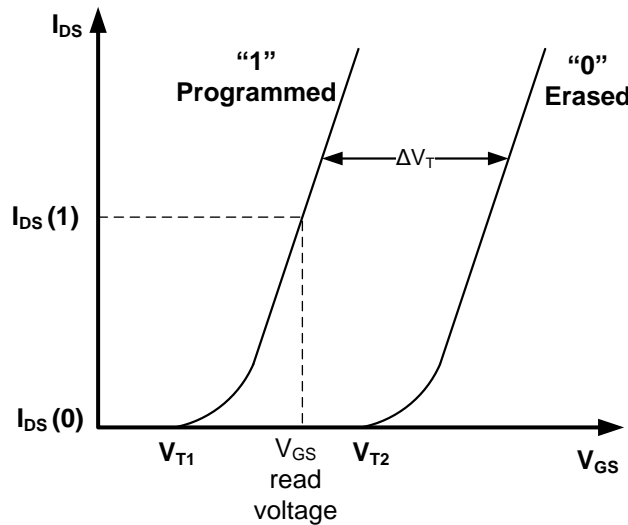


Figure 5-23: Programming window of flash cell [20]

Flash cell is programmed and erased electrically by two possible methods named Fowler Norheim Injection and Channel Hot Electron. They are represented in figure 5-22 as current sources I_{FN} and I_{CHE} respectively.

C_{PP} is the capacitance between floating gate and control gate, C_{OX} is the Capacitance between floating gate and substrate, C_{GS} is the Gate-Source capacitance and C_{GD} is the Gate-Drain capacitance.

The behavior of the floating gate transistors are defined in the triode and saturation regions by equations (15) and (16) respectively [23].

$$\text{Triode region:} \quad I_{DS} = \beta [V_{GS} - V_T] V_{DS} - \frac{1}{2\alpha_G} V_{DS}^2 \quad (15)$$

$$\text{Saturation region} \quad I_{DS} = \frac{\beta}{2} \alpha_G V_{GS} + f V_{DS} - V_T^2 \quad (16)$$

Where

$$\alpha_G = \frac{C_{PP}}{C_T}, \quad f = \frac{C_D}{C_{PP}}, \quad C_T = C_{PP} + C_S + C_{OX} + C_D \quad \text{and} \quad \beta \text{ is a conductivity factor}$$

From the previous equations, it can be deduced that the FG transistor can conduct current even when $|V_{GS}| < |V_T|$. This effect is called “drain turn-on” and it occurs because the channel can be turned on by the drain voltage due to the presence of the term fV_{DS} in equation (16).

In order to read the state of a Flash cell, a bias voltage has to be applied between the control gate and source. The value of this bias voltage has to be in the middle way between the two threshold voltages of the flash cell (figure 5-23). Drain voltage has to be maintained at around 1V.

Table 5-5 shows an example of bias voltages applied on Source, Control Gate and Drain of a typical flash cell during the different operations. The substrate is generally grounded, but by applying negative voltage of -2V can reduce the consumption

Table 5-5: typical bias voltages for flash cell [23]

	Source	Control Gate	Drain
Read	GND	5V	1V
Program	GND	12V	5-7 V
Erase	12V	GND	Floating

5.2.2 Flash cell model

In terms of research collaboration between ISEP and IM2NP lab of Marseille we used their compact model of flash cell [20] in order to validate the concept of its integration in the cardiac stimulation system. The model is built on PSP MOS model of N-type and gate dimensions: $W=90\text{nm}$, $L=180\text{nm}$ and $t_{\text{ox}}=9.8\text{nm}$. Program and erase mechanisms are performed by Fowler Nordheim (FN) and Hot Channel Electron (CHE).

The model of Flash memory cell is presented in figure 5-22 with its three principal components:

- MOS transistor to describe the channel behavior
- Capacitances to isolate the floating gate node
- Current sources to model injection currents

Starting from the VerilogA files of the flash model, we generated a symbol using Mentor Graphics environment in order to facilitate the simulation of the model with our system in Eldo.

In order to verify that our generated cell behavior corresponds to the model behavior, we simulated the Program/Erase sequences on the Flash symbol generated in Mentor Graphics environment.

5.2.2.1 Program Sequence using Channel Hot Electron Method

The flash cell has four functional I/O terminals representing Bulk (B), Source (S), G (Control Gate) and Drain (D). It has another three outputs used to observe the change in threshold voltage (VT), Floating gate voltage (FG) and the injection currents (IG).

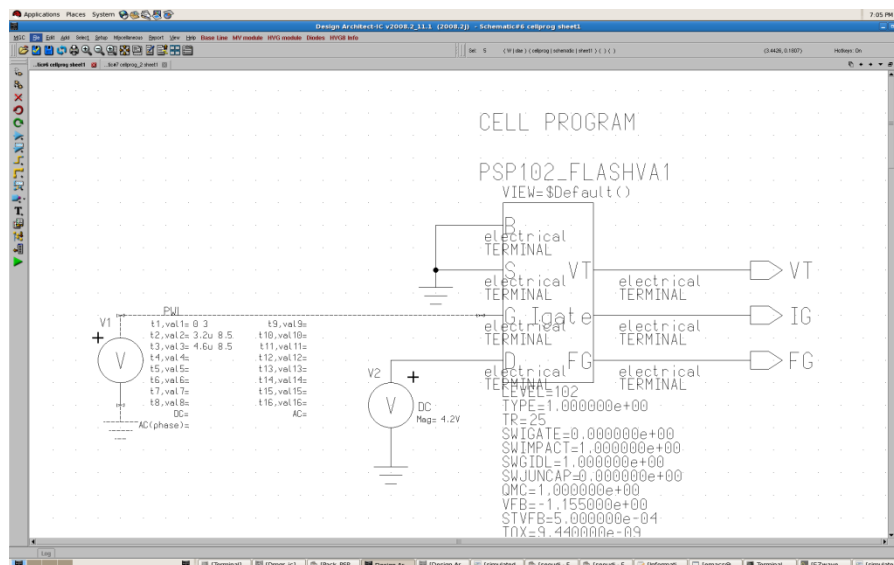


Figure 5-24: symbol for the generated flash cell - Program sequence

A comparison between our simulation results for the cell (fig. 5-26) in reference to the behavior given by the model (fig. 5-25) shows a complete match with only slight difference in V_T values as marked in figures.

We can see from the figures how V_T is increased from $V_{T1}=3.11\text{V}$ to $V_{T2} = 5.8\text{V}$. This shows the state switching from ON (erased) state to OFF (programmed) state.

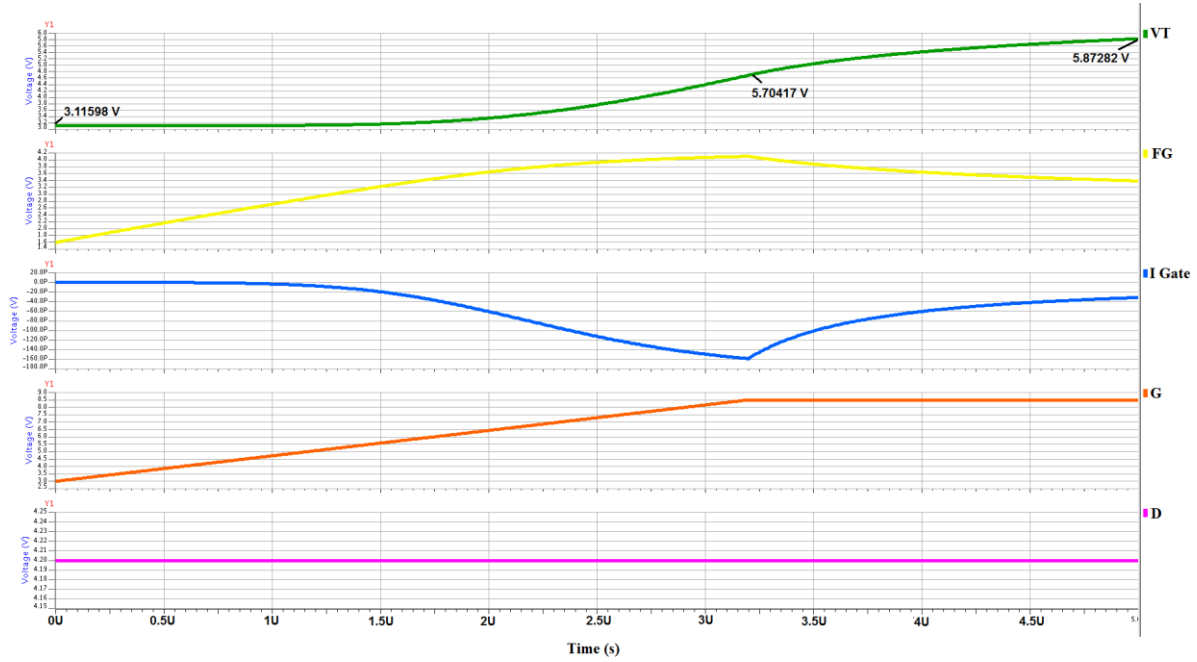


Figure 5-25: Program sequence waveforms for reference VerilogA Flash cell

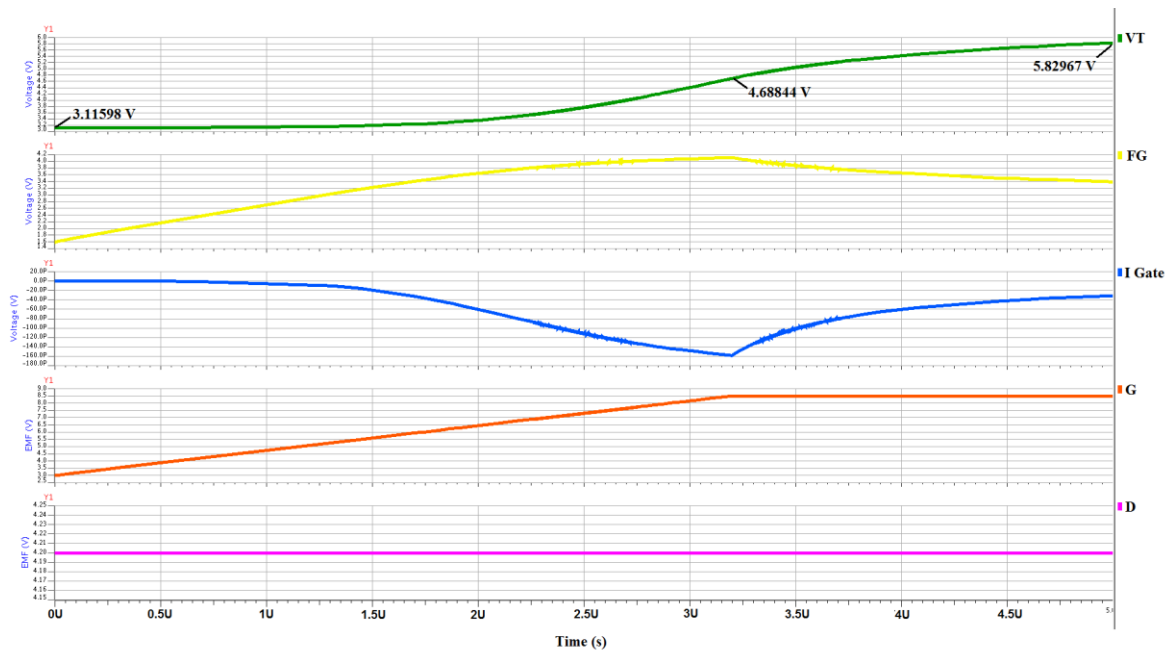


Figure 5-26: Program sequence waveforms for the generated symbol of Flash cell

5.2.2.2 ERASE Sequence using Fowler Nordheim Injection method

Figure 5-26 shows the set up used for erasing the flash cell using Fowler Nordheim Method. Bulk, Source and Drain are tied to the same stepping ramp voltage varying from 3V to 6.9V during about 1ms. Gate is connected to high negative voltage of -10.5V.

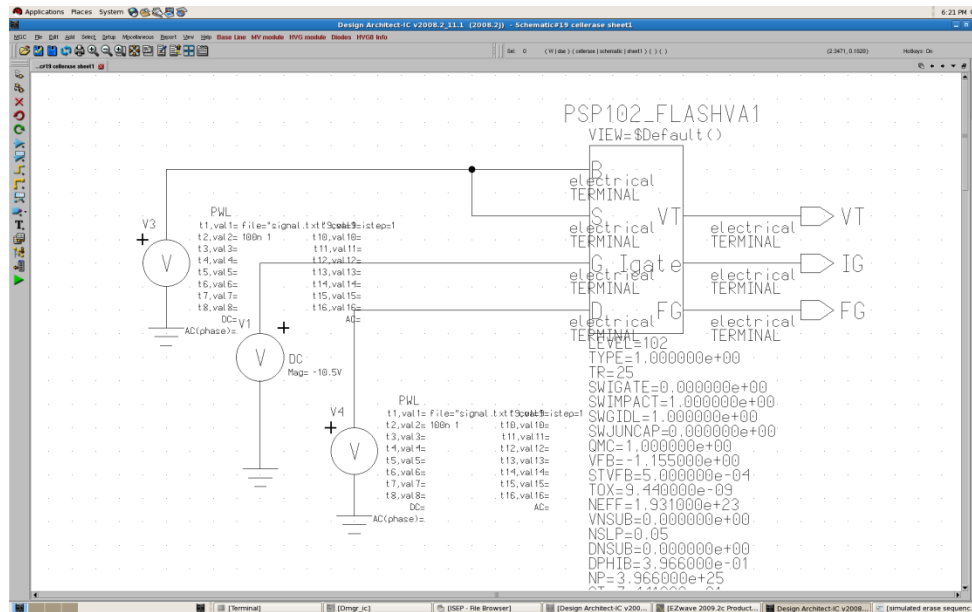


Figure 5-27: Symbol for the generated flash cell - Erase sequence

A comparison between our simulation results for the cell (fig. 5-29) in reference to the behavior given by the model (fig. 5-28) shows a complete match with only slight difference in VT values as marked in figures.

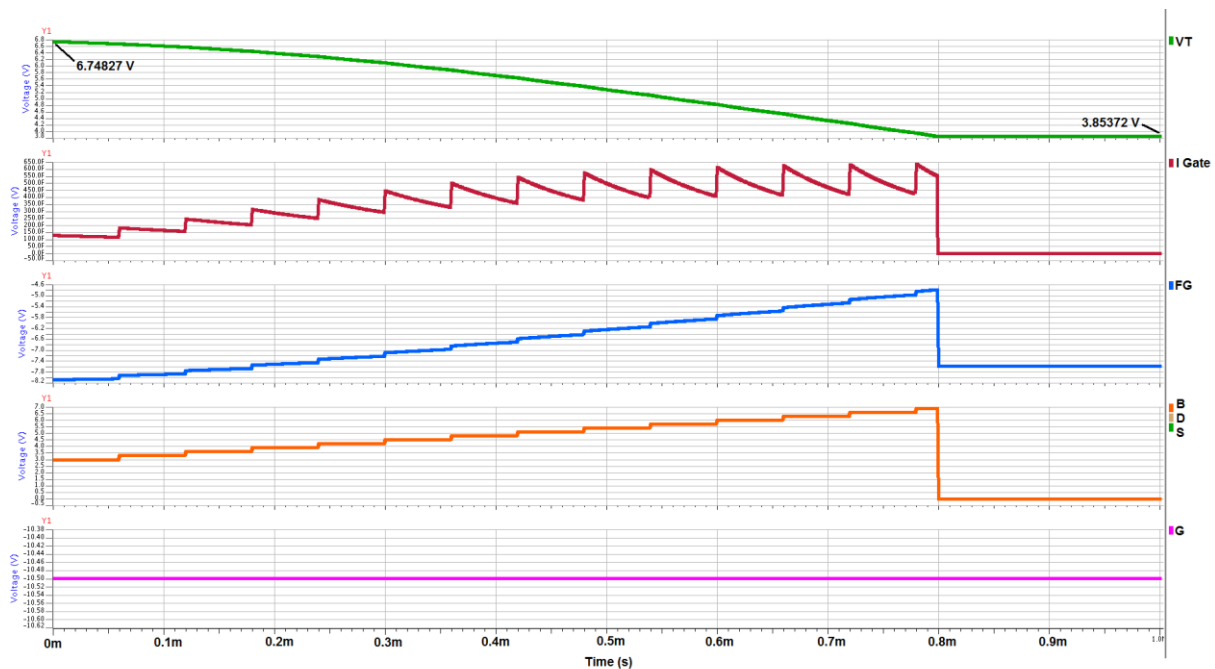


Figure 5-28: Erase sequence waveforms of reference VerilogA Flash cell

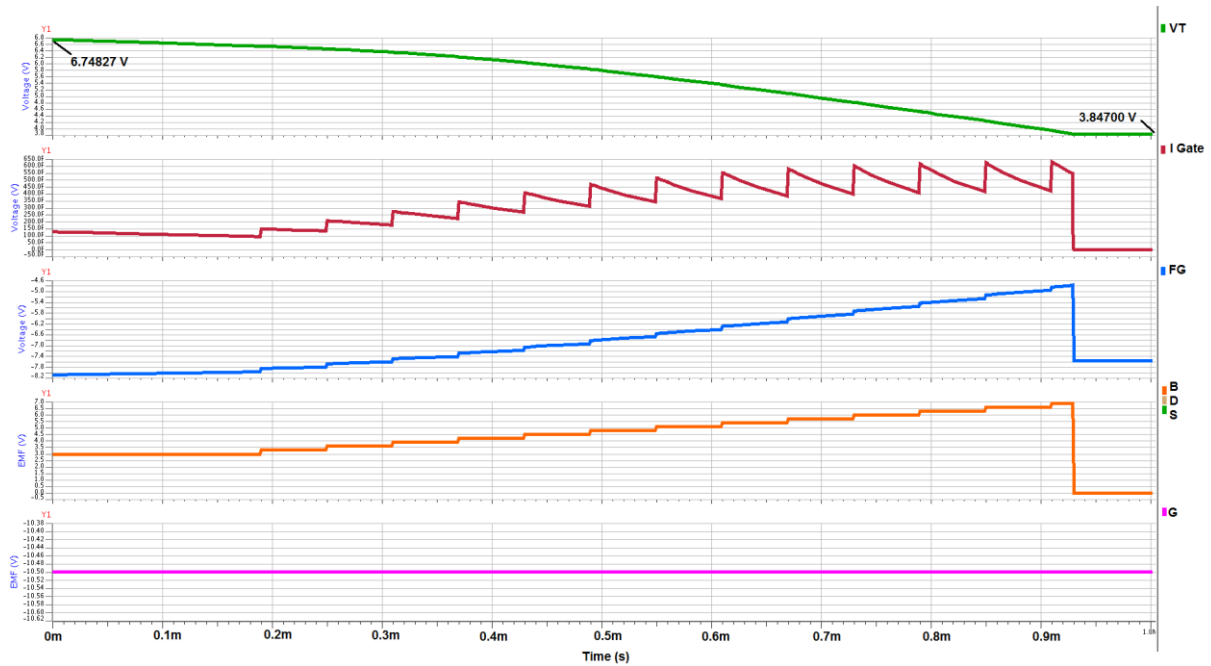


Figure 5-29: Erase sequence waveforms for the generated symbol of Flash cell

5.2.2.3 Observed Characteristics of the Flash Cell

We obtained the same behavior between the reference flash model and the generated flash cell. Table 5-6 summarizes the observed characteristics

Table 5-6: Characteristics summary

Threshold voltage of erased cell V_{T1} (ON)	3.8 V
Threshold voltage of programmed cell V_{T2} (OFF)	6.7 V
Read bias voltage needed	4V

5.2.2.4 Operation Window expansion to adapt with our application

By definition, the operational window is the difference between the erased state threshold voltage and the programmed state threshold voltage [21]. As observed from the default properties of the flash cell model, the operation window is between $V_{T1}=3.11\text{V}$ and $V_{T2} = 6.7\text{V}$.

During the Read phase, it was specified in the flash model operation guidelines that a voltage of a value in the middle of this window has to be applied to the control gate. As shown in (fig. 5-30A), when the flash cell is programmed to have its threshold voltage as V_{T1} , the cell is considered ON if the applied gate-source voltage drop is greater than V_{T1} . When the cell is erased to have its threshold voltage at V_{T2} , the cell is considered OFF if the applied gate-source voltage drop is smaller than V_{T2} .

In our application, we want to use the flash cell as a switch to pass or prevent a wide range of voltages unlike the normal functionality of the cell in the read phase. As an analogy to the basic functionality of the cell, we studied the possibility to extend the operation window to include the functional voltage range $[-2V, -8V]$ of our application. Figure 5-30B shows the flash cell operation window after its expansion. When the flash cell is programmed to have its threshold voltage as V_{T1} , the cell is considered ON if the applied gate-source voltage drop is greater than V_{T1} . When the cell is erased to have its threshold voltage at V_{T2} , the cell is considered OFF if the applied gate-source voltage drop is smaller than V_{T2} .

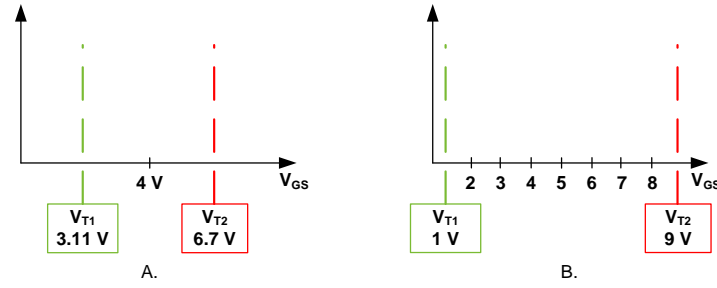


Figure 5-30: (a) default operation window of the flash cell model, (b) application adapted operation window of the model

After consulting an expert in the field of the Flash memories, he confirmed the feasibility of having V_{T1} at 1V but even in sometimes we can obtain a negative V_{T1} if needed. He also confirmed the possibility of expanding V_{T2} value to reach 9V either through increasing the programming pulse amplitude or through increasing the pulse duration. This expanded operation window is obtainable in the existing flash technology with standard cell without affecting the cell's size.

5.2.2.5 Evolution of VT with QFG0 (simulation)

In order to expand the operational window of the flash model, we studied the model behavior in response to change in Q_{FG0} and V_{TUV} parameters. Q_{FG0} is the amount of charge in the floating gate at the initial condition. The quantity of charges trapped inside the floating gate is calculated by equation (16)

$$Q_{FG} = Q_{GI} + Q_{GD} + Q_{GS} + C_{PP}(V_{FG} - V_{CG}) \quad (16)$$

Where, Q_{GI} represents the quantity of charges stored in the gate-substrate capacitance C_{OX} . V_{TUV} is the threshold voltage at zero Floating Gate charge (Q_{FG0}). Normally it corresponds to the middle value between the two threshold values of the flash cell.

The following graph (fig. 5-31) shows the evolution of threshold voltage V_T with different values for Q_{FG0} parameter in the flash cell model.

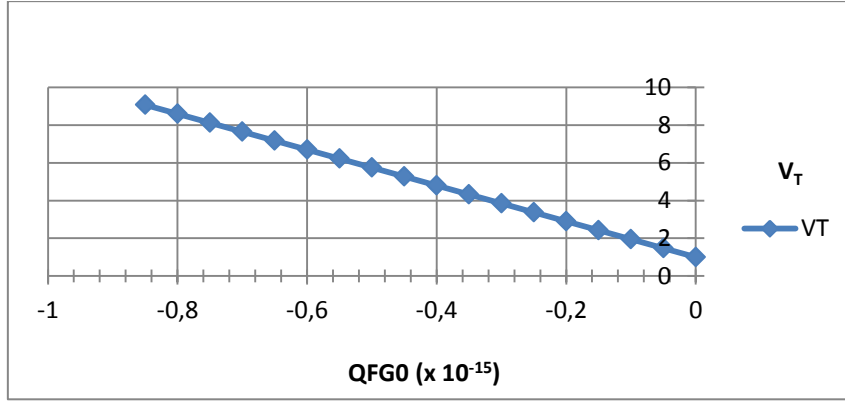


Figure 5-31: Threshold voltage change with varying Q_{FG0} @ $V_{tuv} = 1V$

5.2.3 Non-Volatile Switching Unit Using Flash Memory Cell

We aim to use the flash cells as programmable switches to connect or disconnect each stimulation electrode in the stimulation lead to Anode or Cathode lines. These programmable switches must be able to support stimulation currents (16mA) and voltages (up to 8V). Moreover, these switches have to have low ON resistance to minimize the energy loss in the path between the pacemaker and the patient's heart.

At this important amount of currents, the flash cell risks to be damaged. We found that the flash cells could not be used alone to replace stimulation switches as was the case with NRAM cell of section 5.2 of this chapter.

We thought of architecture for a nonvolatile switching unit in which flash cells are to be associated to ordinary MOS transistors. According to the state of the flash cell ON or OFF, it will drive the MOS transistor to block or pass the stimulation signal between the pacemaker and the configured electrode.

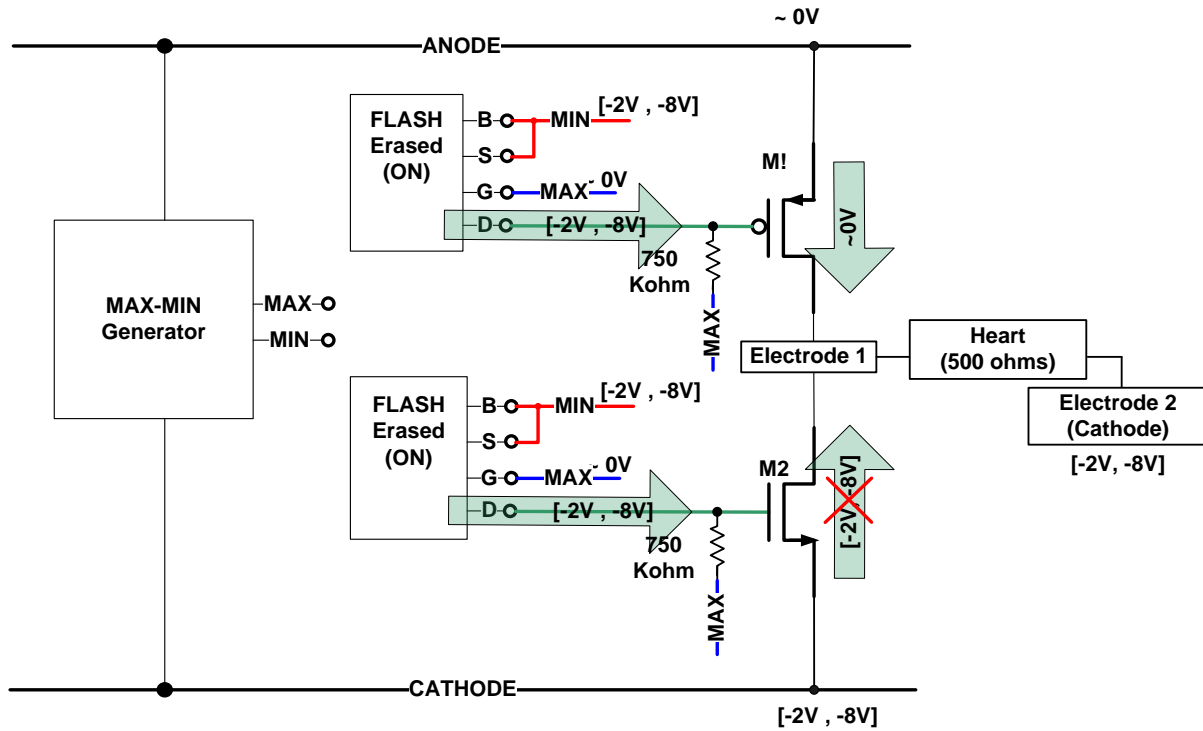


Figure 5-32: concept schematic

Figure 5-32 illustrates a simplified concept schematic for our switching unit architecture. The target of the switching unit is to connect the electrode either to Anode or to Cathode according to the configuration given by the pacemaker. This configuration consists of programming/erasing the two flash cells. Each flash cell has to copy or block voltage signals from its Source to its Drain in order to drive the gate of MOS transistor. By this Flash-MOS association, no important currents pass through the flash cell because the MOS gate does not drain current ($I_G \approx 0$).

The challenge facing this Flash-MOS architecture is that the only power source available during the pacing cycle, comes from the signals running between Anode and Cathode. During stimulation phase as an example the voltage between Anode and Cathode can vary according to configuration between -2V and -8V. Supposing we will use the flash cell in its read mode, we need to apply a VGS of a value between VT1 and VT2 which is not available.

We used a circuit (MAX-MIN generator presented before in section 4.4.1 of chapter 4) to give the maximum voltage (MAX) and the minimum voltage (MIN) found between Anode and Cathode. In our case, MAX will always be around 0V and MIN will take a voltage value in $[-2V, -8V]$ range. We use these two voltages to drive the Flash cell as shown in figure 5-32 so that VGS will have always a positive value.

In the following sections we will present the simulation results obtained for this architecture.

4.3.1 Case 1: MOS Switch connects Cathode to Electrode

In this section we will focus on how to activate or deactivate the MOS switch M2 presented before in (Fig. 5-32), by changing the state of the flash cell.

5.3.1.4.1 Flash cell Erased (ON)

Figure 5-33 shows the connection of the flash cell to the gate of M2. In order to block the connection between Cathode and Electrode1 illustrated in fig. 5-33, the flash cell has to copy MIN voltage from its source to its drain, while its gate is connected to MAX (0V). To do that, the Flash cell has to be Erased (ON) which means that the threshold voltage is modulated to its lowest value.

As the operation window is expanded to be $[-1V, 9V]$, theoretically the flash cell will be able to pass the complete functional voltage range of our application $[-2V, -8V]$ from its source to its drain

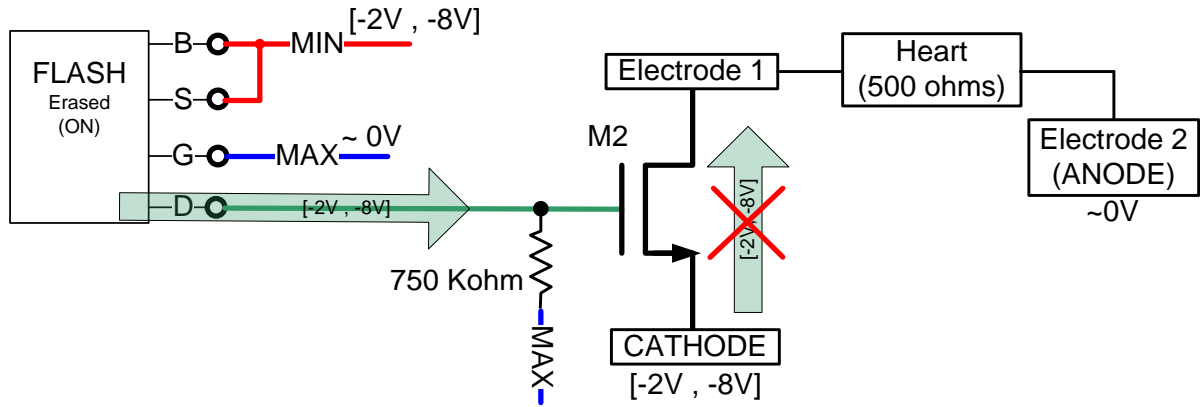


Figure 5-33: Flash cell erased (ON) to block the connection between Cathode and Electrode1

Table 5-7 shows the simulation results for the experiment illustrated in fig. 5-33.

Note: It was observed from simulation, that when MIN voltage is assigned to -2V (V_{GS} Flash = 2V), oppositely to what theoretically assumed, the drain node of flash floats, which means that the cell is OFF. This may be explained by the capacitive effect of the floating gate as given in equation 15 describing the behavior of Flash cell in its triode region, in contrast with the behavior of ordinary MOS transistor.

The role of the pull-up resistor (750 Kohm) connected to the gate of M2, is to ensure a fixed state for M2 when the flash cell is programmed (OFF). This will be clarified in fig.5-34.

Table 5-7: QFG0 = 0 and $V_T = 1V$

ERASED (ON)							
$V_{CATHODE}$	MAX	MIN	V_{DRAIN}	$V_{ELEC1} - V_{ELEC2}$	REF	I_{HEART}	I_{FLASH}
-3V	0V	-3V	-2.73V	0V	0	0 mA	3.64 μA
-4V	0V	-4V	-3.89V	0V	0	0 MA	5.18 μA
-5V	0V	-5V	-4.91V	0V	0	0 MA	6.55 μA
-6V	0V	-6V	-5.92V	0V	0	0 MA	7.89 μA
-7V	0V	-7V	-6.92V	0V	0	0 MA	9.23 μA
-8V	0V	-8V	-7.92V	0V	0	0 MA	10.56 μA

5.3.1.4.2 Flash cell Programmed (OFF)

In order to enable the connection between Cathode and Electrode1 illustrated in fig. 5-34, the flash cell has to block MIN voltage from its source to its drain, while its gate is connected to MAX (0V). To do that, the Flash cell has to be programmed (OFF) which means that the threshold voltage is modulated to its highest value.

As the operation window is expanded to be $[-1V, 9V]$, theoretically the flash cell will be able to block the complete functional voltage range of our application $[-2V, -8V]$ from its source to its drain

To avoid that the gate of M2 be floating after turning OFF the flash cell, a pull-up resistor is used to assign MAX voltage (0V) to M2's gate. This also creates a positive gate-source drop voltage for the NMOS M2, and the connection between Cathode and Electrode1 is activated.

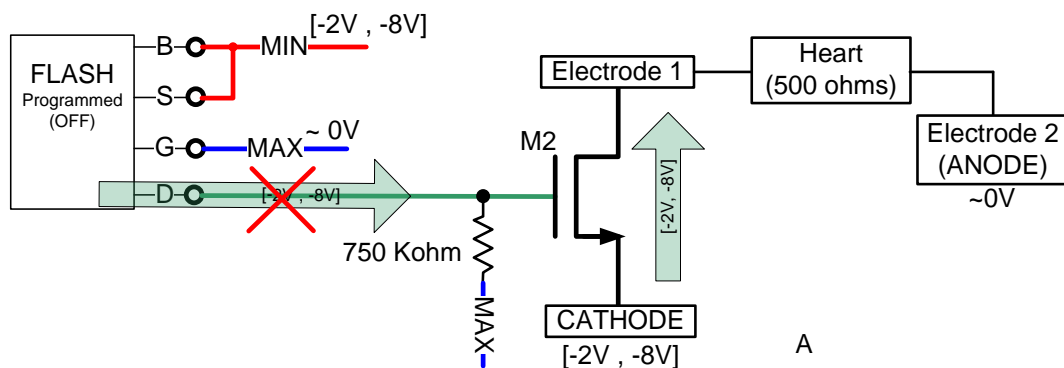


Figure 5-34: Flash cell programmed (off) to enable the connection between Cathode and Electrode1

Table 5-8 shows the simulation results for the experiment illustrated in fig. 5-34.

Table 5-8: $QFG0 = -8.5e-16$ and $V_T = 9.07V$

PROGRAMMED (OFF)							
$V_{CATHODE}$	MAX	MIN	V_{DRAIN}	$V_{ELEC1} - V_{ELEC2}$	REF	I_{HEART}	I_{FLASH}
-3V	0V	-3V	-0.004V	-3V	-3V	-5.9 MA	91 NA
-4V	0V	-4V	-0.018V	-4V	-4V	-7.9 MA	176 NA
-5V	0V	-5V	-0.03V	-4.97V	-5V	-9.9 MA	255 NA
-6V	0V	-6V	-0.11V	-5.96V	-6V	-11.9 MA	385 NA
-7V	0V	-7V	-0.25V	-6.96V	-7V	-13.9 MA	569 NA
-8V	0V	-8V	-0.45V	-7.98V	-8V	-15.9 MA	864 NA

Case 2: MOS Switch connects Anode to Electrode

In this section we will focus on how to activate or deactivate the PMOS switch M1 presented before in Fig. 5-32 by changing the state of the flash cell

5.3.1.4.3 Flash cell Erased (ON)

Figure 5-35 shows the connection of the flash cell to the gate of PMOS M1. In order to enable the connection between Anode and Electrode1, the flash cell has to copy MIN voltage from its source to its drain, while its gate is connected to MAX (0V). To do that, the Flash cell has to be Erased (ON) which means that the threshold voltage is modulated to its lowest value.

As the operation window is expanded to be $[-1V, 9V]$, so theoretically the flash cell will be able to pass the complete functional voltage range of our application $[-2V, -8V]$ from its source to its drain.

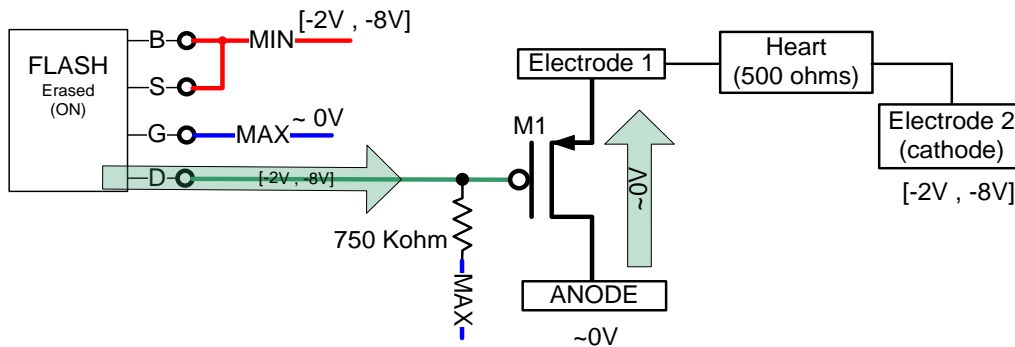


Figure 5-35: Flash cell is erased (ON) to enable the connection between Anode and Electrode1

Table 5-9 shows the simulation results for the experiment illustrated in fig. 5-35.

Note: It was observed that when the MIN voltage goes more negative than -5V, the simulator stops with converging errors. Therefore the functional voltage range in this case is reduced from $[-3V, -8V]$ to be $[-3V, -5V]$. The only difference between this case and the one of fig. 5-33 is the type of switch connecting the electrode (PMOS instead of NMOS).

Table 5-9: $QFG0 = 0$ and $V_T = 1V$

ERASED (ON)							
$V_{Cathode}$	MAX	MIN	V_{Drain}	$V_{ELEC1} - V_{ELEC2}$	REF	I_{FLASH}	I_{HEART}
-3V	0V	-3V	-2.73	-2.82V	-3V	3.64 μA	0 MA
-4V	0V	-4V	-3.89	-3.83V	-4V	5.18 μA	0 MA
-5V	0V	-5V	-4.91	-4.83V	-5V	6.55 μA	0 MA

5.3.1.4.4 Flash cell Programmed (OFF)

In order to disable the connection between Cathode and Electrode1 illustrated in fig. 5-36, the flash cell has to block MIN voltage from its source to its drain, while its gate is connected to MAX (0V). To do that, the Flash cell has to be programmed (OFF) which means that the threshold voltage is modulated to its highest value.

As the operation window is expanded to be $[1V, 9V]$, so theoretically the flash cell will be able to block the complete functional voltage range of our application $[-2V, -8V]$ from its source to its drain.

To avoid that the gate of M1 to be floating after turning OFF the flash cell, a pull-up resistor is used to assign MAX voltage (0V) to M1's gate. This also creates a zero gate-source drop voltage for the PMOS M1, and the connection between Anode and Electrode1 is deactivated.

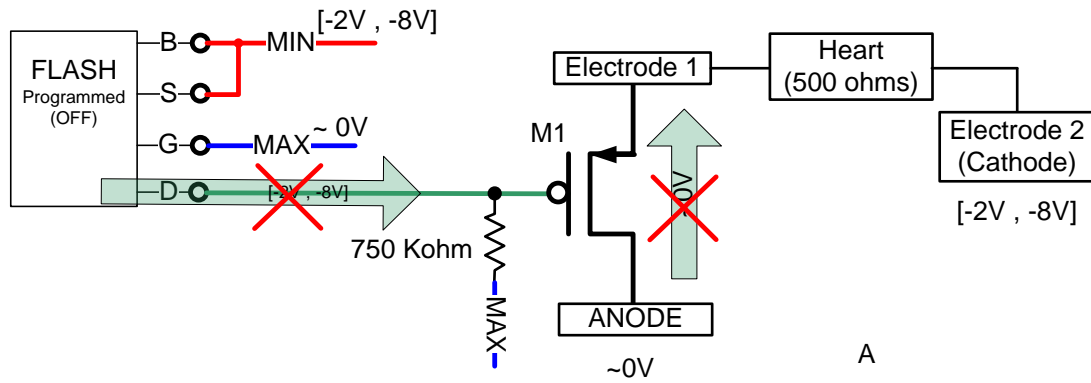


Figure 5-36: Flash cell is programmed to block the connection between Anode and Electrode1

Table 5-10 shows the simulation results for the experiment illustrated in fig. 5-36.

Table 5-10: $Q_{FG0} = -8.5e-16$ and $V_T = 9.07V$

PROGRAMMED (OFF)							
$V_{Cathode}$	MAX	MIN	V_{Drain}	$V_{ELEC1} - V_{ELEC2}$	REF	I_{HEART}	I_{FLASH}
-3V	0V	-3V	0V	0V	0V	0 MA	2.91 NA
-4V	0V	-4V	-0.01V	0V	0V	0 MA	13.7 NA
-5V	0V	-5V	-0.03V	0V	0V	0 MA	52.11 NA
-6V	0V	-6V	-0.11V	0V	0V	0 MA	151 NA
-7V	0V	-7V	-0.25V	0V	0V	0 MA	336 NA
-8V	0V	-8V	-0.45V	0V	0V	0 MA	604 NA

5.2.4 Summary

After exploring the details of both cases 1 and 2, the combination of both cases together is compulsory to meet our system requirements. Our application requires three distinct states for each Electrode as follows:

1. Cathode (fig. 5-11 a)
2. Anode (fig. 5-11 b)
3. Not connected (fig 5-11 c)

Figure 5-37 shows these three cases with the representation of the state of the flash cells as well as the two MOS switches. Table 5-11 summarizes how to configure the electrode by changing the states of the flash cells.

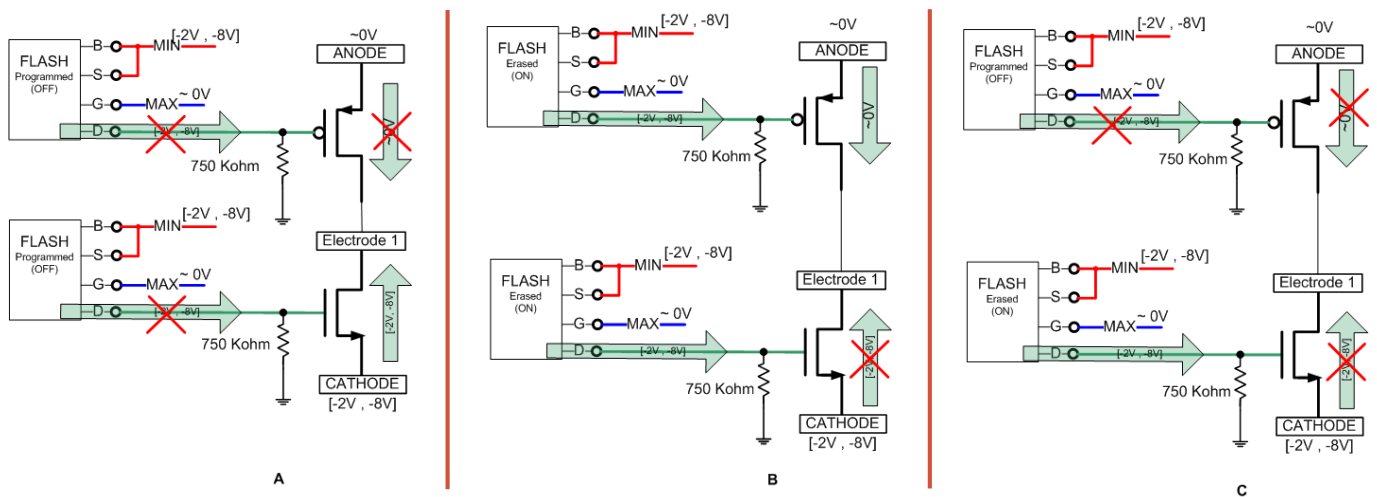


Table 5-11: nonvolatile switching unit's configuration summary

Flash cell 1	Flash cell 2	Electrode State
OFF	OFF	Cathode
ON	ON	Anode
OFF	ON	Floating (not-active)

Figure 5-37: A. Electrode = Cathode, B. Electrode = Anode, C. Electrode = not connected

After all these successful experiments that we performed using the Flash memory cell, we claim the feasibility of the integration of non-volatile memory cells - represented here in flash - within our standard switching unit in order to transform it into a new non-volatile switching unit.

Figure 5-38 gives as an example a part of our new non-volatile switching unit showing two electrodes among the multiple ones in the lead. Each electrode is connected to two MOS switches that define its polarity whether Anode or Cathode according to the state of the flash cell associated to each MOS switch.

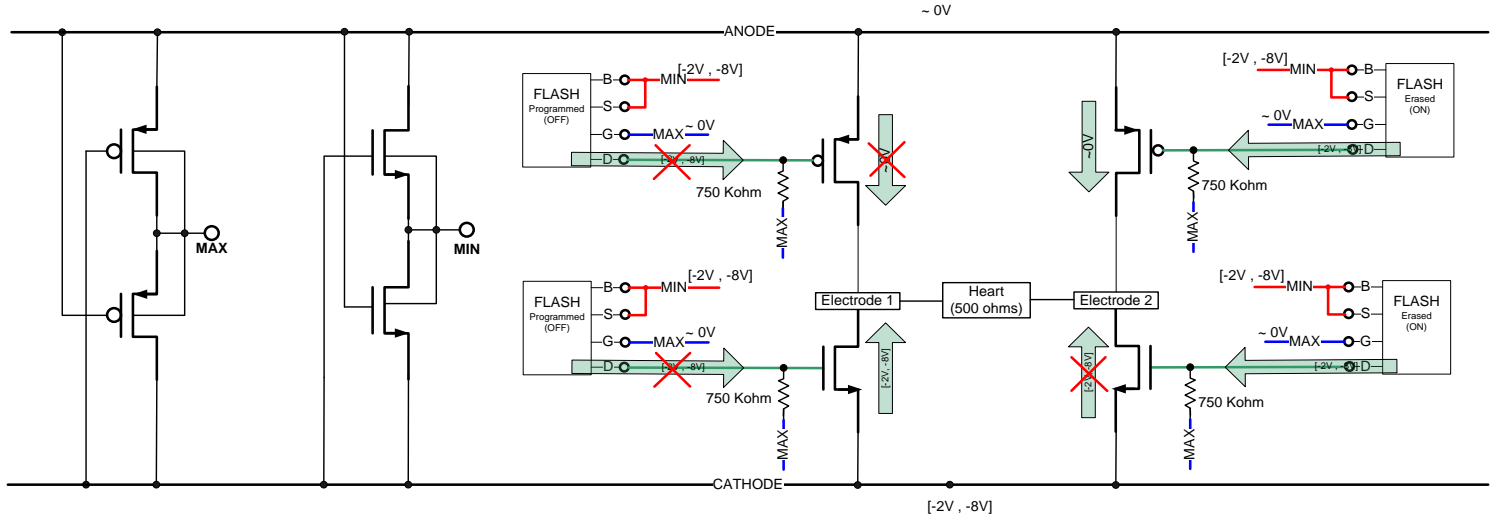


Figure 5-38: example of complete system

The advantage of this structure that the overhead per electrode needed to transform its state from volatile to non-volatile; is the addition of two standard flash cells. Voltages and currents needed for programming and erasing the flash cells can be easily generated using the existing resources of the electrode-controller (charge pumps presented in section 3.4.2.7).

We patented the concept of non-volatile memory technologies integration in the cardiac implants as discussed in this chapter.

5.3 Conclusion

In this chapter we opened a new direction for research through the integration of rising nonvolatile memory technologies within cardiac stimulation system. The employment of such technologies in building a new non-volatile switching unit enhanced our multi-electrode system in several aspects. It suppressed the need of repetitive configuration of electrodes as long as change is not required which is built on its capability of state retention for unlimited durations. It also reduced the latency between stimulation demand and its delivery to the electrodes. Moreover, it alleviates the need of big power storage unit which reduces the overall size of electrode controller. It was also noticed that nonvolatile memory cells are smaller in size than low Ron MOS switches used in conventional switching units.

We saw how promising a technology like NRAM can be for our application. It's no leakage states, very big resistance distinction between its states; speed and small size make it the ideal candidate for our application.

STT MTJ and Memristance were grouped under resistive RAM family for their common features from the application point of view. After our investigations, we reached a conclusion that their integration in our system is not feasible due to their states instability facing stimulation voltages and currents.

Finally we investigated flash memory cells and came up with a new structure where flash cells are associated with MOS transistors. In this structure stimulation voltages and currents passes through the MOS transistors while the flash cells define and retain the state of the MOS transistor.

We patented the concept of non-volatile memory technologies integration in the cardiac implants as discussed in this chapter.

Publications

Patent N° FR1159288, « Module de commutation contrôlée de sonde multiélectrode pour un dispositif médical implantable actif », filed one 13 October 2011

References

- [1] Ch. Muller et al. “Design challenges for prototypical and emerging memory concepts relying on resistance switching” 978-1-4577-0223-5
- [2] W guo, G Prenat, V Javerliac, M El Baraji, N de Mestier, C baraduc and B Dieny “SPICE modeling of magnetic tunnel junctions written by spin-transfer torque”. J. Phys. D: Appl. Phys. 43 (2010) 215001
- [3] Jonathan F. Harms et al. “Spice macromodel of spin-torque-transfer-operated magnetic tunnel junctions” IEEE transactions on electron devices, vol. 57, no. 6, june 2010
- [4] Dynamic compact model of Spin-Transfer Torque based magnetic tunnel junction (MTJ) (ref. Louis-barthelemy Faber et al “Dynamic compact model of Spin-Transfer Torque based magnetic tunnel junction (MTJ)” 2009 IEEE)
- [5] Dmitri B. Strukov, Gregory S. Snider, Duncan R. Stewart and R. Stanley Williams: “The missing memristor found”
- [6] Dalibor Biolek, Zdenek Biolek, Viera Biolkova: “SPICE Modeling of Memristive, Memcapacitive and Meminductive Systems”
- [7] Massimiliano Di Ventra, Yuriy V. Pershin, and Leon O. Chua: “Circuit Elements with Memory: Memristors, Memcapacitors, and Meminductors”
- [8] Tezaswi Raja and Samiha Mourad: “Digital Logic Implementation in Memrstor-based Crossbars”
- [9] Yenpo Ho, Garng M. Huang and Peng Li: “Nonvolatile Memristor Memory: Device Characteristics and design implicatons”
- [10] Sangho Shin, Kyungmin Kim and Sung-Mo Kang “Memristor-Based Fine Resolution Programmable Resistance and Its Applications”
- [11] EVER SPIN TECHNOLOGIE S, IN C. MRAM Technical guide
- [12] MR2A16A Datasheet
- [13] J. P. Nozières « Magnetic Random Access Memories (M-RAM): A truly universal memory? »
- [14] B. N. Engel, J. Åkerman, B. Butcher, R. W. Dave, M. DeHerrera, M. Durlam, G. Grynkewich, J. Janesky, S. V. Pietambaram, N. D. Rizzo, J. M. Slaughter, K. Smith, J. J. Sun, and S. Tehrani “A 4-Mb Toggle MRAM Based on a Novel Bit and Switching Method”
- [15] US Patent 6545906
- [16] R.F. Smith, T. Ruekes, S. Konsek, J.W. Ward, D.K. Brock, and B.M. Segal “Carbon Nanotube Based Memory Development and Testing”

- [17] Thomas Rueckes, Kyoung-ha Kim, Ernesto Joselevich, Greg Y. Tseng, Chin-Li Cheung, and Charles M. Lieber “Carbon Nanotube-Based Nonvolatile Random Access Memory for Molecular Computing”
- [18] Journal of Nuclear Medicine JNM figure
- [19] Daniel Batas and Horst Fiedler “A Memristor SPICE Implementation and a New Approach for Magnetic Flux-Controlled Memristor Modeling” IEEE transactions on Nanotechnology, Vol. 10, no. 2, March 2011
- [20] A. Maure, P. Canet, F. Lalande, B. Delsuc, J. Devin « Flash Memory cell compact modelling using PSP model » Proceedings of the IEEE BMAS, 2008
- [29] S. S. Chung, S. T. Liaw, C. M. Yih, Z. H. Ho, C. J. Lin, D. S. Kuo, and M. S. Liang “N-channel versus p-channel Flash EEPROM – which one has better reliabilities” Reliability Physics Symposium, 2001.
- [22] Nantero, Inc. “Mass Insight PowerPoint” 2005
- [23] P. Pavan, R. Bez, P. Olivo, E. Zanoni “Flash Memory Cells – An Overview” Proceedings of the IEEE, vol. 85, no. 8, august 1997
- [24] US Patent 7652337 “Nanotube-based switching element”, Nantero Inc. 2006

Chapter 6

Conclusion

This thesis started by presenting the structure of human heart and the different disorders affecting it that may raise the need for cardiac implants. We saw how cardiac implants evolution led to better treatment for patients suffering from cardiovascular diseases. We then explored the building blocks of cardiac implants and how they interact with cardiac tissues to analyze the patient's state and deliver the adequate treatment. By the end of chapter 2, the importance of biventricular pacing (CRT) was cleared as well as the limitations of using bipolar leads in left ventricular stimulation.

In chapter 3, we addressed those limitations by our multi-electrode system for left ventricular stimulation. We presented this system in its two structures (centralized and distributed). We showed how we modified the implant's control in order to drive our custom-designed electrode-controller inserted inside the lead.

Our system added more flexibility for the choice of stimulation sites through its selective control of up to 8 electrodes with the possibility of interchangeable polarity for each. The re-configurability of lead electrodes suppresses the need for post-implant surgery in case of inhibition of patient response to stimulation caused by lead displacement.

The communication between the two parts of our multi-electrode system (implant and the electrode-controller) was implemented by our one-wire protocol doted by a tolerance to difference in oscillator frequencies between both sides. According to this protocol, power pulses and configuration bits shared the same line, leaving Anode and Cathode lines for stimulation and sensing purposes. This enabled the isolation of patient's heart from data and power pulses. Moreover it resulted in a norm-compliant 3-wire connector interface.

Another notable feature in our system is its capability of delivering two consecutive stimulation pulses of same or different polarities as configured. This feature enables biphasic stimulation which may reduce the discharge period that follows the stimulation phase.

Our system is distinguished by ensuring compatibility of our multi-electrode lead with any pacemaker in the market thanks to its auxiliary switching unit. The concept was proved using discrete JFET switches.

In chapter 4 we presented an ameliorated solution for the problem of multi-electrode lead compatibility with any pacemaker device in the market; named Default Connection Unit (DCU). This unit which was integrated within the electrode-controller chip process alleviates this challenge by transforming the multi-electrode lead into a standard bipolar lead through the activation of two electrodes that it shares their control with the main switching unit found in the electrode-controller chip.

We showed how the DCU was designed to use the available stimulation energy to activate its paths between Anode, Cathode and default electrodes without the need for a power source (battery). It also stores a part of this energy in order to retain its state for a period that at least covers the discharge phase duration. DCU paths are equipped with resistances that enable it to continue ensuring the connection between electrodes and the pacemaker during the duration of the sensing phase which depends on each patient.

DCU distinguishes our multi-electrode system and takes a step forward compared to the auxiliary switching unit using JFET presented in chapter 3 as it is integrated in the technology process used in the electrode-controller chip.

As the DCU is assigned to only two electrodes in the multi-electrode lead, this may show some limitations to the site of stimulation for the new pacemaker connected to the lead. In chapter 5 we introduced a new solution to address this issue. We showed how nonvolatile memories and its underlying implementation technologies offer us ways to maintain the last configured stimulation site and thereby allowing us to circumvent the fixed site limitation imposed by the DCU.

This opened a new direction for research through the integration of rising nonvolatile memory technologies within cardiac stimulation system. The employment of such technologies in building a new non-volatile switching unit enhanced our multi-electrode system in several aspects. It suppressed the need of repetitive configuration of electrodes as long as change is not required which is built on its capability of state retention for unlimited durations. It also reduced the latency between stimulation demand and its delivery to the electrodes. Moreover, it alleviates the need of big power storage unit which reduces the overall size of electrode controller. It was also noticed that nonvolatile memory cells are smaller in size than low Ron MOS switches used in conventional switching units.

We saw how promising a technology like NRAM can be for our application. It's no leakage states, very big resistance distinction between its states; speed and small size make it the ideal candidate for our application.

STT MTJ and Memristance were grouped under resistive RAM family for their common features from the application point of view. After our investigations, we reached a conclusion that their integration in our system is not feasible due to their states instability facing stimulation voltages and currents.

Finally we investigated flash memory cells and came up with a new structure where flash cells are associated with MOS transistors. In this structure stimulation voltages and currents passes through the MOS transistors while the flash cells define and retain the state of the MOS transistor.

We patented the concept of non-volatile memory technologies integration in the cardiac implants.

We believe much work can be done at all levels in the multi-electrode system. While there are new technologies which need to be explored in more detail through silicon proven chips and characterization, even the traditional approach can be improved by re-looking at the design aspects. For example we can rethink the communication protocol in the multi-electrode lead; we can also reexamine the circuit implementations of the analog/digital blocks of our system. In the non-volatile memories, we can investigate the design of circuitry used for programming and erasing memory cells. This make the system more integrated hence electronically more performant.

As technology matures and new technologies come to the fore and new solutions to manage cardiovascular ailments will come into being. Like any technology design, there would be elements of tradeoff; some approaches will offer better power consumption figures versus others which are more performant. Moreover, as we saw in the previous chapters, technologies are in different states of maturity and one of the key elements of industrial design is to judiciously select the technologies and make design decisions which are backward compatible and take less implementation time. The experience gained during the thesis has helped us to understand these subtle choices and look at new approaches with a pragmatic angle.

List of Publications

1. I. Seoudi, K. Amara, F. Gayral, A. Amara, R. Dal Molin “Multi-electrode system for pacemaker applications” IEEE ICECS 2011
http://ieeexplore.ieee.org/xpl/freeabs_all.jsp?arnumber=6122230
2. I. Seoudi, K. Amara, F. Gayral, A. Amara, R. Dal Molin “Innovative Multi-electrode Communication Scheme for Cardiac Pacemakers” TBME 2012 (submitted – under review)
3. I. Seoudi, J-F. Debroux, M. Laflutte, A. Makdissi, K. Amara, A. Amara, R. Dal Molin “Default connection in multi-electrode leads for cardiac pacemakers” accepted in NEWCAS 17-20 June 2012
4. Patent N° FR1159288, « Module de commutation contrôlée de sonde multiélectrode pour un dispositif médical implantable actif », filed one 13 October 2011